Ginzburg-Landau theory of type II superconductors in magnetic field

Baruch Rosenstein*

Electrophysics Department, National Chiao Tung University, 30010 Hsinchu, Taiwan, Republic of China

Dingping Li†

Department of Physics, Peking University, 100871 Beijing, China

(Published 26 January 2010)

Thermodynamics of type II superconductors in electromagnetic field based on the Ginzburg-Landau theory is presented. The Abrikosov flux lattice solution is derived using an expansion in a parameter characterizing the "distance" to the superconductor-normal phase transition line. The expansion allows a systematic improvement of the solution. The phase diagram of the vortex matter in magnetic field is determined in detail. In the presence of significant thermal fluctuations on the mesoscopic scale (for example, in high T_c materials) the vortex crystal melts into a vortex liquid. A quantitative theory of thermal fluctuations using the lowest Landau level approximation is given. It allows one to determine the melting line and discontinuities at melt, as well as important characteristics of the vortex liquid state. In the presence of quenched disorder (pinning) the vortex matter acquires certain "glassy" properties. The irreversibility line and static properties of the vortex glass state are studied using the "replica" method. Most of the analytical methods are introduced and presented in some detail. Various quantitative and qualitative features are compared to experiments in type II superconductors, although the use of a rather universal Ginzburg-Landau theory is not restricted to superconductivity and can be applied with certain adjustments to other physical systems, for example, rotating Bose-Einstein condensate.

DOI: 10.1103/RevModPhys.82.109 PACS number(s): 74.25.Uv, 74.25.Dw, 74.40.−n

CONTENTS

*vortex@yahoo.com
†lidp@pku.edu.cn

I. INTRODUCTION

Phenomenon of superconductivity was initially defined by two basic properties of classic superconductors (which belong to type I, see below): zero resistivity and perfect diamagnetism (or Meissner effect). The phenomenon was explained by the Bose-Einstein condensation (BEC) of pairs of electrons (Cooper pairs carrying a charge $-e^*=-2e$, constant e^* considered positive throughout) below a critical temperature T_c. The transition to the superconducting state is described phenomenologically by a complex order parameter field $\Psi(\mathbf{r}) = |\Psi(\mathbf{r})|e^{i\chi(\mathbf{r})}$ with $|\Psi|^2$ proportional to the density of Cooper pairs and its phase χ describing the BEC coherence. Magnetic and transport properties of another group of materials, the type II superconductors, are more complex. An external magnetic field H and even, under certain circumstances, electric field do penetrate into a type II superconductor. The study of type II superconductor group is important for both fundamental science and applications.

A. Type II superconductors in magnetic field

1. Abrikosov vortices and some other basic concepts

Below a certain field, the first critical field H_{c1}, the type II superconductor is still a perfect diamagnet, but in fields just above H_{c1} magnetic flux does penetrate the material. It is concentrated in well-separated "vortices"

of size λ, the magnetic penetration depth, carrying one unit of flux,

$$\Phi_0 \equiv hc/e^*. \quad (1)$$

The superconductivity is destroyed in the core of a smaller width ξ called the coherence length. The type II superconductivity refers to materials in which the ratio $\kappa=\lambda/\xi$ is larger than $\kappa_c=1/\sqrt{2}$ (Abrikosov, 1957). The vortices strongly interact with each other, forming highly correlated stable configurations such as the vortex lattice; they can vibrate and move. The vortex systems in such materials became an object of experimental and theoretical study early on.

Discovery of high T_c materials focused the attention to certain particular situations and novel phenomena within the vortex matter physics. They are "strongly" type II superconductors $\kappa \sim 100 \gg \kappa_c$, and are "strongly fluctuating" due to high T_c and large anisotropy in a sense that thermal fluctuations of the vortex degrees of freedom are not negligible, as was the case in "old" superconductors. In strongly type II superconductors the lower critical field H_{c1} and the higher critical field H_{c2} at which the material becomes "normal" are well separated $H_{c2}/H_{c1} \sim \kappa^2$ leading to a typical situation $H_{c1} \ll H < H_{c2}$ in which magnetic fields associated with vortices overlap, the superposition becoming nearly homogeneous, while the order parameter characterizing superconductivity is still highly inhomogeneous. The vortex degrees of freedom dominate in many cases the thermodynamic and transport properties of the superconductors.

Thermal fluctuations significantly modify the properties of the vortex lattices and might even lead to its melting. A new state, the vortex liquid, is formed. It has distinct physical properties from both the lattice and the normal metals. In addition to interactions and thermal fluctuations, disorder (pinning) is always present, which may also distort the solid into a viscous glassy state, so the physical situation becomes quite complicated leading to rich phase diagram and dynamics in multiple time scales. A theoretical description of such systems is a subject of the present review. Two ranges of fields, $H \ll H_{c2}$ and $H \gg H_{c1}$, allow different simplifications and consequently different theoretical approaches to describe them. For large κ there is a large overlap of their applicability regions.

2. Two major approximations: The London and the homogeneous field Ginzburg-Landau models

In the fields range $H \ll H_{c2}$ vortex cores are well separated and one can employ a picture of linelike vortices interacting magnetically. In this approach one ignores the detailed core structure. The value of the order parameter is assumed to be a constant Ψ_0 with an exception of thin lines with phase winding around the lines. Magnetic field is inhomogeneous and obeys a linearized London equation. This model was developed for low T_c superconductors and subsequently elaborated to describe the high T_c materials as well. It was comprehensively described in numerous reviews and books (Blatter *et al.*, 1994; Brandt, 1995; Tinkham, 1996; Kopnin, 2001) and will not be covered here.

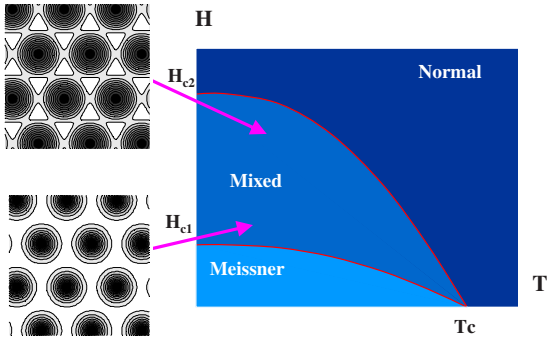

FIG. 1. (Color online) Schematic magnetic phase diagram of a type II superconductor.

The approach, however, becomes invalid as fields of order of H_{c2} are approached; since then the cores cannot be considered as linelike and profile of the depressed order parameter becomes important. The temperature dependence of the critical lines is shown in Fig. 1. The region in which the London model is inapplicable includes typical situations in high T_c materials as well as in novel "conventional" superconductors. However precisely under these circumstances different simplifications are possible. This is a subject of the present review. When distance between vortices is smaller than λ (at fields of several H_{c2}) the magnetic field becomes homogeneous due to overlaps between vortices. This means that magnetic field can be described by a number rather than by a field. This is the most important assumption of the Landau level theory of the vortex matter. One therefore can focus solely on the order parameter field $\Psi(\mathbf{r})$. In addition, in various physical situation the order parameter Ψ is greatly depressed compared to its maximal value Ψ_0 due to various "pair breaking" effects such as temperature, magnetic and electric fields, disorder, etc. For example, in an extreme case of $H \sim H_{c2}$ only small "islands" between core centers remain superconducting, yet superconductivity dominates electromagnetic properties of the material. One can rely on expansion of energy in powers of the order parameter, a method known as the Ginzburg-Landau (GL) approach, which is introduced next.

To conclude, while in the London approximation one assumes constant order parameter and operates with degrees of freedom describing the vortex lines, in the GL approach the magnetic field is constant and one operates with key notions such as Landau wave functions describing the order parameter.

B. Ginzburg-Landau model and its generalizations

An important feature of the present treatise is that we discuss a great variety of complex phenomena using a single well-defined model. The mathematical methods used are also quite similar in various parts of the review

and almost invariably range from perturbation theory to the so-called variational Gaussian approximation and its improvements. This consistency often allows us to consider a smooth limit of a more general theory to a particular case. For example, a static phenomenon is obtained as a small velocity limit of the dynamical one, the clean case is a limit of zero disorder, and the mean field is a limit of small mesoscopic thermal fluctuations. The model is motivated and defined below, while methods of solution will be the subject of the following sections. The complexity increases gradually.

1. Landau theory near T_c for a system undergoing a second order phase transition

Near a transition in which the U(1) phase symmetry, $\Psi \to e^{i\chi}\Psi$, is spontaneously broken a system is effectively described by the following Ginzburg-Landau free energy (Mazenko, 2006):

$$F[\Psi] = \int d\mathbf{r}dz \left\{ \frac{\hbar^2}{2m^*}|\nabla\Psi|^2 + \frac{\hbar^2}{2m_c^*}|\nabla\Psi|^2 + a'|\Psi|^2 + \frac{b'}{2}|\Psi|^4 \right\} + F_n. \quad (2)$$

Here $\mathbf{r}=(x,y)$ and we assumed equal effective masses in the x-y plane, $m_a^*=m_b^*\equiv m^*$, both possibly different from the one in the z direction, $m_c^*/m^*=\gamma_a^2$. This anticipates application to layered superconductors for which the anisotropy parameter γ_a can be very large. The last term F_n, the normal free energy, is independent of order parameter but might depend on temperature. The GL approach is generally an effective mesoscopic approach, in which one assumes that microscopic degrees of freedom are "integrated out." It is effective when higher powers of order parameter and gradients, neglected in Eq. (2), are indeed negligible. Typically, but not always, it happens near a second order phase transition.

All the terms in Eq. (2) are of order $(1-t)^2$, where $t \equiv T/T_c$, while one neglects (as "irrelevant") terms of order $(1-t)^3$ like $|\Psi|^6$ and quadratic terms containing higher derivatives. Generally parameters of the GL model [Eq. (2)] are functions of temperature, which can be determined by a microscopic theory or considered phenomenologically. They take into account thermal fluctuations of the microscopic degrees of freedom (integrated out in the mesoscopic description). Consistently one expands the coefficients "near," with coefficient a' vanishing at T_c as $1-t$,

$$a'(T) = T_c[\alpha(1-t) + \alpha'(1-t)^2 + \cdots],$$
$$b'(T) = b' + b''(1-t) + \cdots, \quad (3)$$
$$m^*(T) = m^* + m^{*\prime}(1-t) + \cdots.$$

The second and higher terms in each expansion are omitted since their contributions are also of order $(1-t)^3$ or higher. Therefore, when temperature deviates significantly from T_c, one cannot expect the model to provide a good precision. Minimization of the free energy [Eq. (2)], with respect to Ψ, below the transition temperature determines the value of the order parameter in a homogeneous superconducting state,

$$|\Psi|^2 = |\Psi_0|^2(1-t), \quad |\Psi_0|^2 = \alpha T_c/b'. \quad (4)$$

Substituting this into the last two terms in the square bracket in Eq. (2), one estimates them to be of order $(1-t)^2$, while one of the terms dropped, $|\Psi|^6$, is indeed of higher order. The energy of this state is lower than the energy of normal state with $\Psi=0$, namely, F_n by

$$F_0/\mathrm{vol} = -F_{\mathrm{GL}}(1-t), \quad \text{where } F_{\mathrm{GL}} = (b'/2)|\Psi_0|^4, \quad (5)$$

is the condensation energy density of the superconductor at zero temperature.

The gradient term determines the scale over which fluctuations are typically extended in space. Such a length ξ, called in the present context the coherence length, is determined by comparing the first two terms in the free energy,

$$\nabla^2\Psi \sim \xi^{-2}\Psi \propto (1-t)\Psi, \quad \xi = \hbar/\sqrt{2m^*\alpha T_c}. \quad (6)$$

So typically gradients are of order $(1-t)^{1/2}$, and the first term in the free energy [Eq. (2)] is therefore also of the order $(1-t)^2$. Since the order parameter field describing the Bose-Einstein condensate of Cooper pair is charged, minimal coupling principle generally provides an unambiguous procedure to include effects of electromagnetic fields.

2. Minimal coupling to magnetic field

Generalization to the case of magnetic field is a straightforward use of the local gauge invariance principle (or the minimal substitution) of electromagnetism. The free energy becomes

$$F[\Psi,\mathbf{A}] = \int d\mathbf{r}dz \left[\frac{\hbar^2}{2m^*}|\mathbf{D}\Psi|^2 + \frac{\hbar^2}{2m_c^*}|D_z\Psi|^2 + a'|\Psi|^2 + \frac{b'}{2}|\Psi|^4 \right] + G_n[\mathbf{A}], \quad (7)$$

while the Gibbs energy is

$$G[\Psi,\mathbf{A}] = F[\Psi] + \int \frac{(\mathbf{B}-\mathbf{H})^2}{8\pi}. \quad (8)$$

Here $\mathbf{B}=\nabla\times\mathbf{A}$ and we assume that "external" magnetic field (considered homogeneous, see above) is oriented along the positive z axis, $\mathbf{H}=(0,0,H)$. The covariant derivatives are defined by

$$\mathbf{D} \equiv \nabla + i(2\pi/\Phi_0)\mathbf{A}. \quad (9)$$

The "normal electron" contribution $G_n[\mathbf{A}]$ is a part of free energy independent of the order parameter but can, in principle, depend on external parameters such as temperature and fields. Minimization with respect to Ψ and $\mathbf{A}$ leads to a set of static GL equations, the nonlinear Schrödinger equation,

$$\frac{\delta}{\delta\psi^*}G = -\frac{\hbar^2}{2m^*}\mathbf{D}^2\Psi - \frac{\hbar^2}{2m_c^*}D_z^2\Psi + a'\Psi + b'|\Psi|^2\Psi = 0, \tag{10}$$

and the supercurrent equation,

$$c\frac{\delta}{\delta\mathbf{A}}G = \frac{c}{4\pi}\nabla \times \mathbf{B} - \mathbf{J}_s - \mathbf{J}_n = 0, \tag{11}$$

where the supercurrent and the normal current are given by

$$\begin{aligned}\mathbf{J}_s &= \frac{ie^*\hbar}{2m^*}(\Psi^*\mathbf{D}\Psi - \Psi\mathbf{D}\Psi^*)\\ &= \frac{ie^*\hbar}{2m^*}(\Psi^*\nabla\Psi - \Psi\nabla\Psi^*) - \frac{e^{*2}}{cm^*}\mathbf{A}|\Psi|^2,\\ \mathbf{J}_n &= -\frac{\delta}{\delta\mathbf{A}}G_n[\mathbf{A}].\end{aligned} \tag{12}$$

$\mathbf{J}_n$ can be typically represented by the Ohmic conductivity $\mathbf{J}_n = \sigma_n\mathbf{E}$ and vanishes if the electric field is absent.

Comparing the second derivative with respect to $\mathbf{A}$ term in Eq. (11) with the last term in the supercurrent equation [Eq. (12)], one determines the scale of typical variations of the magnetic field inside superconductor, the magnetic penetration depth,

$$\nabla^2\mathbf{A} \sim \lambda^{-2}(1-t)\mathbf{A} \sim \frac{4\pi e^{*2}}{c^2m^*}\mathbf{A}(1-t)|\Psi_0|^2. \tag{13}$$

This leads to

$$\lambda = \frac{c}{2e^*}\sqrt{\frac{mb'}{\pi\alpha T_c}}. \tag{14}$$

The two scales' ratio defines the GL parameter $\kappa \equiv \lambda/\xi$. The second equation shows that supercurrent in turn is small since it is proportional to $|\Psi|^2 < \Psi_0^2$. Therefore magnetization is much smaller than the field since it is proportional both to the supercurrent creating it and to $1/\kappa^2$. Since magnetization is so small, especially in strongly type II superconductors, inside superconductor $B \approx H$ and consistently disregard the "supercurrent" equation [Eq. (11)]. Therefore the following vector potential,

$$\mathbf{A} = (-By, 0, 0) \simeq (-Hy, 0, 0), \tag{15}$$

(Landau gauge) will be use throughout. The validity of this significant simplification can be then checked *a posteriori.*

The upper critical field will be related in Sec. II to the coherence length [Eq. (6)] by

$$H_{c2} = \Phi_0/2\pi\xi^2. \tag{16}$$

The energy density difference between the superconductor and the normal states F_{GL} in Eq. (2) can therefore be reexpressed as

$$F_{\mathrm{GL}} = H_{c2}^2/16\pi\kappa^2. \tag{17}$$

3. Thermal fluctuations

Thermal fluctuations on the microscopic scale have already been taken into account by the temperature dependence of the coefficients of the GL free energy. However, in high T_c superconductors temperature can be high enough, so that one cannot neglect additional thermal fluctuations which occur on the mesoscopic scale. These fluctuations can be described by a statistical sum,

$$Z = \int \mathcal{D}\Psi(\mathbf{r})\mathcal{D}\Psi^*(\mathbf{r})\exp\left\{-\frac{F[\Psi^*,\Psi]}{T}\right\}, \tag{18}$$

where a functional integral is taken over all configurations of the order parameter. In principle thermal fluctuations of magnetic field should also be considered, but it turns out that they are unimportant even in high T_c materials (Halperin *et al.*, 1974; Dasgupta and Halperin, 1981; Lobb, 1987; Herbut and Tešanović, 1996; Herbut, 2007).

The Ginzburg parameter, the square of the ratio of T_c to the superconductor energy density times correlation volume,

$$\mathrm{Gi} = 2(T_c/16\pi F_{\mathrm{GL}}\xi^2\xi_c)^2 = 2(4\pi^2T_c\kappa^2\xi\gamma_a/\Phi_0^2)^2, \tag{19}$$

generally characterizes the strength of the thermal fluctuations on the mesoscopic scale (Levanyuk, 1959; Ginzburg, 1960; Larkin and Varlamov, 2005), where $\Phi_0 \equiv hc/e^*$. The definition of Gi is the standard one as in Blatter *et al.* (1994), contrary to the previous definition used early in our papers, for example, in Li and Rosenstein (2002a, 2003). Here $\xi_c = \gamma_a^{-1}\xi$ is the coherence length in the field direction. The Ginzburg parameter is significantly larger in high T_c superconductors compared to the low temperature one. While for metals this dimensionless number is very small (of order 10^{-6} or smaller), it becomes significant for relatively isotropic high T_c cuprates such as $YBa_2Cu_3O_{7-\delta}$ (YBCO) (10^{-4}) and even large for very anisotropic cuprate $Bi_2Sr_2CaCu_2O_{8+\delta}$ (BSCCO) (up to Gi=0.1–0.5). The physical reasons behind the enhancement are the small coherence length, high T_c, and, in the case of BSCCO, large anisotropy, $\gamma_a \sim 150$. Therefore the thermal fluctuations play a much larger role in these new materials. In the presence of magnetic field the importance of fluctuations is further enhanced. Strong magnetic field effectively suppresses long wavelength fluctuations in the direction perpendicular to the field reducing dimensionality of the fluctuations by two. Under these circumstances fluctuations influence various physical properties and even lead to new observable qualitative phenomena such as the vortex lattice melting into a vortex liquid far below the mean field phase transition line.

Several remarkable experiments determined that the vortex lattice melting in high T_c superconductors is first order with magnetization jumps (Zeldov *et al.*, 1995; Willemin *et al.*, 1998; Nishizaki *et al.*, 2000; Beidenkopf *et al.*, 2005, 2007) and spikes in specific heat (it was found that in addition to the spike there is also a jump in spe-

cific heat which was measured as well) (Schilling *et al.*, 1996, 1997; Nishizaki *et al.*, 2000; Bouquet *et al.*, 2001; Lortz *et al.*, 2006, 2007). These and other measurements such as the resistivity and shear modulus point toward a need to develop a quantitative theoretical description of thermal fluctuations in vortex matter (Pastoriza *et al.*, 1994; Liang *et al.*, 1996; Matl *et al.*, 2002; Okazaki *et al.*, 2008). To tackle the difficult problem of melting, the description of both the solid and the liquid phases should reach the precision level below 1% since the internal energy difference between the phases near the transition temperature is quite small.

4. Quenched disorder

In any superconductor there are impurities either present naturally or systematically produced using the proton or electron irradiation. The inhomogeneities on both the microscopic and the mesoscopic scales greatly affect thermodynamic and especially dynamic properties of type II superconductors in magnetic field. Abrikosov vortices are pinned by disorder. As a result of pinning the flux flow may be stopped and the material restores the property of zero resistivity (at least at zero temperature, otherwise thermal fluctuations might depin the vortices) and make various quantities such as magnetization become irreversible. Disorder on the mesoscopic scale can be modeled in the framework of the Ginzburg-Landau approach adding a random component to its coefficients (Larkin, 1970). The random component of the coefficient of the quadratic term $W(r)$ is called δT disorder since it can be interpreted as a local deviation of the critical temperature from T_c. The simplest such a model is the (white noise) with local variance,

$$a' \to a'[1 + W(r)], \quad \overline{W(r)W(r')} = n\xi^2\xi_c\delta(r - r'). \quad (20)$$

A dimensionless disorder strength n, normalized to the coherence volume, is proportional to the density of the short range point like pinning centers and average "strength" of the center. The disorder average of a static physical quantity A, denoted by $\bar{A}$ in this case, is a Gaussian measure,

$$\bar{A} = N\int \mathcal{D}W A[W]\exp\left(-\frac{1}{2n\xi^2\xi_c}\int_r W(r)^2\right),$$
$$N^{-1} \equiv \int \mathcal{D}W \exp\left(-\frac{1}{2n\xi^2\xi_c}\int_r W(r)^2\right). \quad (21)$$

The averaging process and its limitations are the subject of Sec. IV, where the replica formalism is introduced and used to describe the transition to the glassy (pinned) states of the vortex matter. They are characterized by irreversibility of various processes. The quenched disorder greatly affects the dynamics. Disordered vortex matter is depinned at certain "critical current" J_c and the flux flow ensues. Close to J_c the flow proceeds slowly via propagation of defects (elastic flow) before becoming a fast plastic flow at larger currents. The I-V curves of the disordered vortex matter therefore are nonlinear. Disorder creates a variety of "glassy" properties involving slow relaxation, memory effects, etc. Thermal fluctuations in turn also greatly influence phenomena caused by disorder in both statics and dynamics. The basic effect is the thermal depinning of single vortices or domains of the vortex matter. The inter-relations between the interactions, disorder, and thermal fluctuations are, however, very complex. The same thermal fluctuations can soften the vortex lattice and actually can also cause better pinning near peak effect region. Critical current might have a "peak" near the vortex lattice melting.

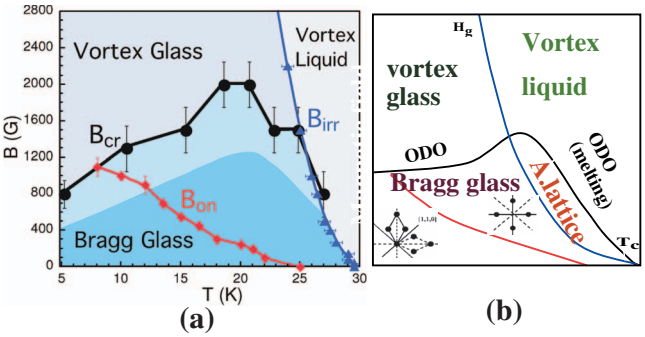

FIG. 2. (Color) Magnetic phase diagram of high T_c. (a) Experimentally determined phase diagram of LaSCO. From Divakar *et al.*, 2004. (b) Theoretical phase diagram advocated in this article.

C. Complexity of the vortex matter physics

In the previous section we encountered several major complications pertinent to the vortex physics: interactions, dynamics, thermal fluctuations, and disorder. These lead to a multitude of various "phases" or states of the vortex matter. It resembles the complexity of (atomic) condensed matter, but, as we learn along the way, there are some profound differences. For example, there is no transition between liquid and gas and therefore no critical point. A typical magnetic (T-B) phase diagram advocated here (Li, Rosenstein, and Vinokur, 2006) is shown in Fig. 2(b). It resembles for example, an experimental phase diagram of high T_c superconductor (Sasagawa *et al.*, 2000; Divakar *et al.*, 2004), LaSCO [Fig. 2(a)]. Here we mention various phases and transitions between them and direct the interested reader to the relevant section in which the theory can be found. We start the tour from the low T and B corner of the phase diagram in which, as discussed above, vortices form a stable Abrikosov lattice. Vortex solid might have several crystalline structures very much like an ordinary atomic solid. In the particular case shown at lower fields the lattice is rhombic, while at elevated fields it undergoes a structural transformation into a square lattice (red line in Fig. 2). These transitions are discussed in Sec. II. Thermal fluctuations can melt the lattice into a liquid (the "melting" segment of the black line) (Sec. III), while disorder can turn both a crystal and a homogeneous liquid into a glassy state, Bragg glass and vortex glass, respectively (Sec. IV). The corresponding continuous tran-

sition line (blue line in Fig. 2) is often called an irreversibility line since glassiness strongly affects transport properties leading to irreversibility and memory effects.

To summarize we have several transition lines:

(1) The first order (Zeldov *et al.*, 1995; Schilling *et al.*, 1996, 1997; Bouquet *et al.*, 2001) melting line due to thermal fluctuations was shown to merge with the "second magnetization peak" line due to pinning forming the universal order-disorder phase transition line (Fuchs *et al.*, 1998; Radzyner *et al.*, 2002). At low temperatures the location of this line strongly depends on disorder and generally exhibits a positive slope [termed also the "inverse" melting (Paltiel, Zeldov, Myasoedov, Rappaport, *et al.*, 2000; Paltiel, Zeldov, Myasoedov, Shtrikman, *et al.* 2000), while in the melting section it is dominated by thermal fluctuations and has a large negative slope. The resulting maximum at which the magnetization and the entropy jump vanish is a Kauzmann point (Li and Rosenstein, 2003). This universal "order-disorder" transition (ODT) line, which appeared first in the strongly layered superconductors [BSCCO (Fuchs *et al.*, 1998)], was extended to the moderately anisotropic superconductors [$La_{2-x}Sr_xCuO_4$ (LaSCO) (Radzyner *et al.*, 2002)] and to the more isotropic ones such as YBCO (Pal *et al.*, 2001, 2002; Li and Rosenstein, 2003). The symmetry characterization of the transition is clear: spontaneous breaking of both the continuous translation and the rotation symmetries down to a discrete symmetry group of the lattice.

(2) The "irreversibility line" or the "glass" transition (GT) line is a continuous transition (Deligiannis *et al.*, 2000; Taylor *et al.*, 2003; Taylor and Maple, 2007; Senatore *et al.*, 2008). The almost vertical in the T-B plane glass line clearly represents effects of disorder although the thermal fluctuations affect the location of the transition due to thermal depinning. Experiments in BSCCO (Fuchs *et al.*, 1998; Beidenkopf *et al.*, 2005, 2007) indicate that the line crosses the ODT line right at its maximum and continues deep into the ordered (Bragg) phase. This proximity of the glass line to the Kauzmann point is reasonable since it signal both the region of close competition of the disorder and the thermal fluctuation effects. In more isotropic materials the data are more confusing. In LaSCO (Sasagawa *et al.*, 2000; Divakar *et al.*, 2004) the GT line is closer to the melting section of the ODT line still crossing it. It is more difficult to characterize the nature of the GT transition as a "symmetry breaking." The common wisdom is that "replica" symmetry is broken in the glass (either via "steps" or via "hierarchical" continuous process) as in most of the spin glass theories (Fischer and Hertz, 1991; Dotsenko, 2001). The dynamics in this phase exhibits zero resistivity (neglecting exponentially small creep) and various irreversible features due to multitude of metastable states. Critical current at which the vortex matter starts moving is nonzero. It is different in the crystalline and homogeneous pinned phases.

(3) Sometimes there are one or more structural transitions in the lattice phase (Keimer *et al.*, 1994; McK. Paul *et al.*, 1998; Johnson *et al.*, 1999; Sasagawa *et al.*, 2000; Eskildsen *et al.*, 2001; Gilardi *et al.*, 2002; Divakar *et al.*, 2004; Jaiswal-Nagar *et al.*, 2006; Li, Lin, *et al.*, 2006). They might be either first or second order and also lead to a peak in the critical current (Chang *et al.*, 1998a, 1998b; Park and Huse, 1998; Rosenstein, 1999; Klironomos and Dorsey, 2003; Rosenstein *et al.*, 2005).

D. Guide for a reader

1. Notations and units

Throughout the article we use two different systems of units. In sections not dealing with thermal fluctuations, namely, in Secs. II and IV.A we use units which do not depend on "external" parameters T and H, just on material parameters and universal constants (for example, the unit of length is the coherence length ξ). More complicated parts of the review involving thermal fluctuations utilize units dependent on T and H. For example, the unit of length in directions perpendicular to the field direction becomes magnetic length $l=\xi\sqrt{H_{c2}/B}$. However, throughout the review basic equations and important results, which might be used for comparison with experiments and other theories, are also stated in regular physical units.

a. The mean field units and definitions of dimensionless parameters

The Ginzburg-Landau free energy [Eq. (2)] contains three material parameters m^*, m_c^* (in the a-b directions perpendicular to the field and in the field direction, respectively), and αT_c, b'. If in addition the δT_c disorder, introduced in Eq. (20), is present, it is described by the disorder strength n. These material parameters are usually expressed via physically more accessible lengths and time units ξ, ξ_c, λ,

$$\xi_c = \hbar/\sqrt{2m_c^*\alpha T_c}. \tag{22}$$

Despite the fact that one often uses temperature dependent coherence length and penetration depth, which as seen in Eqs. (6) and (13) might be considered as divergent near T_c, we prefer to write factors of $1-t$ explicitly.

From the above scales one can form the following dimensionless material parameters: Gi,

$$\kappa = \lambda/\xi, \quad \gamma_a^2 = m_c^*/m^*. \tag{23}$$

From the scales one can form units of magnetic and electric fields, current density, and conductivity,

$$H_{c2} = \Phi_0/2\pi\xi^2, \tag{24}$$

as well as energy density $F_{\rm GL}$. These can be used to define dimensionless parameters, temperature T, and magnetic and electric fields H, E,

$$t = T/T_c, \quad b = B/H_{c2}, \quad h = H/H_{c2}, \tag{25}$$

from which other convenient dimensionless quantity describing the proximity to the mean field transition line is formed,

$$a_H = (1 - t - b)/2. \tag{26}$$

The unit of the order parameter field (or square root of the Cooper pair density) is determined by the mean field value $|\Psi_0|^2 = \alpha T_c/b'$,

$$\bar{\Psi} = \Psi/\sqrt{2}|\Psi_0| = (b'/2\alpha T_c)^{1/2}\Psi, \tag{27}$$

and the Boltzmann factor and the disorder correlation in the physics units (length is in unit of ξ in x-y plane and in unit of ξ_c along c axis and order parameter in unit as defined by the equation above) are

$$\frac{F[\Psi^*,\Psi]}{T} = \frac{1}{\omega_t}\int d^3x\left\{\frac{1}{2}|D\psi|^2 + \frac{1}{2}|\partial_z\psi|^2 - \frac{1-t}{2}[1 + W(r)]|\psi|^2 + \frac{1}{2}|\psi|^4\right\},$$

$$\frac{G[\Psi,\mathbf{A}]}{T} = \frac{F[\Psi^*,\Psi]}{T} + \frac{1}{\omega_t}\int d^3x\frac{(\mathbf{b}-\mathbf{h})^2}{4},$$

$$\overline{W(r)W(r')} = n\delta(r-r') \quad \omega_t = \sqrt{2\mathrm{Gi}}\pi t.$$

b. The LLL scaled units

When dealing with thermal fluctuations, the following units depend on parameters T, H, and E. The unit of length in directions perpendicular to the field can be conveniently chosen to be the magnetic length,

$$l = \xi\sqrt{H_{c2}/B}, \tag{28}$$

in the field direction, while in the field direction it is different,

$$\xi_c(\sqrt{\mathrm{Gi}}tb/4)^{-1/3}. \tag{29}$$

Motivation for these fractional powers of both temperature and magnetic field will become clear in Sec. III. We rescale the order parameter to ψ by an additional factor,

$$\Psi = \Psi_0(\sqrt{\mathrm{Gi}}tb/4)^{1/3}\psi. \tag{30}$$

Instead of a_H or $a_{H,E}$ it will be useful to use "Thouless LLL scaled temperature" (Thouless, 1975; Ruggeri and Thouless, 1976; Ruggeri, 1978),

$$a_T = -\frac{a_H}{(\sqrt{\mathrm{Gi}}tb/4)^{2/3}} = -\frac{1-t-b}{2(\sqrt{\mathrm{Gi}}tb/4)^{2/3}}. \tag{31}$$

The scaled energy is defined by

$$\mathcal{F} = \frac{H_{c2}^2}{2\pi\kappa^2}\left(\frac{\sqrt{\mathrm{Gi}}tb}{4}\right)^{4/3} f(a_T) \tag{32}$$

and magnetization by

$$\frac{M}{H_{c2}} = \frac{1}{4\pi\kappa^2}\left(\frac{\sqrt{\mathrm{Gi}}tb}{4}\right)^{2/3} m(a_T), \qquad m(a_T) = -\frac{d}{da_T}f(a_T). \tag{33}$$

The disorder is characterized by the ration of the strength of pinning to that of thermal fluctuations

$$r = \frac{(1-t)^2}{\pi\mathrm{Gi}^{1/2}t}n. \tag{34}$$

2. Analytical methods described in this article

Discussion of properties of the GL model in magnetic fields utilizes a number of general and special theoretical techniques. We chose to describe some of them in detail, while others are mentioned in the last section. We do not describe numerous results obtained using the elasticity theory or numerical methods such as Monte Carlo and molecular dynamics simulations, although comparison with both is made when possible.

The techniques and special topics include the following:

(1) Translation symmetries in gauge theories (electromagnetic translations) in Sec. II.A. In their representations, the quasimomentum basis (Sec. III.B) is used throughout to discuss excitations of vortex matter either thermal or elastic.

(2) Perturbation theory around a bifurcation point of a nonlinear differential equations containing partial derivatives. This is very different from the perturbation theory used in linear systems, for example, in quantum mechanics

(3) Variational Gaussian approximation to field theory (Kleinert, 1990) is widely used in Secs. III and IV. It is defined in Sec. III.C in the path integral form and subsequently shown to be the leading order of a convergent series of approximants, the so-called optimized perturbation series (OPS). The next to leading order, the post-Gaussian approximation, which is related to the Cornwall-Jackiw-Tomboulis method, is sometimes used, while higher approximants are difficult to calculate and are obtained to date for the vortex liquid only.

(4) Ordinary perturbation theory in field theory is developed in the beginning of every section with enough details to follow. Spatial attention is paid to infrared (IR) and sometimes ultraviolet divergencies. We generally do not use the renormalization group (RG) resummation, except in Sec. III.D, where it is presented in a form of Borel-Pade approximants.

(5) The replica method to treat quenched disorder is introduced in Sec. IV.B and used to describe the static and thermodynamic properties of pinned vortex matter. Most of the presentation is devoted to the replica symmetric case, while more general hierarchial matrices are introduced in Sec. IV.D following Parisi's approach (Parisi, 1980; Mezard, 1991).

Some technical details are contained in Appendixes A and B. We compare with available experiments on type II superconductors in magnetic field, while application or adaptation of the results to other fields in which the model can be useful is not attempted.

3. Results

All important results (in both regular physical units and the special units described above) are provided in a form of MATHEMATICA file, which can be found on our website.

II. MEAN FIELD THEORY OF THE ABRIKOSOV LATTICE

In this section we construct, following Abrikosov original ideas (Abrikosov, 1957), a vortex lattice solution of the static GL equations [Eq. (10)] near the $H_{c2}(T)$ line. In a region of the magnetic phase diagram in which the order parameter is significantly reduced from its maximal value Ψ_0 [Eq. (4)], one does not really see well-separated "vortices" since, as explained in the previous section, their magnetic fields strongly overlap. Very close to $H_{c2}(T)$ even cores approach each other and consequently the order parameter is greatly reduced. Only small islands between the core centers remain superconducting. Despite this superconductivity dominates electromagnetic, transport, and sometimes thermodynamic properties of the material. One still has a well-defined "centers" of cores: zeros of the order parameter. They still repel each other and thereby organize themselves into an ordered periodic lattice.

To see this we first employ a heuristic Abrikosov's argument based on linearization of the GL equations and then develop a systematic perturbative scheme with a small parameter—the "distance" from the $H_{c2}(T)$ line on the T-H plane. The heuristic argument naturally leads to the lowest Landau level (LLL) approximation, widely used later to describe various properties of the vortex matter. The systematic expansion allows us to ascertain how close one should stay from the H_{c2} line in order to use the LLL approximation. Having established the lattice solution, spectrum of excitations around it (the flux waves or phonon) is obtained in the next section. This in turn determines elastic, thermal, and transport properties of vortex matter.

A. Solution of the static GL equations: Heuristic solution near H_{c2}

1. Symmetries, units, and expansion in κ^{-2}

a. Broken and unbroken symmetries

Generally, before developing mathematical tools to analyze a complicated model described by free energy [Eq. (2)] and its generalizations, it is important to make full use of various symmetries of the problem. The free energy (including the external magnetic field) is invariant under both the three-dimensional translations and rotations in the x-y (a-b) plane. However, some of the symmetries in the x-y plane are broken spontaneously below the $H_{c2}(T)$ line. The symmetry which remains unbroken is the continuous translation along the magnetic field direction z. As a result the configuration of the order parameter is homogeneous in the z direction, $\Psi(\mathbf{r},z)=\Psi(\mathbf{r})$, $\mathbf{r}\equiv(x,y)$. Hence the gradient term can be disregarded and the problem becomes two dimensions (here we consider the mean field equations only; when thermal fluctuations or pointlike disorder is present the simplification is no longer valid).

b. Units, free energy, and GL equations

To describe the physics near $H_{c2}(T)$, it is reasonable to use the coherence length $\xi=\hbar/\sqrt{2m^*\alpha T_c}$ as a unit of length (assuming for simplicity $m_a^*=m_b^*\equiv m^*$) and the value of the field Ψ_0 at which the "potential" part is minimal [Eq. (4)] (times $\sqrt{2}$) will be used as a scale of the order parameter field,

$$\bar{x}=x/\xi, \quad \bar{y}=y/\xi, \quad \bar{\Psi}=(b'/2\alpha T_c)^{1/2}\Psi, \tag{35}$$

while the (zero temperature energy) density difference between the normal and the superconductor states F_{GL} of Eq. (17) determines a unit of energy density. Therefore dimensionless two-dimensional (2D) energy $\bar{F}\equiv F/8L_z\xi^2F_{\mathrm{GL}}$, where L_z is the sample's size in the field direction, and Eq. (8) takes a form

$$\bar{F}=\int d\bar{x}d\bar{y}\left[\bar{\Psi}^*\hat{H}\bar{\Psi}-a_H|\bar{\Psi}|^2+\frac{1}{2}|\bar{\Psi}|^4+\frac{\kappa^2(\mathbf{b}-\mathbf{h})^2}{4}\right]. \tag{36}$$

Dimensionless temperature and magnetic fields are $t\equiv T/T_c$, $b\equiv B/H_{c2}$, $h\equiv H/H_{c2}$, and $\kappa\equiv\lambda/\xi$. The units of temperature and magnetic field are therefore T_c and $H_{c2}\equiv\Phi_0/2\pi\xi^2$.

The linear operator $\hat{H}$ is defined as

$$\hat{H}=-\tfrac{1}{2}(D_x^2+\partial_y^2+b). \tag{37}$$

It coincides with the quantum mechanical operator of a charged particle in a constant magnetic field. The covariant derivative (with all the bars omitted from now on) is $D_x=\partial_x-iby$ and the constant is defined as

$$a_H = (1 - t - b)/2. \tag{38}$$

The constant is positive in the superconducting phase and vanishes on the $H_{c2}(T)$ line, as shown in the next section. The reason why $\hat{H}$ is "shifted" by a constant $-b/2$ compared to a standard Hamiltonian of a particle in magnetic field will become clear there. In rescaled units the GL equation takes a form

$$\hat{H}\bar{\Psi} - a_H\bar{\Psi} + |\bar{\Psi}|^2\bar{\Psi} = 0. \tag{39}$$

The equation for magnetic field takes a form

$$\kappa^2\varepsilon_{ij}\partial_j b = \frac{i}{2}\bar{\Psi}^* D_i\bar{\Psi} + \text{c.c.} \tag{40}$$

with boundary condition involving the external field h.

c. Expansion in powers of κ^{-2}

In physically important cases one encounters strongly type II superconductors for which $\kappa \gg 1$. For example, all high T_c cuprates have κ of order 100, and even low T_c superconductors which are useful in applications have κ of order 10. In such cases it is reasonable to expand the second equation in powers of κ^{-2},

$$b = h + \kappa^{-2}b^{(1)} + \cdots,$$
$$\bar{\Psi} = \bar{\Psi}^{(0)} + \kappa^{-2}\bar{\Psi}^{(1)} + \cdots. \tag{41}$$

It can be seen from Eqs. (39) and (40) that to leading order in κ^{-2} magnetic field b is equal to the external field h considered constant. Therefore one can ignore Eq. (40) and use external field in the first equation. Corrections will be calculated consistently. For example, magnetization will appear in the next to leading order.

From now on we drop bars over Ψ and consider the leading order in κ^{-2}. Even this nonlinear differential equation is still quite complicated. It has an obvious normal metal solution $\Psi = 0$ but might have also a nontrivial one. A simplistic way to find the nontrivial one is to linearize the equation. Indeed naively the nonlinear term contains the "small" fields Ψ compared to one in the linear term. This assumption is problematic since, for example, the coefficient of the Ψ term is also small, but this will follow this reasoning, nevertheless leaving a rigorous justification to Sec. II.B.

2. Linearization of the GL equations near H_{c2}

Naively dropping the nonlinear term in Eq. (39), one is left with the usual linear Schrödinger eigenvalue equation of quantum mechanics for a charged particle in the homogeneous magnetic field,

$$\hat{H}\Psi = a_H\Psi. \tag{42}$$

The Landau gauge that we use, defined in Eq. (15), still maintains a manifest translation symmetry along the x direction, while the y translation invariance is "masked" by this choice of gauge. Therefore one can disentangle the variables,

$$\Psi(x,y) = e^{ik_x x} f(y), \tag{43}$$

resulting in the shifted harmonic oscillator equation,

$$\left[-\frac{1}{2}\partial_y^2 + \frac{b^2}{2}(y - Y)^2\right] f = \frac{1 - t}{2} f, \tag{44}$$

where $Y \equiv k_x/b$ is the y coordinate of the center of the classical Larmor orbital. For a finite sample k_x is discretized in units of $2\pi\xi/L_x$, while the Larmor orbital center is confined inside the sample, $-L_y/2 < Y\xi < L_y/2$, leading to $BL_xL_y/\Phi_0 \equiv N_L$ values of k_x.

Nontrivial $f(y) \neq 0$ solutions of the *linearized* equation exist only for special values of magnetic field since the operator $\hat{H}$ has a discrete spectrum

$$E_N = Nb \tag{45}$$

for any Y (the Landau levels are therefore N_L times degenerate). These fields b_N satisfy

$$\frac{1 - t}{2} = \left(N + \frac{1}{2}\right) b_N, \tag{46}$$

and the eigenfunctions are

$$\phi_{Nk_x}(\mathbf{r}) = \pi^{-1/4}\sqrt{\frac{b}{2^N N!}} H_N[b^{1/2}(y - k_x/b)] \times e^{ik_x x - (b/2)(y - k_x/b)^2}, \tag{47}$$

where $H_N(x)$ are Hermite polynomials. As we will see shortly, the *nonlinear* GL equation [Eq. (39)] acquires a nontrivial solution also at fields different from b_N. The solution with $N = 0$ (the lowest Landau level or LLL, corresponding to the highest $b_N = 1$) appears at the bifurcation point

$$1 - t - b_0(t) = 0 \tag{48}$$

or $a_H = 0$. It defines the $H_{c2}(T) = H_{c2}(1 - T/T_c)$ line.

For yet higher fields the only solution of nonlinear GL equations is the trivial one: $\Psi = 0$. This is seen as follows. The operator $\hat{H}$ is positive definite, as its spectrum [Eq. (45)] demonstrates. Therefore for $a_H < 0$ all three terms in the free energy [Eq. (36)] are non-negative and in this case the minimum is indeed achieved by $\Psi = 0$. For $a_H > 0$ the minimum of the nonlinear equations should not be very different from a solution of the linearized equation at $B = H_{c2}(T)$.

Since the LLL, $B = H_{c2}(T)$, solutions

$$\phi_{k_x}(\mathbf{r}) = (b^{1/2}/\pi^{1/4}) e^{ik_x x - (b/2)(y - k_x/b)^2} \tag{49}$$

are degenerate, it is reasonable to try the most general LLL function,

$$\Psi(\mathbf{r}) = \sum_{k_x} C_{k_x}\phi_{k_x}(\mathbf{r}), \tag{50}$$

as an approximation for a solution of the nonlinear GL equation just below $H_{c2}(T)$. However how should one chose the correct linear combination? Perhaps the one with the lowest nonlinear energy: the quartic term in energy [Eq. (36)] will lift the degeneracy. Unfortunately

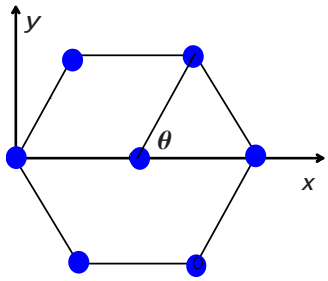

FIG. 3. (Color online) Symmetry of the vortex lattice. Unit cell.

the number of the variational parameters in Eq. (50) is clearly unmanageable. To narrow possible choices of the coefficients, one has to utilize all the symmetries of the lattice solution. Therefore we digress to discuss symmetries in the presence of magnetic field, the magnetic translations, returning later to the Abrikosov solution equipped with minimal group theoretical tools.

3. Digression: Translation symmetries in gauge theories

a. Translation symmetries in gauge theories

Consider a solution of the GL equations invariant under two arbitrary translation vectors. Without loss of generality one of them $\mathbf{d}_1$ can be aligned with the x axis. Its length will be denoted by d. The second is determined by two parameters,

$$\mathbf{d}_1 = d(1,0), \quad \mathbf{d}_2 = d(\rho,\rho'). \tag{51}$$

We consider only rhombic lattices (sufficient for most applications), which are obtained for $\rho=1/2$. The angle θ between $\mathbf{d}_1$ and $\mathbf{d}_2$ is shown in Fig. 3. Flux quantization (assuming one unit of flux per unit cell) will be

$$d^2\rho' b = 2\pi, \quad \rho' = \tfrac{1}{2}\tan\theta. \tag{52}$$

Generally an arbitrary translation in the x direction in the particular gauge that we have chosen [Eq. (15)] is very simple,

$$T_{\mathbf{d}_1}\Psi(x,y) = \Psi(x+d,y) = e^{i\hat{p}_x d}\Psi(x,y), \tag{53}$$

where $\hat{\mathbf{p}} \equiv -i\nabla$ is the "momentum" operator. Periodicity of the order parameter in the x direction with lattice constant d (in units of ξ as usual) means that the wave vector k_x in Eq. (49) is quantized in units of $2\pi/d$, $k_x = (2\pi/d)n$, $n=0,\pm1,\pm2,\ldots$, and the variational problem of Eq. (50) simplifies considerably,

$$\Psi(\mathbf{r}) = \sum_n C_n \phi_n(\mathbf{r}),$$
$$\phi_n(\mathbf{r}) = \pi^{-1/4} b^{1/2} e^{i(2\pi/d)nx-(b/2)[y-(2\pi/d)(1/b)n]^2}. \tag{54}$$

Periodicity with lattice vector $\mathbf{d}_2$ is only possible only when absolute values of coefficients $|C_n|$ are the same and, in addition, their phases are periodic in n.

b. Hexagonal lattice

In this case the basic lattice vectors are $\mathbf{d}_1 = d_\Delta(1,0)$, $\mathbf{d}_2 = d_\Delta(1/2,\sqrt{3}/2)$ (see Fig. 3), $\theta=60°$. As a next simplest guess to construct a lattice configuration out of Landau harmonics one can try a two parameter ansatz $C_{n+2} = C_n$,

$$\Psi(x,y) = C_0 \sum_{n\ \text{even}} \pi^{-1/4} b^{-1/2} e^{i(2\pi/d_\Delta)nx-(b/2)[y-(2\pi/d_\Delta)(1/b)n]^2} + C_1 \sum_{n\ \text{odd}} \pi^{-1/4} b^{-1/2} e^{i(2\pi/d_\Delta)nx-(b/2)[y-(2\pi/d_\Delta)(1/b)n]^2}. \tag{55}$$

For the hexagonal (also called sometimes triangular) flux line lattice (FLL) $C_1 = iC_0 = iC$. Geometry and the flux quantization give us now $\xi^2 d_\Delta^2 = 2\Phi_0/\sqrt{3}B$, which becomes (in rescaled units of ξ)

$$d_\Delta^2 = \frac{2\pi}{b}\frac{2}{\sqrt{3}}. \tag{56}$$

We are therefore left again with just one variational parameter,

$$\varphi_\Delta(x,y) = \frac{C}{b^{1/2}\pi^{1/4}}\left\{\sum_{n\ \text{odd}} e^{i(2\pi/d_\Delta)nx-(b/2)[y-(\sqrt{3}d_\Delta/2)n]^2} + i\sum_{n\ \text{even}} e^{i(2\pi/d_\Delta)nx-(b/2)[y-(\sqrt{3}d_\Delta/2)n]^2}\right\}. \tag{57}$$

Naive nonmagnetic translation in the "diagonal" direction (see Fig. 3) now gives

$$\varphi_\Delta(x+d_\Delta/2, y+\sqrt{3}d_\Delta/2) = ie^{i(2\pi/d_\Delta)x}\varphi_\Delta(x,y). \tag{58}$$

This is again a "regauging," which generally accompanies a symmetry transformation. The "magnetic translation" now will be

$$T_{\mathbf{d}_2} = e^{-i[(2\pi/d_\Delta)x+\pi/2]}e^{i[(d_\Delta/2)p_x+(\sqrt{3}d_\Delta/2)p_y]}. \tag{59}$$

The normalization is

$$\frac{1}{\text{vol}}\int_{\text{cell}} |\varphi(x,y)|^2 = 1, \tag{60}$$

which gives $|c|^2 = 3^{1/4}\pi^{1/2}b$. Combining the even and the odd parts, the normalized function can also be written in a form

$$\varphi_\Delta(\mathbf{r}) = \varphi(b^{1/2}\mathbf{r}),$$
$$\varphi(\mathbf{r}) = 3^{1/8}\sum_{l=-\infty}^{\infty} e^{i[(\pi/2)l^2+3^{1/4}\pi^{1/2}lx]-(1/2)(y-3^{1/4}\pi^{1/2}l)^2}. \tag{61}$$

This form will be used extensively in the following sections.

c. General rhombic lattice

All rhombic lattices with magnetic field b are obtained from the ansatz $C_{n+2}=C_n$ by assuming the phase $C_1 = iC_0$,

$$\varphi(x,y,b) \equiv \pi^{1/4} b^{-1/4} \sqrt{2/d_\theta} \times \sum_{l=-\infty}^{\infty} e^{i[(2\pi/d_\theta)xl+(\pi/2)l^2]-(b/2)[y-(2\pi/d_\theta b)l]^2}. \quad (62)$$

The hexagonal lattice corresponds to $\theta=60°$ (see Fig. 3). One can check that a rhombic lattice indeed is invariant under magnetic translations by $\mathbf{d}_1$ and $\mathbf{d}_2$. The flux quantization takes a form

$$\tfrac{1}{2} d_\theta^2 \tan\theta = 2\pi/b. \quad (63)$$

One notices $d_\theta = d_\theta(b) = d_\theta(1)/\sqrt{b}$ and that generally we have a following relation:

$$\varphi(x,y,b) \equiv \varphi(b^{1/2}x, b^{1/2}y), \quad (64)$$

where the right-hand side equation $\varphi(x,y)$ is the solution in the case of $b=1$ and we replace x,y by $\sqrt{b}x, \sqrt{b}y$. There are of course infinitely many invariant functions differing by a "fractional" translation as well as by rotation of the lattice. These symmetries are "broken spontaneously" by the lattice. According to the Goldstone theorem, they lead to the existence of soft phonon modes in the crystalline phase and will be studied in Sec. III.

d. General magnetic translations and their algebra

We generalize the discussion by considering an arbitrary Landau gauge. Using the experience with regauging of the two nontrivial translations in our gauge, which generally defined a matrix,

$$\mathcal{B} = \begin{pmatrix} 0 & b \\ 0 & 0 \end{pmatrix}, \quad A_i = \mathcal{B}_{ij} r_j. \quad (65)$$

Magnetic translation operator for a general vector $\mathbf{d}$ should be defined as

$$T_{\mathbf{d}} = e^{-i[(1/2)d_i\mathcal{B}_{ij}+r_i\mathcal{B}_{ij}]d_j} e^{i\mathbf{d}\cdot\hat{\mathbf{p}}} = e^{i\mathbf{d}\cdot\hat{\mathbf{P}}}, \quad (66)$$

with a generator $\hat{\mathbf{P}}$ defined by

$$\hat{P}_i = -i\partial_i - \mathcal{B}_{ji} r_j = \hat{p}_i - \mathcal{B}_{ji} r_j. \quad (67)$$

This can be derived using the general formula

$$e^K e^L = e^{K+L+(1/2)[K,L]}, \quad (68)$$

which is valid when commutator $[K,L]$ is proportional to the identity operator. Applying the formula to the case of the expression [Eq. (66)] with $K=-i[(1/2)d_i\mathcal{B}_{ij}+r_i\mathcal{B}_{ij}]d_j$, $L=i\hat{\mathbf{p}}\cdot\mathbf{d}$, and using the basic algebra $[r_i,\hat{p}_j]=i\delta_{ij}$, one indeed obtains a number

$$[K,L] = [r_i\mathcal{B}_{ij}d_j, \hat{\mathbf{p}}\cdot\mathbf{d}] = id_i\mathcal{B}_{ij}d_j. \quad (69)$$

The expression for magnetic translations can also be derived from a requirement that they commute with "Hamiltonian" $\hat{H}$ defined in Eq. (37). In fact, they commute with both covariant derivatives D_i,

$$D_i = \partial_i + i\mathcal{B}_{ij} r_j, \quad (70)$$

as well. However, using the same basic algebra, one also observes that magnetic translations generally do not commute: $T_{\mathbf{d}_1}T_{\mathbf{d}_2}$ differs from $T_{\mathbf{d}_2}T_{\mathbf{d}_1}$ by a phase. This is a consequence of the Campbell-Baker-Hausdorff formula $e^K e^L = e^L e^K e^{[K,L]}$, which follows immediately from Eqs. (68) and (69),

$$e^{i\mathbf{d}_1\cdot\hat{\mathbf{P}}} e^{i\mathbf{d}_2\cdot\hat{\mathbf{P}}} = e^{i\mathbf{d}_2\cdot\hat{\mathbf{P}}} e^{i\mathbf{d}_1\cdot\hat{\mathbf{P}}} e^{-[\mathbf{d}_1\cdot\hat{\mathbf{P}},\mathbf{d}_2\cdot\hat{\mathbf{P}}]}, \quad (71)$$

with the constant commutator given by $[\mathbf{d}_1\cdot\hat{\mathbf{P}},\mathbf{d}_2\cdot\hat{\mathbf{P}}] = ib\mathbf{d}_1\times\mathbf{d}_2$. The group property therefore is

$$T_{\mathbf{d}_1}T_{\mathbf{d}_2} = e^{-ib\mathbf{d}_1\times\mathbf{d}_2} T_{\mathbf{d}_2}T_{\mathbf{d}_1}, \quad (72)$$

from which the requirement to have an integer number of fluxons per unit cell of a lattice is as follows:

$$b\mathbf{d}_1\times\mathbf{d}_2 = 2\pi\times\text{integer}. \quad (73)$$

Note that the generator of magnetic translations is not proportional to covariant derivative $D_i=\partial_i - i\mathcal{B}_{ij}r_j$. The relation is nonlocal,

$$P_i = -iD_i + \varepsilon_{ij} r_j, \quad (74)$$

where ε_{ij} is the antisymmetric tensor.

4. The Abrikosov lattice solution: Choice of the lattice structure based on minimization of the quartic contribution to energy

a. The Abrikosov β constant of a lattice structure

To lift the degeneracy between all possible "wave functions" with arbitrary normalization on the ground Landau level, one can try to minimize the quartic term in free energy [Eq. (36)]. It is reasonable to assume that more "symmetric" configurations will have an advantage. In particular lattices will be preferred over "chaotic" inhomogeneous ones. Moreover, hexagonal lattice should be perhaps the leading candidate due to its relative isotropy and high symmetry. This configuration is preferred to the London limit (Tinkham, 1996) since vortices repel each other and try to self-assemble into the most homogeneous configuration. A simpler square lattice was considered, in fact, as the best candidate by Abrikosov and we start from this lattice to try to fix the variational parameter C. The energy constrained to the LLL is

$$G = \int d\mathbf{r} \left[-a_H|\Psi|^2 + \frac{1}{2}|\Psi|^4 + \frac{\kappa^2}{4}(\mathbf{b}-\mathbf{h})^2 \right]. \quad (75)$$

The quartic contribution to energy density is proportional to the space average of $|\varphi|^4$ which is called the Abrikosov $\beta_\diamond$,

$$\beta_\diamond = \frac{1}{d_\diamond^2}\int_{-d_\diamond/2}^{d_\diamond/2} dx \int_{-d_\diamond/2}^{d_\diamond/2} dy |\varphi_\diamond(x,y)|^4$$
$$= \frac{1}{d_\diamond^2}\int_{-d_\diamond/2}^{d_\diamond/2} dx \int_{-d_\diamond/2}^{d_\diamond/2} dy \times \sum_{n_i} e^{i(2\pi/d_\diamond)(n_1-n_2+n_3-n_4)x} \times e^{-(b/2)[(y-d_\diamond n_1)^2+(y-d_\diamond n_2)^2+(y-d_\diamond n_3)^2+(y-d_\diamond n_4)^2]}. \quad (76)$$

In principle, one can slightly generalize the method we used to calculate analytically both integrals and sums (Saint-James *et al.*, 1969), however, we will refrain from doing so here, since in Appendix A a more efficient method will be presented. The result is $\beta_\diamond = 1.18$. More generally it is shown there that for any lattice this constant is given by

$$\beta_\theta = \sum_{n_1,n_2=-\infty}^{\infty} e^{-[b\mathbf{X}^2(n_1,n_2)/2]}, \quad (77)$$

where the summation is over the lattice sites $\mathbf{X}(n_1,n_2) = n_1\mathbf{d}_1 + n_2\mathbf{d}_2$. For example, $\beta_\Delta = 1.16$ for the hexagonal lattice.

b. Energy, entropy, and specific heat

The free energy density of the leading order solution is indeed negative. Substituting a variational solution, one has

$$\frac{1}{\text{vol}}\int_{\mathbf{r}} \bar{F} = \frac{1}{\text{vol}}\int_{\mathbf{r}} |C|^2\left[\varphi^*\hat{H}\varphi - \frac{1-t-b}{2}|\varphi|^2 + \frac{1}{2}|C|^2|\varphi|^4\right] = -|C|^2 a_H + \frac{1}{2}|C|^4\beta_\diamond. \quad (78)$$

The FLL and the transition to the normal state can therefore be described well by a "dimensionally reduced" $D=0$ U(1) symmetric model with the complex "order parameter" C. It is similar to the Meissner state in the absence of magnetic field but in $D=0$ with the only difference being that between β_A and 1 (which is about 10%). One minimizes it with respect to C,

$$|C|^2 = a_H/\beta_\diamond. \quad (79)$$

The average energy density at minimum (still on the subspace of square lattices) is given by

$$\frac{1}{\text{vol}}\int_{\mathbf{r}} \bar{F} = -\frac{a_H^2}{2\beta_\diamond} = -\frac{(1-b-t)^2}{8\beta_\diamond} \quad (80)$$

or, returning to the unscaled units, the energy density is

$$\frac{F}{\text{vol}} = -\frac{H_{c2}^2}{4\pi\kappa^2}\frac{a_H^2}{\beta_\diamond}. \quad (81)$$

The first derivative with respect to temperature T, the entropy density

$$S = -(H_{c2}^2/4\pi\kappa^2\beta_A T_c)a_H, \quad (82)$$

smoothly vanishes at transition to the normal phase. On the other hand, the second derivative, the specific heat divided by temperature, jumps to a constant

$$C_v/T = H_{c2}^2/8\pi\kappa^2\beta_A T_c^2 \quad (83)$$

from zero in the normal phase. Note that in this section we use a simple GL model which neglects the normal state contribution to free energy [Eq. (2)], retaining only terms depending on the order parameter. The additional term is a smooth "background," also referred to as a contribution of normal electrons.

Of course a similar argument is valid for any lattice symmetry with corresponding Abrikosov parameter β_A. What is the correct shape of the vortex lattice? To minimize the energy in this approximation is equivalent to the minimization of β_θ with respect to shape of the lattice. This is achieved for the hexagonal lattice, although differences are not large. The square lattice incidentally has the largest energy among all rhombic structures, some 2% higher than that of the hexagonal lattice. This sounds rather small, but for a comparison the typical latent heat at melting (difference in internal energies between lattice and homogeneous liquid) is of the same order of magnitude.

c. Magnetization to leading order in $1/\kappa^2$

Magnetization can be obtained via minimization of the Gibbs free energy with respect to magnetic induction B. In our units and within LLL approximation one can differentiate Eq. (75) and the Maxwell term with respect to b,

$$\kappa^2[h - b(\mathbf{r})] = 4\pi\kappa^2 m(\mathbf{r}) = |\Psi(\mathbf{r})|^2. \quad (84)$$

The magnetization $m(\mathbf{r})$ is therefore proportional to the superfluid density $|\Psi(\mathbf{r})|^2$ and is thus highly inhomogeneous. Its space average is

$$m \equiv \frac{1}{4\pi\,\text{vol}}\int_{\mathbf{r}} m(\mathbf{r}) = \frac{C^2|\varphi_\diamond(\mathbf{r})|^2}{4\pi\kappa^2} = -\frac{1-t-b}{8\pi\kappa^2\beta_\diamond}. \quad (85)$$

For large κ (typical value for high T_c superconductors is $\kappa = 100$) the magnetization is of order $1/\kappa^2$ compared to H and therefore negligible. This justifies an assumption of constant magnetic induction, which can be slightly corrected,

$$b = \frac{-(1-t)/2\beta_\diamond + \kappa^2 h}{\kappa^2 - 1/2\beta_\diamond} \simeq h - \frac{1-t-h}{2\kappa^2\beta_\diamond}. \quad (86)$$

Rescaling back to regular units, one has

$$M = \frac{1}{4\pi}(B-H) \simeq -\frac{H_{c2}}{4\pi\kappa^2}\frac{a_H}{\beta_\diamond}, \quad (87)$$

with

$$a_H = \frac{1}{2}\left(1 - \frac{T}{T_c} - \frac{B}{H_{c2}}\right) \simeq \frac{1}{2}\left(1 - \frac{T}{T_c} - \frac{H}{H_{c2}}\right), \quad (88)$$

which is valid up to corrections of order κ^{-2}.

d. A general relation between the current density and the superfluid density on LLL

The pattern of supercurrent flow around vortex cores can be readily obtained by substituting the Abrikosov vortex approximation into the expression for the supercurrent density [Eq. (12)]. We derive here a general relation between an arbitrary static LLL function [Eq. (50)] and the supercurrent. It will be helpful for understanding the mechanism behind the flux flow, occurring in dynamical situations, when electric field is able to penetrate a superconductor. The covariant derivatives acting on the LLL basis elements give

$$\begin{aligned} D_x\phi_{k_x} &= (\partial_x - iby)\{\pi^{-1/4}b^{1/2}e^{ik_x x-(b/2)(y-k_x/b)^2}\} \\ &= -i\pi^{-1/4}b^{1/2}(by-k_x)e^{ik_x x-(b/2)(y-k_x/b)^2} \\ &= i(b/2)^{1/2}\phi_{N=1,k_x}, \\ D_y\phi_{k_x} &= \partial_y\{\pi^{-1/4}b^{1/2}e^{ik_x x[-(b/2)(y-k_x/b)^2]}\} \\ &= -\pi^{-1/4}b^{1/2}(by-k_x)e^{ik_x x-(b/2)(y-k_x/b)^2} \\ &= (b/2)^{1/2}\phi_{N=1,k_x}. \end{aligned} \tag{89}$$

The covariant derivatives, which are linear combinations of "raising" and "lowering" Landau level operators,

$$\begin{aligned} &D_x = i\sqrt{\frac{b}{2}}(\hat{a}^\dagger + \hat{a}), \quad D_y = \sqrt{\frac{b}{2}}(\hat{a}^\dagger - \hat{a}), \\ &\hat{a}^\dagger = \frac{-i\partial_x + \partial_y - by}{\sqrt{2b}}, \quad \hat{a} = -\frac{-i\partial_x + \partial_y + by}{\sqrt{2b}}, \end{aligned} \tag{90}$$

therefore raise an LLL function to the first LL. One can check that the following relation is valid:

$$i\Psi^*(\mathbf{r})D_i\Psi(\mathbf{r}) + \text{c.c.} = \varepsilon_{ij}\partial_j[|\Psi(\mathbf{r})|^2], \tag{91}$$

where ε_{ij} is the antisymmetric tensor. We therefore have established an exact relation between the current density and [scaled with $J_{\rm GL}=c\Phi_0/2\pi^2\kappa^2\xi^3$, $J_{\rm GL}=c\Phi_0/4\pi^2\kappa^2\xi^3$ according to Eq. (24)] superfluid density,

$$\bar{J}_i(\mathbf{r}) = J_i(\mathbf{r})/J_{\rm GL} = -\tfrac{1}{2}\varepsilon_{ij}\bar{\partial}_j[|\bar{\Psi}(\bar{\mathbf{r}})|^2], \tag{92}$$

which is valid, however, on LLL states only. In regular units the current density is related to (unscaled) order parameter field by

$$J_i(\mathbf{r}) = -(e^*\hbar/2m^*)\varepsilon_{ij}\partial_j[|\Psi(\mathbf{r})|^2]. \tag{93}$$

The supercurrent indeed creates a vortex around a dip in the superfluid density (Fig. 4). The overall current is of course zero since the bulk integral is transformed into a surface one. An approximate solution described in this section is perhaps valid near the $H_{c2}(T)$ line, however to estimate the range of validity and to obtain a better approximation, one would prefer a systematic perturbative scheme over an uncontrollable variational principle. This is provided by the a_H expansion.

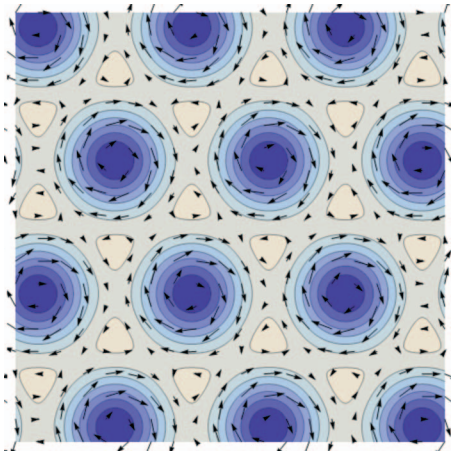

FIG. 4. (Color) Superflow around the vortex centers in the hexagonal lattice.

B. Systematic expansion around the bifurcation point

1. Expansion and the leading order

We have defined the operator $\hat{H}$ in Eq. (37) in such a way that its spectrum will start from zero. This allows the development of the bifurcation point perturbation theory for the GL equation [Eq. (39)]. This type of the perturbation theory is quite different from the one used in linear equations like the Schrödinger equation.

One develops a perturbation theory in small a_H around the $H_{c2}(T)$ line

$$\Psi = \sqrt{a_H}(\Psi^{(0)} + a_H\Psi^{(1)} + a_H^2\Psi^{(2)} + \cdots). \tag{94}$$

Note the fractional power of the expansion parameter in front of the "regular" series. This is related to the mean field critical exponent for a ϕ^4 type equation being 1/2, so that all the terms in the free energy have the same power a_H^2 and are "relevant," as mentioned in Introduction. Substituting this series into Eq. (39) one observes that the leading ($a_H^{1/2}$) order equation gives the lowest LLL restriction already motivated in the heuristic approach of the previous section,

$$\hat{H}\Psi^{(0)} = 0, \tag{95}$$

resulting in $\Psi^{(0)}=C^{(0)}\varphi$ with normalization undetermined. It will be determined by the next order. The next to leading ($a_H^{3/2}$) order equation is

$$\hat{H}\Psi^{(1)} - C^{(0)}\varphi + C^{(0)}|C^{(0)}|^2\varphi|\varphi|^2 = 0. \tag{96}$$

Multiplying it with φ^* and integrating over coordinates, one obtains

$$\int_{\mathbf{r}} \varphi^*[\hat{H}\Psi^{(1)} - C^{(0)}\varphi + C^{(0)}|C^{(0)}|^2\varphi|\varphi|^2] = 0. \tag{97}$$

The first term vanishes since Hermitian operator $\hat{H}$ in the scalar product, defined as

$$\frac{1}{L_x L_y}\int_{\mathbf{r}} f^*(r)g(r) \equiv [f|g], \tag{98}$$

can be applied on it and vanished by virtue of Eq. (95). This way one recovers the "naive" result of Eq. (79),

$$-1+|C^{(0)}|^2\frac{1}{L_x L_y}\int_{\mathbf{r}}|\varphi|^4 = -1+|C^{(0)}|^2\beta_\Delta = 0. \tag{99}$$

Note that to this order different lattices or in fact any LLL functions are "approximate solutions."

2. Higher order corrections to the solution

a. Next to leading order

Higher order corrections would, in principle, contain higher Landau level (HLL) eigenfunctions in the basis of solutions of the linearized GL equation [Eq. (42)] for eigenvalues E_N [Eq. (47)]. As on the LLL for higher Landau levels one can combine them into a lattice with a certain (here hexagonal) symmetry,

$$\varphi_{\Delta N}(\mathbf{r}) = \int_{k_x} C_{k_x}\phi_{Nk_x}(\mathbf{r}) = \varphi_N(b^{1/2}\mathbf{r}),$$
$$\varphi_N(\mathbf{r}) = \frac{3^{1/8}}{\sqrt{2^N N!}}\sum_{l=-\infty}^{\infty} e^{il[\pi l/2+3^{1/4}\pi^{1/2}x]-(1/2)(y-3^{1/4}\pi^{1/2}l)^2}. \tag{100}$$

The coefficients are the same as given in the previous section [Eq. (57)].

The order $(a_H)^{i+1/2}$ correction can be expanded in the Landau levels basis [Eq. (100)] as

$$\Psi^i(\mathbf{r}) = C^{(i)}\varphi(b^{1/2}\mathbf{r}) + \sum_{N=1}^{\infty} C_N^{(i)}\varphi_N(b^{1/2}\mathbf{r}) \tag{101}$$

(to simplify notations the LLL coefficient is denoted simply $C^{(i)}$ rather than $C_0^{(i)}$, suppressing $N=0$, the convention we have been using already for $\varphi\equiv\varphi_0$). Inserting this into Eq. (96), one obtains to order $a_H^{3/2}$,

$$\sum_{N=1}^{\infty} NbC_N^{(1)}\varphi_N = C^{(0)}\varphi - C^{(0)}|C^{(0)}|^2\varphi|\varphi|^2. \tag{102}$$

The scalar product with φ^N determines $C_N^{(1)}$,

$$C_N^{(1)} = -\beta_N/Nb\beta_\Delta^{3/2}, \tag{103}$$

where

$$\beta_N \equiv \frac{1}{\mathrm{vol}}\int_{\mathbf{r}}|\varphi|^2\varphi_N\varphi^*. \tag{104}$$

To find $C^{(1)}$ we need in addition also the order $a_H^{5/2}$ equation,

$$\hat{H}\Psi_2 = \sum_{N=1}^{\infty} NbC_N^{(2)}\varphi_N = \Psi_1 - (C^{(0)})^2(2\Psi_1|\varphi|^2 + \Psi_1^*\varphi^2). \tag{105}$$

Inner product with φ gives

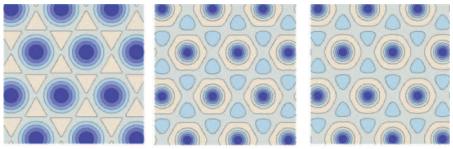

(a) (b) (c)

FIG. 5. (Color) Convergence of the bifurcation perturbation theory.

$$C^{(1)} = \frac{3}{2}\sum_{N=1}^{\infty}\frac{(\beta_N)^2}{Nb\beta_\Delta^{5/2}}. \tag{106}$$

The expansion can be relatively easily continued. Figure 5 shows three successive approximation. The convergence is quite fast even as far from the $H_{c2}(T)$ line for $b=0.1$, $t=0.5$.

b. Orders a_H^2 and a_H^3 in the expansion of free energy

The mean field expression for the free energy to order a_H^2 was already obtained using heuristic approach [Eq. (80)]. Inserting the next correction [Eqs. (106) and (103)] into Eq. (36) one obtains the free energy density,

$$\frac{F^{(2)}+F^{(3)}}{4\mathrm{vol}\Delta} = -\frac{a_H^2}{2\beta_\Delta} - \frac{a_H^3}{\beta_\Delta^3 b}\sum_{N=1}^{\infty}\frac{(\beta_N)^2}{N}$$
$$= -0.43a_H^2 - 0.0078\frac{a_H^3}{b}, \tag{107}$$

where $\Delta = H_{c2}^2/8\pi\kappa^2$ is the unit of energy density.

It is interesting to note that $\beta_N \neq 0$ only when $n=6j$, where j is an integer. This is due to hexagonal symmetry of the vortex lattice (Lascher, 1965). For $n=6j$ it decreases very fast with j: $\beta_6=-0.2787$, $\beta_{12}=0.0249$. Because of this the coefficient of the next to leading order is very small (additional factor of 6 in the denominator). We might preliminarily conclude therefore that the perturbation theory in a_H works much better that might be naively anticipated and can be used very far from transition line. If we demand that the correction is smaller than the main contribution, the corresponding line on the phase diagram will be $b=0.015(1-t)$. For example, the LLL melting line corresponds to $a_H\sim 1$. This overly optimistic conclusion is, however, incorrect as calculation of the following term shows.

c. How precise is LLL?

Now we discuss in what region of the parameter space the expansion outlined above can be applied. First note that all contributions to Ψ_1 are proportional to $1/b$. This is a general feature: the actual expansion parameter is a_H/b. One can ask whether the expansion is convergent and, if yes, what is its radius of convergence. Looking just at the leading correction and comparing it to the LLL one gets a very optimistic estimate. For this purpose higher order coefficients were calculated (Li and Rosenstein, 1999a). The results for the Ψ_2 are the following:

$$C_N^{(2)} = \frac{1}{Nb}\left[C_N^{(1)} - \frac{1}{\beta_\Delta}\sum_{M=0}^{\infty} C_M^{(1)}(2[N,0|M,0] + [0,0|M,N])\right] \quad (108)$$

and

$$C^{(2)} = -\frac{3}{2\beta_\Delta}\beta_N C_N^{(2)} - \frac{1}{2\sqrt{\beta_\Delta}}\sum_{L,M=0}^{\infty} C_L^{(1)} C_M^{(1)}([0,0|L,M] + 2[M,0|L,0]), \quad (109)$$

where

$$[K,L|M,N] \equiv \frac{1}{\mathrm{vol}}\int_{\mathbf{r}} \varphi_K^* \varphi_L^* \varphi_M \varphi_N. \quad (110)$$

We can already see that $C_N^{(2)}$ and $C^{(2)}$ are proportional to $C_N^{(1)}$ and in addition there is a factor of $1/N$. Since due to hexagonal lattice symmetry all the $C_N^{(1)}$, $N \neq 6j$, vanish, so do $C_N^{(2)}$. We have checked that there is no more small parameters, so we conclude that the leading order coefficient is much larger than first (factor 6×5), but the second is only six times larger than the third. The correction to free energy density is

$$\frac{F^{(4)}}{4\mathrm{vol}\Delta} = \frac{0.056}{6^2}\frac{a_H^4}{b^2}. \quad (111)$$

Accidental smallness by factor $1/6$ of the coefficients in the a_H/b expansion due to symmetry means that the range of validity of this expansion is roughly $a_H < 6b$ or $B < H_{c2}(T)/13$. Moreover, additional smallness of all the HLL corrections compared to the LLL means that they constitute just several percent of the correct result inside the region of applicability. To illustrate this point we plot in Fig. 5 the perturbatively calculated solution for $b=0.1$, $t=0.5$. One can see that although the leading LLL function has very thick vortices [Fig. 5(a)], the first nonzero correction makes them of order of the coherence length [Fig. 5(b)]. Following correction of the order $(a_H/b)^2$ makes it practically indistinguishable from the numerical solution. Amazingly the order parameter between the vortices approaches its vacuum value. Paradoxically starting from the region close to H_{c2} the perturbation theory knows how to correct the order parameter so that it looks very similar to the London approximation (valid only close to H_{c1}) result of well-separated vortices.

We conclude therefore that the expansion in a_H/b works in the mean field better that one can naively expect.

III. THERMAL FLUCTUATIONS AND MELTING OF THE VORTEX SOLID INTO A LIQUID

In this section a theory of thermal fluctuations and of melting of the vortex lattice in type II superconductors in the framework of Ginzburg-Landau approach is presented. Far from $H_{c1}(T)$ the lowest Landau level approximation can be used. Within this approximation the model simplifies and results depend just on one parameter: the LLL reduced temperature. To obtain an accurate description of both the vortex lattice and the vortex liquid different methods are applied. In the crystalline phase basic excitations are phonons. Their spectrum and interactions are rather unusual and the low temperature perturbation theory requires to develop a certain technique. Generally perturbation theory to the two loop order is sufficient, but for certain purposes (like finding a spinodal in which metastable crystalline state becomes unstable) a self-consistent "Gaussian" approximation is required. In the liquid state both the perturbation theory and Gaussian approximations are insufficient to get a precision required to describe the first order melting transition and one utilizes more sophisticated methods. Already the Gaussian approximation shows that the metastable liquid state persists (within LLL) until zero temperature. The high temperature renormalized series (around the Gaussian variational state) supplemented by interpolation to a $T=0$ metastable "perfect liquid" state are sufficient. The melting line location is determined and magnetization and specific heat jumps along it are calculated. The magnetization of liquid is larger than that of solid by 1.8%, irrespective of the melting temperature, while the specific heat jump is about 6% and decreases slowly with temperature.

A. The LLL scaling and the quasimomentum basis

1. The LLL scaling

a. Units and the LLL scaled temperature

If the magnetic field is sufficiently high, we can keep only the $N=0$ LLL modes. This is achieved by enforcing the following constraint:

$$-\frac{\hbar^2}{2m^*}\mathbf{D}^2\Psi = \frac{\hbar e^*}{2m^* c}B\Psi, \quad (112)$$

where covariant derivatives were defined in Eq. (9). Using it the free energy [Eq. (8)] simplifies

$$G[\Psi,\mathbf{A}] = \int dr\left\{\frac{\hbar^2}{2m_c^*}|\partial_z\Psi|^2 + \alpha T_c(1-t-b)|\Psi|^2 + \frac{\beta}{2}|\Psi|^4 + \frac{(\mathbf{B}-\mathbf{H})^2}{8\pi}\right\}. \quad (113)$$

Originally the Ginzburg-Landau statistical sum [Eq. (18)] had five dimensionless parameters, three material parameters $\kappa=\lambda/\xi, \gamma_a=(m_c^*/m^*)^{1/2}$, and the Ginzburg number, defined by

$$\mathrm{Gi} \equiv (e^{*2}\kappa^2\xi T_c\gamma_a/2\pi c^2\hbar^2)^2 \quad (114)$$

and two external parameters $t=T/T_c$ and $b=B/H_{c2}$. However, since there is now no gradient term in directions perpendicular to the field, one independent parameter is missing. The Gibbs energy,

$$\mathcal{G} = -T\log\left\{\int_{\Psi,B}\exp\left[-\frac{1}{T}\int G[\Psi,\mathbf{B}]\right]\right\}, \tag{115}$$

thus possesses the "LLL scaling" (Lee and Shenoy, 1972; Thouless, 1975; Ruggeri and Thouless, 1976; Ruggeri, 1978). To exhibit these scaling relations, it is useful to use units of coordinates and fields, which are dependent not just on material parameters (as those used in Sec. II) but also on external parameters, magnetic field, and temperature. One uses the magnetic length rather than coherence length as a unit of length in directions perpendicular to magnetic field, $x=(\xi/\sqrt{b})\bar{x}$, $y=(\xi/\sqrt{b})\bar{y}$, while in the field direction a different factor is used, $z=(\xi/\gamma_a)(\sqrt{\mathrm{Gi}}tb/4)^{-1/3}\bar{z}$. The magnetic field is rescaled as before with H_{c2}, while the order parameter field has an additional factor: $\Psi^2=2\Psi_0^2(\sqrt{\mathrm{Gi}}tb/4)^{2/3}\psi^2$. With the usefulness of the fractional powers additional factors will become clear later.

The dimensionless Boltzmann factor becomes

$$g[\psi,b] \equiv \frac{G[\Psi,\mathbf{A}]}{T} = \frac{1}{2^{5/2}\pi}f[\psi] + \frac{\kappa^2}{2^{5/2}\pi}\left(\frac{\sqrt{\mathrm{Gi}}tb}{4}\right)^{-4/3} \times \int d\bar{r}\frac{(\mathbf{b}-\mathbf{h})^2}{4}, \tag{116}$$

$$f[\psi] = \int d\bar{r}\left[\frac{1}{2}|\partial_{\bar{z}}\psi|^2 + a_T|\psi|^2 + \frac{1}{2}|\psi|^4\right], \tag{117}$$

where the LLL scale "temperature" is

$$a_T = -\left(\frac{\sqrt{\mathrm{Gi}}tb}{4}\right)^{-2/3}a_H = -\frac{1-t-b}{2}\left(\frac{\sqrt{\mathrm{Gi}}tb}{4}\right)^{-2/3}. \tag{118}$$

The constant a_H was defined in Eq. (38) and extensively used in the previous section. The scaled temperature therefore is the only remaining dimensionless parameter in Eq. (116) in addition to the coefficient of the last term. Factors of $2^{5/2}\pi$ in the definition of "dimensionless free energy" f in Eq. (116) are traditionally kept and will appear frequently in what follows. Assuming nonfluctuating constant magnetic field, one can disregard the last term in Eq. (116) and consider the thermal fluctuations of the order parameter only. This assumption is typically valid in almost all applications and will be discussed in Sec. III.E. Certain physical quantities, the "LLL scaled" ones, are functions of this parameter only. We list the most important such quantities below.

b. Scaled quantities

The scaled free energy density is

$$f_d(a_T) = -\frac{2^{5/2}\pi}{V'}\ln\int \mathcal{D}\psi\mathcal{D}\psi^* e^{-1/2^{5/2}\pi f[\psi]}, \tag{119}$$

where V' is the rescaled volume and $f(a_T)$ is related to the free energy density in unscaled units by

$$\mathcal{F}_d = \left(\frac{\sqrt{\mathrm{Gi}}tb}{4}\right)^{4/3}\frac{H_{c2}^2}{2\pi\kappa^2}f_d(a_T). \tag{120}$$

Focusing on magnetization, We return to conventional units [Eq. (113)] and neglect fluctuations of magnetic field [considered by Halperin *et al.* (1974), Dasgupta and Halperin (1981), Lobb (1987), Herbut and Tešanović (1996), and Herbut (2007). Within LLL magnetization in the presence of thermal fluctuations is determined from

$$\frac{\delta}{\delta B}\mathcal{G} = Z^{-1}\int_\Psi \frac{\delta}{\delta B}G[\Psi,B]\exp\left(-\frac{1}{T}\int G[\Psi,B]\right) = 0. \tag{121}$$

Taking the derivative, one obtains

$$-Z^{-1}\int_\Psi\left[\int_r \frac{\alpha T_c}{H_{c2}}|\Psi|^2 + \frac{B-H}{4\pi}\right]\exp\left(-\frac{1}{T}\int G[\Psi,B]\right) = -\frac{\alpha T_c}{H_{c2}}\langle|\Psi|^2\rangle - \frac{B-H}{4\pi} = 0, \tag{122}$$

where from now on $\langle\cdots\rangle$ denotes the thermal average. The magnetization on LLL is therefore proportional to the superfluid density

$$M = -(\alpha T_c/H_{c2})\langle|\Psi|^2\rangle. \tag{123}$$

This motivates the definition of the LLL scaled magnetization proportional to $\langle|\Psi|^2\rangle$,

$$m(a_T) = -\langle|\psi|^2\rangle = -\frac{\partial}{\partial a_T}f_d(a_T), \tag{124}$$

which is related to magnetization by

$$\frac{M}{H_{c2}} = \frac{1}{4\pi\kappa^2}\left(\frac{\sqrt{\mathrm{Gi}}}{4}tb\right)^{2/3}m(a_T). \tag{125}$$

Consequently, $M/(TB)^{3/2}$ depends on a_T only, the statement called the LLL scaling proposed by Thouless (1975), Ruggeri and Thouless (1976), Ruggeri (1978), Tešanović *et al.* (1992), and Tešanović and Andreev (1994). It has been experimentally demonstrated in numerous experiments.

The specific heat contribution due to the vortex matter is generally defined by $C=-T\frac{\partial^2}{G(T,H)}\partial T^2$. Usually, since the GL approach is applied near T_c, one can replace T by T_c in the Boltzmann factor, leaving the temperature dependence just inside the coefficient of $|\Psi|^2$ in Eq. (113). In this case the normalized specific heat is defined as

$$c = C/C_{\mathrm{mf}}, \tag{126}$$

where $C_{mf}=H_{c2}^2T/8\pi\kappa^2\beta_\Delta T_c^2$ is the mean field specific heat of solid calculated in the previous section. Substituting $G(T,H)$, if very near phase transition temperature, we can put $t=1$ in the scaling factor $(\sqrt{\mathrm{Gi}}/4)tb$, in this case, we obtain

$$c = -\beta_\Delta \frac{\partial^2}{\partial a_T^2} f_d(a_T). \tag{127}$$

Since the range of applicability of LLL can extend beyond vicinity of T_c, especially at strong fields (since they depress order parameter), one should use a more complicated formula which does not utilize $T \simeq T_c$,

$$c = -\beta_A \left[\frac{16}{9t^2}(bt)^{4/3} f_d(a_T) - \frac{4(b-1-t)}{3t^2}(bt)^{2/3} f'(a_T) + \frac{(2-2b+t)}{9t^2} 2 f_d''(a_T) \right]. \tag{128}$$

It no longer possesses the LLL scaling.

2. Magnetic translations and the quasimomentum basis

It is necessary to use the representations of translational symmetry in order to classify various excitations of both the Abrikosov lattice and a homogeneous state created when thermal fluctuations become strong enough. As we have seen in Sec. II.B, presence of magnetic field makes the use of the translational symmetry a nontrivial task due to the need to "regauge." Here we use an algebraic approach to construct the quasimomenta basis and then to determine the excitation spectrum of the lattice and the liquid, which in turn determines its elastic and thermal properties.

a. The quasimomentum basis

We motivated the definition of the magnetic translation symmetries [Eq. (66)] by the property that they transform various lattices onto themselves. More formally the x-y plane translation operators T_d [Eq. (66)] represent symmetries since they commute with Hamiltonian $\hat{H}$ of Eq. (37). Excitations of the lattice are no longer invariant under the symmetry transformations. This in particular means that we cannot longer consider the problem as two dimensional. However, as in the solid state physics, it is convenient to expand them in the basis of eigenfunctions of the generators of the magnetic translation operators defined in Eq. (66) and simple translations in the field z direction,

$$\hat{\mathbf{P}}\varphi_{Nk} = \mathbf{k}\varphi_{Nk}, \quad T_{\mathbf{d}}\varphi_{Nk} = e^{i\mathbf{k}\cdot\mathbf{d}}\varphi_{Nk}, \qquad \hat{p}_z\varphi_{Nk} = k_z\varphi_{Nk}, \quad T_{d_z}\varphi_{Nk} = e^{ik_z d_z}\varphi_{Nk}, \tag{129}$$

with the commutation relation [Eq. (72)] $T_{\mathbf{d}_1}T_{\mathbf{d}_2} = e^{-ib\mathbf{d}_1\times\mathbf{d}_2}T_{\mathbf{d}_2}T_{\mathbf{d}_1}$. The three-dimensional quasimomentum vector is denoted by $k \equiv (\mathbf{k}, k_z)$. It is easy to construct these functions explicitly. On the Nth Landau level the 2D quasimomentum $\mathbf{k}$ function is given by

$$\varphi_{N\mathbf{k}}(\mathbf{r}) = T_{\tilde{\mathbf{k}}}\varphi_N(\mathbf{r}), \tag{130}$$

where $\tilde{k}_i = \varepsilon_{ij}k_j$ for $i = x, y$ and $\varphi_N(\mathbf{r})$ for a given lattice symmetry was constructed in Sec. II.A. Here we take the hexagonal lattice functions of Eq. (100). Indeed

$$T_{\mathbf{d}}\varphi_{N\mathbf{k}} = T_{\mathbf{d}}T_{\tilde{\mathbf{k}}}\varphi_N = e^{-i\mathbf{d}\times\tilde{\mathbf{k}}}T_{\tilde{\mathbf{k}}}T_{\mathbf{d}}\varphi_N = e^{i\mathbf{k}\cdot\mathbf{d}}\varphi_{N\mathbf{k}}. \tag{131}$$

To write it explicitly, the most convenient form of the magnetic translation is that of Eq. (66), which gives

$$\varphi_{N\mathbf{k}} = e^{-i[(1/2)\tilde{k}_i\mathcal{B}_{ij}\tilde{k}_j + x_i\mathcal{B}_{ij}\tilde{k}_j]}e^{i\tilde{\mathbf{k}}\cdot\mathbf{p}}\varphi_N. \tag{132}$$

Since $T_{\mathbf{d}}$ is unitary, the normalization is the same as that of φ_N. On LLL in our gauge one has

$$\varphi_{\mathbf{k}} = e^{ixk_x}\varphi_0(\mathbf{r}+\tilde{\mathbf{k}}) = 3^{1/8}\sum_{l=-\infty}^{\infty} e^{i[\pi l^2/2 + 3^{1/4}\pi^{1/2}(x+k_y)l + xk_x] - (1/2)[y - k_x - 3^{1/4}\pi^{1/2}l]^2}. \tag{133}$$

In the direction along the field one uses the usual momentum,

$$\varphi_k(r) = e^{ik_z z}\varphi_{\mathbf{k}}(\mathbf{r}), \tag{134}$$

where, as before, we use the notation $r \equiv (\mathbf{r}, z)$.

The values of the quasimomentum cover a Brillouin zone in the x-y plane. As usual, it is convenient to work in basis vectors of the reciprocal lattice, $\mathbf{k} = k_1\tilde{\mathbf{d}}_1 + k_2\tilde{\mathbf{d}}_2$, with the basis vectors

$$\tilde{\mathbf{d}}_1 = \frac{\sqrt{3^{1/2}}}{\sqrt{\pi}}\left(1, -\frac{1}{\sqrt{3}}\right), \quad \tilde{\mathbf{d}}_2 = \frac{\sqrt{3^{1/2}}}{\sqrt{\pi}}\left(0, \frac{2}{\sqrt{3}}\right). \tag{135}$$

The measure is

$$\int_{B.z.} dk_x dk_y \equiv 2\pi\int_0^1 dk_1 \int_0^1 dk_2, \qquad \int_k d^3k \equiv \int_{-\infty}^{\infty} dk_z \int_{B.z.} d\mathbf{k}. \tag{136}$$

Beyond LLL the quasimomentum basis consists of $\varphi_{\mathbf{k}}^N(\mathbf{r})$, Nth Landau level wave functions with quasimomentum $\mathbf{k}$,

$$\varphi_{\mathbf{k}}^N(\mathbf{r}) = \sqrt{\frac{3^{1/4}}{2^N N!}}\sum_{l=-\infty}^{\infty} H_n(y - k_x - 3^{1/4}\pi^{1/2}l) \times e^{i[\pi l^2/2 + 3^{1/4}\pi^{1/2}(x+k_y)l + xk_x] - (1/2)[y - k_x - 3^{1/4}\pi^{1/2}l]^2}. \tag{137}$$

The construction is identical to LLL. Even in the homogeneous liquid state, which is obviously more symmetric than the hexagonal lattice, we find it convenient to use this basis,

$$\psi(r) = \frac{1}{(2\pi)^{3/2}}\int_k \sum_{N=0}^{\infty} \varphi_k^N(r)\psi_k^N. \tag{138}$$

b. Energy in the quasimomentum basis

As discussed in Sec. II, the lowest energy configurations belong to LLL. There is an energy gap to any $N > 0$ configuration, so it is reasonable that, for tempera-

tures small enough, their contribution is small. Restricting the set of states over which we integrate to LLL

$$\psi(r) = \frac{1}{(2\pi)^{3/2}} \int_k \varphi_k(r) \psi_k, \tag{139}$$

one has the Boltzmann factor $(1/2^{5/2}\pi) f[\psi]$ [Eq. (117)] and other physical quantities via new variables ψ_k. The first two terms in Eq. (117) are simple,

$$f_0[\psi] = \frac{1}{(2\pi)^3} \int_k (k_z^2/2 + a_T) \int_r \varphi_k^*(r) \varphi_l(r) \psi_k^* \psi_l$$
$$= \int_k (k_z^2/2 + a_T) \psi_k^* \psi_k. \tag{140}$$

The quartic term is

$$f_{\rm int}[\psi] = \frac{L_x L_y}{2(2\pi)^5} \int_{k,l,k',l'} \delta(k_z + l_z - k_z' - l_z') \times [\mathbf{k},\mathbf{l}|\mathbf{k}',\mathbf{l}'] \psi_k^* \psi_l^* \psi_{k'} \psi_{l'}, \tag{141}$$

with

$$[\mathbf{k},\mathbf{l}|\mathbf{k}',\mathbf{l}'] \equiv \frac{1}{L_x L_y} \int_{\mathbf{r}} \varphi_{\mathbf{k}}^*(\mathbf{r}) \varphi_{\mathbf{l}}^*(\mathbf{r}) \varphi_{\mathbf{k}'}(\mathbf{r}) \varphi_{\mathbf{l}'}(\mathbf{r}) \tag{142}$$

calculated in Appendix A. Generally the expression is not very simple due to the so-called "umklapp" processes since when four quasimomenta involved We turn now to the first application of this basis: calculation of harmonic excitations spectrum of the vortex lattice.

B. Excitations of the vortex lattice and perturbations around it

1. Shift of the field and the excitation spectrum

a. Shift of the field and diagonalization of the quadratic part

For negative a_T and neglecting thermal fluctuations the minimum of energy is achieved by choosing one of the degenerate lattice solutions, the hexagonal lattice φ_Δ in our case. This was the main subject of the previous section. When thermal fluctuations are weak, one can expand in temperature around the mean field solution. The zero quasimomentum field is then shifted by the mean field solutions. In our new LLL units we therefore express the complex fields ψ_k via two "shifted" real fields ($O_k = O_{-k}^*$, $A_k = A_{-k}^*$),

$$\psi_k = v_0 (2\pi)^{3/2} \delta_k + \frac{c_{\mathbf{k}}}{\sqrt{2}} (O_k + iA_k), \tag{143}$$

with value of the field found in Sec. II in the LLL units being

$$v_0 = \sqrt{-a_T/\beta_\Delta}. \tag{144}$$

Notations O and A indicate an analogy to optical and acoustic phonons in atomic crystals. The constants $c_{\mathbf{k}}$ will be chosen later and will help us to diagonalize the quadratic part of the free energy. Substituting this into the energy [Eqs. (140) and (141)], one obtains a constant "mean field" energy density of Sec. II,

$$f_{\rm mf}/{\rm vol} = -a_T^2/2\beta_A, \tag{145}$$

while the quadratic part is

$$f_2 = \frac{1}{2} \int_k [k_z^2/2 - a_T + 2v_0^2 |c_{\mathbf{k}}|^2 \beta_{\mathbf{k}}] (O_k^* - iA_k^*)(O_k + iA_k)$$
$$+ \frac{v_0^2}{4} \int_k [\gamma_{\mathbf{k}} c_{\mathbf{k}}^2 (O_k^* + iA_k^*)(O_k + iA_k) + {\rm c.c.}], \tag{146}$$

where functions

$$\beta_{\mathbf{k}} = \frac{1}{\rm vol} \int_{\mathbf{r}} |\varphi(\mathbf{r})|^2 |\varphi_{\mathbf{k}}(\mathbf{r})|^2 = [\mathbf{0},\mathbf{k}|\mathbf{0},\mathbf{k}],$$
$$\gamma_{\mathbf{k}} = \frac{1}{\rm vol} \int_{\mathbf{r}} \varphi^{*2}(\mathbf{r}) \varphi_{\mathbf{k}}(\mathbf{r}) \varphi_{-\mathbf{k}}(\mathbf{r}) = [\mathbf{0},\mathbf{0}|\mathbf{k},-\mathbf{k}] \tag{147}$$

are calculated and given explicitly in Appendix A. There is no linear term since we shifted by the mean field solution.

The choice

$$c_{\mathbf{k}} = \sqrt{\gamma_{\mathbf{k}}^*/|\gamma_{\mathbf{k}}|} \tag{148}$$

eliminates the OA terms, diagonalizing f_2:

$$f_2 = \frac{1}{2} \int_k \varepsilon_k^O O_k^* O_k + \varepsilon_k^A A_k^* A_k. \tag{149}$$

The resulting spectrum is

$$\varepsilon_k^O = \mu_{O\mathbf{k}}^2 + k_z^2/2, \quad \varepsilon_k^A = \mu_{A\mathbf{k}}^2 + k_z^2/2,$$
$$\mu_{O\mathbf{k}}^2 = a_T + v_0^2(2\beta_{\mathbf{k}} + |\gamma_{\mathbf{k}}|) = -\frac{a_T}{\beta_\Delta}(2\beta_{\mathbf{k}} + |\gamma_{\mathbf{k}}| - \beta_\Delta), \tag{150}$$
$$\mu_{A\mathbf{k}}^2 = a_T + v_0^2(2\beta_{\mathbf{k}} - |\gamma_{\mathbf{k}}|) = -\frac{a_T}{\beta_\Delta}(2\beta_{\mathbf{k}} - |\gamma_{\mathbf{k}}| - \beta_\Delta).$$

The cubic and quartic terms describing the anharmonicities or interactions of the excitations (phonons) are

$$f_3 = \int_{k,l,m} \delta(k_z - l_z - m_z) \Lambda_3(\mathbf{k},\mathbf{l},\mathbf{m}) [(O_k^* - iA_k^*) \times (O_l + iA_l)(O_m + iA_m) + {\rm c.c.}], \tag{151}$$

$$f_4 = \int_{k,l,k',l'} \delta(k_z - l_z + k_z' - l_z') \Lambda_4(\mathbf{k},\mathbf{l},\mathbf{k}',\mathbf{l}') (O_k^* - iA_k^*) \times (O_l + iA_l)(O_{k'}^* - iA_{k'}^*)(O_{l'} + iA_{l'}), \tag{152}$$

where

$$\Lambda_3(\mathbf{k},\mathbf{l},\mathbf{m}) \equiv v_0 \frac{L_x L_y}{2^5 \pi^{7/2}} [\mathbf{k},\mathbf{0}|\mathbf{l},\mathbf{m}] c_{\mathbf{k}}^* c_{\mathbf{l}} c_{\mathbf{m}}, \tag{153}$$

$$\Lambda_4(\mathbf{k},\mathbf{l},\mathbf{k}',\mathbf{l}') \equiv \frac{L_x L_y}{2^8 \pi^5} [\mathbf{k},\mathbf{k}'|\mathbf{l},\mathbf{l}'] c_{\mathbf{k}}^* c_{\mathbf{l}} c_{\mathbf{k}'}^* c_{\mathbf{l}'}, \tag{154}$$

with $[\mathbf{k},\mathbf{k}'|\mathbf{l},\mathbf{l}']$ defined in Eq. (142).

b. Supersoft Goldstone (shear) modes

While the O mode is "massive" even for small quasimomenta, the A mode is a Goldstone boson resulting from spontaneous breaking of several continuous symmetries and is therefore "massless." The broken symmetries include the electric charge U(1), (magnetic) translations, and rotations. The spectrum of Goldstone modes is typically "soft" and quadratic in momentum. This is indeed the case, as far as the field direction z is concerned [Eq. (150)] but the situation in the perpendicular directions is different (Eilenberger, 1967; Lee and Shenoy, 1972).

We use expansion of the functions $\beta_{\mathbf{k}}$ and $\gamma_{\mathbf{k}}$ [Eq. (147)] derived in Appendix A,

$$\beta_{\mathbf{k}} = \beta_\Delta - \frac{\beta_\Delta}{4}\mathbf{k}^2 + \beta_{4\Delta}\mathbf{k}^4,$$
$$\gamma_{\mathbf{k}} = \beta_\Delta - \frac{\beta_\Delta}{2}\mathbf{k}^2 - i\beta_\Delta k_x k_y + i\frac{\beta_\Delta k_x k_y \mathbf{k}^2}{2} + \frac{\beta_\Delta}{8}(\mathbf{k}^4 - 4k_x^2 k_y^2) \tag{155}$$

with constants given in Appendix A, $\beta_{4\Delta}=0.132$. The acoustic spectrum consequently has the following expansion at small momenta:

$$\mu_{A\mathbf{k}}^2 = (2\beta_{4\Delta} - \beta_\Delta/8)v_0^2|\mathbf{k}|^4 + \cdots = 0.1a_H|\mathbf{k}|^4 \tag{156}$$

All quadratic terms cancel and the Goldstone bosons are "supersoft."

One can further investigate the structure of these supersoft modes and identify them with "shear modes" (Moore, 1989, 1992; Zhuravlev and Maniv, 1999, 2002). To conclude, there are many broken continuous symmetries (translations in two directions, rotations and the U(1) phase transformations, forming a rather uncommon in physics Lie group) leading to a single Goldstone mode. The commutators of the magnetic translations generators $\hat{\mathbf{P}}$ and the U(1) generator $\hat{Q}=1$ are (using the explicit form [Eq. (67)])

$$[\hat{P}_x,\hat{P}_y] = i\hat{Q}, \quad [\hat{P}_x,\hat{Q}] = 0, \quad [\hat{P}_y,\hat{Q}] = 0, \tag{157}$$

and form the so-called Heisenberg-Weyl algebra. However, the Goldstone mode is much softer than the regular one: $|\mathbf{k}|^4$ instead of $|\mathbf{k}|^2$. The situation is not entirely unique since ferromagnetic spin waves, Tkachenko modes in superfluid, and excitations in 2D electron gas within LLL share this property. A rigorous general derivation of the modification of the Goldstone theorem in this case is still not available. Note also that, when the magnetic part is not neglected, the modes become massive via a kind of Anderson-Higgs mechanism, which gives them a small "mass" of order $1/\kappa^2$ in our units.

This exceptional "softness" apparently should lead to an instability of the vortex lattice against thermal fluctuations. Indeed naive calculation of the correlator in perturbation theory shows that certain quantities including superfluid density $|\psi|^2$ are infrared (IR) divergent (Maki and Takayama, 1971). This was even considered an indication that the vortex lattice does not exist (Nikulov, 1995; Nikulov *et al.*, 1995; Moore, 1997), despite the large body of experimental evidence, even at that time. As a result, the perturbation theory around the Abrikosov solution was not developed beyond the one-loop order for a long time. One could argue (Brandt, 1995) that real physics is dominated by the small mass $1/\kappa^2$ of the shear mode, acting as a cutoff that prevents IR divergencies, but basic physical properties related to thermal fluctuations near $H_{c2}(T)$ seemed to be independent of the cutoff, especially for high T_c superconductors. Rosenstein (1999) reconsidered the IR divergencies and found that they all cancel exactly at each order in physical quantities such as free energy, magnetization, etc. We therefore systematically consider the (renormalized) perturbation theory for free energy up to two loops and then turn to other physical quantities.

2. Feynman diagrams: Perturbation theory to one loop

a. Feynman diagrams for the loop expansion

To develop a perturbation theory, the coefficient in front of the Boltzmann factor [Eq. (117)] is considered large,

$$f = (1/\alpha)[f_0 + f_2 + f_3 + f_4]. \tag{158}$$

The small parameter α is actually 1 but will be useful to organize the perturbation theory before the actual expansion parameter is uncovered in the process of assembling the series. One does not have to consider a linear in fields term f_1 since it involves only the $k=0$ Goldstone excitations and does not contribute to bulk energy density (Jevicki, 1977). The free energy is calculated from Eq. (119) by expanding exponent of "vertices" $f_3[\psi]$ and $f_4[\psi]$, so that all integrals become Gaussian,

$$\begin{aligned} f(a_T) &= \frac{1}{\alpha}f_{\mathrm{mf}} - 2^{5/2}\pi \log\left\{\int_\psi e^{-(1/\alpha)(f_2+f_3+f_4)}\right\} \\ &= \frac{1}{\alpha}f_0 - 2^{5/2}\pi \log\left\{\int_\psi e^{-(1/\alpha)f_2}\left[1 - \frac{1}{\alpha}(f_3+f_4) + \cdots\right]\right\} \\ &= \frac{1}{\alpha}f_0 - 2^{5/2}\pi \log\left\{\int_\psi e^{-(1/\alpha)f_2}\right\} \\ &\quad + \text{connected diagrams}. \end{aligned} \tag{159}$$

The propagators entering Feynman diagrams [Figs. 6(a) and 6(b)] are read from the quadratic part [Eq. (140)],

$$G_0^{O,A}(k) = \alpha 2^{5/2}\pi/\epsilon_k^{O,A}. \tag{160}$$

The leading order propagators are denoted by dashed and solid lines for the A and the O modes, respectively. Nonquadratic parts of the free energy are the three-leg and the four-leg vertices [Fig. 6(c)–6(f) and Figs. 6(g)–6(k), respectively]. It is important for disappearance of "spurious" IR divergencies (to be discussed later) to realize that vertices involving the A field are "soft," namely, at small momentum they behave like

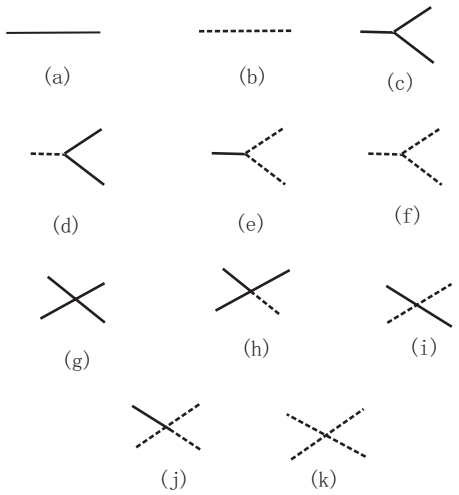

FIG. 6. Feynman rules for vortex lattice.

powers of k. For example, the $A_k A_l A_m$ vertex [Fig. 6(f)], is very soft. At small momenta it is proportional to the fourth power of momenta.

The power of α^{L-1}, $L=\frac{1}{2}(3N_3+4N_4)-N_3-N_4+1$, where N_3, N_4 are numbers of the three-leg and the four-leg vertices, in front of a contribution means that topologically the number of "loops" is L (Itzykson and Drouffe, 1991). The leading term, the mean field energy, is of order α^{-1}.

b. Energy to the one loop order

An important point to note is that in the "ordered" phase, despite the fact that we are talking about perturbation theory, the shift or, in other words, definition of the "physical" excitation fields O_k and A_k in terms of the original fields ψ_k can change from order to order (Itzykson and Drouffe, 1991). The shift v in Eq. (143) is therefore renormalized, that is,

$$v^2 = v_0^2 + \alpha v_1^2 + \cdots . \tag{161}$$

One finds v_1 in the same way v_0 was found, namely, by minimizing the effective free energy at the minimal order in which it appears. We therefore explicitly write several leading contributions to the energy

$$f = (1/\alpha) f_0 + f_1 + \alpha f_2 + \cdots . \tag{162}$$

We start from the mean field part in Eq. (159),

$$\begin{aligned}\frac{f_{\rm mf}}{\rm vol} &= \frac{1}{\alpha}\left[-a_T v^2 + \frac{1}{2}\beta_\Delta v^4\right] \\ &= \frac{1}{\alpha}\left[-a_T v_0^2 + \frac{1}{2}\beta_\Delta v_0^4\right] + \left[-a_T v_1^2 + \beta_\Delta v_0^2 v_1^2\right] \\ &\quad + \alpha\left[\frac{1}{2}\beta_\Delta v_1^4\right] + O(\alpha^2).\end{aligned} \tag{163}$$

The leading order is α^{-1} and comes solely from the mean field contribution, which is therefore the leading contribution in Eq. (159) and coincides with Eq. (145),

$$f_0/{\rm vol} = -a_T^2/\beta_\Delta . \tag{164}$$

This part of energy can also be viewed as an equation determining v_0.

Substituting v_0 into the expression in the second square bracket in Eq. (163) makes it zero. The only contribution to the order α^0 comes from the second term in Eq. (159), the "tr log," $-2^{5/2}\pi \log\{\int_\psi e^{-(1/\alpha)f_2}\}$, which is equal to

$$\begin{aligned}&= \frac{1}{2^{3/2}\pi^2}\int_k \{\log[G_0^O(k)] + \log[G_0^A(k)]\} \\ &= \frac{1}{2^{3/2}\pi^2}\int_k [\log(\mu_{O\mathbf{k}}^2 + k_z^2/2) + \log(\mu_{A\mathbf{k}}^2 + k_z^2/2)].\end{aligned} \tag{165}$$

When we take the leading order in the expansion of the excitation spectrum in powers of α,

$$\begin{aligned}(\mu_{\mathbf{k}}^{O,A})^2 &= a_T + v^2(2\beta_{\mathbf{k}} \pm |\gamma_{\mathbf{k}}|) \\ &= a_T + v_0^2(2\beta_{\mathbf{k}} \pm |\gamma_{\mathbf{k}}|) + \alpha v_1^2(2\beta_{\mathbf{k}} \pm |\gamma_{\mathbf{k}}|) + \cdots \\ &= (\mu_{0\mathbf{k}}^{O,A})^2 + \alpha v_1^2(2\beta_{\mathbf{k}} \pm |\gamma_{\mathbf{k}}|) + \cdots ,\end{aligned} \tag{166}$$

the one loop energy becomes

$$\begin{aligned}\frac{f_1}{\rm vol} &= \frac{1}{2^{3/2}\pi^2}\int_k \{\log[(\mu_{0\mathbf{k}}^O)^2 + k_z^2/2] + \log[(\mu_{0\mathbf{k}}^A)^2 + k_z^2/2]\} \\ &= \frac{1}{\pi}\int_{\mathbf{k}} (\mu_{0\mathbf{k}}^O + \mu_{0\mathbf{k}}^A) = 2.848|a_T|^{1/2}.\end{aligned} \tag{167}$$

3. Renormalization of the field shift and spurious infrared divergencies

a. Energy to two loops: Infrared divergent renormalization of the shift

To order α, corresponding to two loops, one has the first contribution from the mean field part, which contains v_1, namely, the third square bracket in Eq. (163). The tr log term [Eq. (165)] contributes due to leading correction to the excitation spectrum [Eq. (166)],

$$\begin{aligned}&\frac{1}{2^{3/2}\pi^2}\alpha v_1^2 \int_k \left[\frac{2\beta_{\mathbf{k}} + |\gamma_{\mathbf{k}}|}{(\mu_{0\mathbf{k}}^O)^2 + k_z^2/2} + \frac{2\beta_{\mathbf{k}} - |\gamma_{\mathbf{k}}|}{(\mu_{0\mathbf{k}}^A)^2 + k_z^2/2}\right] \\ &\quad = \alpha v_1^2 \frac{1}{2\pi}\int_{\mathbf{k}} \left[\frac{2\beta_{\mathbf{k}} + |\gamma_{\mathbf{k}}|}{\mu_{0\mathbf{k}}^O} + \frac{2\beta_{\mathbf{k}} - |\gamma_{\mathbf{k}}|}{\mu_{0\mathbf{k}}^A}\right],\end{aligned} \tag{168}$$

while the rest of the contributions in Eq. (159) are drawn as Feynman two-loop diagrams in Fig. 7 and cannot contain v_1 since propagators and vertices already provide one factor α. The minimization with respect to v_1^2 results in

$$\begin{aligned}v_1^2 &= -\frac{1}{2\pi\beta_\Delta}\int_{\mathbf{k}} \left[\frac{2\beta_{\mathbf{k}} + |\gamma_{\mathbf{k}}|}{\mu_{0\mathbf{k}}^O} + \frac{2\beta_{\mathbf{k}} - |\gamma_{\mathbf{k}}|}{\mu_{0\mathbf{k}}^A}\right] \\ &= -\frac{1}{2\pi}\int_{\mathbf{k}} \frac{1}{\mu_{0\mathbf{k}}^A} - \frac{1}{2\pi\beta_\Delta}\int_{\mathbf{k}} \left[\frac{2\beta_{\mathbf{k}} + |\gamma_{\mathbf{k}}|}{\mu_{0\mathbf{k}}^O} - \frac{\beta_\Delta}{a_T}\mu_{0\mathbf{k}}^A\right].\end{aligned} \tag{169}$$

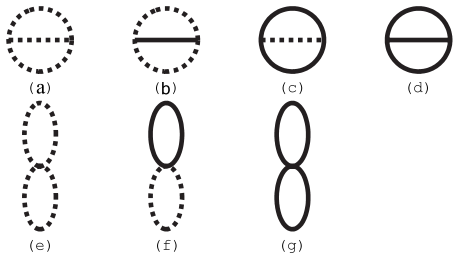

FIG. 7. Two loops connected diagrams contributing to free energy.

Due to additional softness of the A mode $e^A_{0\mathbf{k}} \propto |\mathbf{k}|^4$, the first ("bubble") integral diverges logarithmically near $\mathbf{k} \to \mathbf{0}$,

$$\int d^2\mathbf{k}(\mu^A_{0\mathbf{k}})^{-1} \simeq \left[-\frac{1}{a_T(2\beta_{4\Delta}/\beta_\Delta - 1/8)} \right]^{1/2} \times \int \frac{d^2\mathbf{k}}{|\mathbf{k}|^2} \propto \log L. \tag{170}$$

This means apparently that for the infinite infrared cutoff fluctuations destroy the inhomogeneous ground state, namely, the state with lowest energy is a homogeneous liquid. It is plausible that since the divergence is logarithmic, we might be at lower critical dimensionality in which an analog of Mermin-Wagner theorem (Mermin and Wagner, 1966; Itzykson and Drouffe, 1991) is applicable. Even this does not necessarily means that perturbation theory starting from ordered ground state is useless (Jevicki, 1977). A rigorous way to proceed in these situations has been found while considering simpler models such as the "φ^4 model," $F=\frac{1}{2}(\nabla\varphi^a)^2 + V(\varphi^{a2})$, in $D=2$ with number of components larger than 1, say $a=1,2$. Considering the corresponding statistical sum, one first integrates exactly zero modes, existing due to spontaneous breaking of a continuous symmetry [U(1) in our case; field rotations in the φ^4 model], and then develops a perturbation theory via steepest descent method for the rest of the variables. When the zero mode (the above mentioned Goldstone boson with $k=0$) is taken out, there appears a single configuration with lowest energy and the steepest descent is well defined. For invariant quantities such as energy this procedure simplifies: one actually can forget for a moment about integration over zero mode and proceed with the calculation as if it is done in the ordered phase. The invariance of the quantities ensures that the zero mode integration trivially factorizes. This is no longer true for noninvariant quantities for which the machinery of "collective coordinate method" should be used (Rajaraman, 1982). In our case, we first note that the shift of the field is not a U(1) or translation invariant quantity, so invariant quantities such as energy might be still calculable. Moreover, the sign of the divergence is negative and a physically reasonable possibility that the shift decreases as a power of cutoff,

$$v^2 \approx v_0^2\left[1 - \alpha c \log L + \frac{1}{2}(\alpha c \log L)^2 + \cdots\right] \approx v_0^2 e^{-\alpha c \log L} = \frac{v_0^2}{L^{\alpha c}}. \tag{171}$$

b. IR divergences in energy: The "nondiagrammatic" mean field and Tr log contributions

Substituting the IR divergent correction v_1 [Eq. (169)] back into the free energy [Eqs. (163) and (168)], one obtains a divergent contribution for the nondiagrammatic terms in the following equation:

$$\frac{1}{2}\beta_\Delta v_1^4 + v_1^2\frac{1}{2\pi}\int_{\mathbf{k}}\left[\frac{2\beta_{\mathbf{k}} + |\gamma_{\mathbf{k}}|}{\mu^O_{0\mathbf{k}}} + \frac{2\beta_{\mathbf{k}} - |\gamma_{\mathbf{k}}|}{\mu^A_{0\mathbf{k}}}\right] = -\frac{1}{2(2\pi)^2\beta_\Delta}\left\{\int_{\mathbf{k}}\frac{\beta_\Delta}{\mu^A_{0\mathbf{k}}} + \int_{\mathbf{k}}\left(\frac{2\beta_{\mathbf{k}} + |\gamma_{\mathbf{k}}|}{\mu^O_{0\mathbf{k}}} - \frac{\beta_\Delta}{a_T}\mu^A_{0\mathbf{k}}\right)\right\}^2, \tag{172}$$

containing both the $(\log L)^2$,

$$\frac{f^1_{\text{div}}}{\text{vol}} = -\frac{\beta_\Delta}{2(2\pi)^2}\int_{\mathbf{k},\mathbf{l}}\frac{1}{\mu^A_{0\mathbf{k}}\mu^A_{0\mathbf{l}}} \tag{173}$$

and the subleading $\log L$ divergences. However, we have not finished yet with the order α. They also likely to have divergences naively even worse than logarithmic. We therefore return to the rest of contributions to the two loop order.

c. "Setting sun" diagrams

One gets several classes of diagrams in Fig. 7; some of them IR divergent. The naively most divergent diagram [Fig. 2(a)] actually converges. It contains however two AAA vertices, each one of them is proportional to the fourth power of momenta. The integrals over k_z and l_z can be explicitly performed using

$$\frac{1}{2\pi}\int_{k_z}\int_{l_z}\frac{1}{k_z^2/2 + \mu^2_{\mathbf{k}}}\frac{1}{l_z^2/2 + \mu^2_{\mathbf{l}}}\frac{1}{(k_z + l_z)^2/2 + \mu^2_{\mathbf{k}+\mathbf{l}}} = \frac{\pi}{\mu_{\mathbf{k}}\mu_{\mathbf{l}}\mu_{\mathbf{k}+\mathbf{l}}(\mu_{\mathbf{k}} + \mu_{\mathbf{l}} + \mu_{\mathbf{k}+\mathbf{l}})}. \tag{174}$$

The divergences appear when one or more factors in the denominator belong to the A mode for which $\mu_{\mathbf{k}} \propto |\mathbf{k}|^2$ for small $\mathbf{k}$. However, if the numerator vanishes at these momenta, the diagram is finite. The numerators contain vertices involving the same supersoft field A and typically vertices in theories with spontaneous symmetry breaking are also soft (this fact is known in field theoretical literature as "soft pion" theorem due to their appearance in particle physics). In the present case they are supersoft. The AAA vertex function [Eq. (154)] is

$$\Lambda_3^{AAA}(\mathbf{k},\mathbf{l},\mathbf{m}) = \frac{iL_xL_y}{2^5\pi^{7/2}}\frac{v_0}{3}\{c_{\mathbf{k}}^* c_{\mathbf{l}} c_{\mathbf{m}}[0,-\mathbf{k}|\mathbf{l},\mathbf{m}] + c_{\mathbf{l}}^* c_{\mathbf{k}} c_{\mathbf{m}}[0,-\mathbf{l}|\mathbf{k},\mathbf{m}] + c_{\mathbf{m}}^* c_{\mathbf{l}} c_{\mathbf{k}}[0,-\mathbf{m}|\mathbf{l},\mathbf{k}] - c_{\mathbf{k}} c_{\mathbf{l}}^* c_{\mathbf{m}}^*[-\mathbf{l},-\mathbf{m}|0,\mathbf{k}] - c_{\mathbf{l}} c_{\mathbf{k}}^* c_{\mathbf{m}}^*[-\mathbf{k},-\mathbf{m}|0,\mathbf{l}] - c_{\mathbf{m}} c_{\mathbf{l}}^* c_{\mathbf{k}}^*[-\mathbf{l},-\mathbf{k}|0,\mathbf{m}]\}. \quad (175)$$

One easily sees that for each of the "dangerous" momenta $\mathbf{k}=\mathbf{0}$, $\mathbf{l}=\mathbf{0}$, or $\mathbf{m}=\mathbf{0}$ each one of the two vertices vanishes. For example, when $\mathbf{k}=\mathbf{0}$,

$$\Lambda_3^{AAA}(\mathbf{0},\mathbf{l},\mathbf{m}) = i\frac{L_xL_y}{2^5\pi^{7/2}}\frac{v_0}{3}\{c_{\mathbf{l}} c_{\mathbf{m}}[0,0|\mathbf{l},\mathbf{m}] + c_{\mathbf{l}}^* c_{\mathbf{m}}[0,-\mathbf{l}|\mathbf{0},\mathbf{m}] + c_{\mathbf{m}}^* c_{\mathbf{l}}[0,-\mathbf{m}|\mathbf{l},\mathbf{0}] - c_{\mathbf{l}}^* c_{\mathbf{m}}^*[-\mathbf{l},-\mathbf{m}|0,\mathbf{0}] - c_{\mathbf{l}} c_{\mathbf{m}}^*[0,-\mathbf{m}|0,\mathbf{l}] - c_{\mathbf{m}} c_{\mathbf{l}}^*[-\mathbf{l},\mathbf{0}|0,\mathbf{m}]\}$$
$$= v_0 i\frac{1}{2^3\pi^{3/2}}\frac{1}{3}\delta_{\mathbf{l}+\mathbf{m}}\{|\gamma_{\mathbf{l}}| + 2\beta_{\mathbf{l}} - |\gamma_{\mathbf{l}}| - 2\beta_{\mathbf{l}}\}$$
$$= 0. \quad (176)$$

This means that there are at least two powers of k in the numerator and the integral converges. There are no other powerwise divergencies left to the two loop order. Analogous analysis of the OOA vertex shows that the OOA setting sun diagram [Fig. 7(c)] is also convergent.

Naively logarithmically divergent AAO setting sun diagram, Fig. 7(b) actually has both the $\log^2 L$ and the $\log L$ divergences. The AAO vertex function is

$$\Lambda_3^{AAO}(\mathbf{k},\mathbf{l},\mathbf{m}) = \frac{v_0L_xL_y}{2^5\pi^{7/2}}\{c_{\mathbf{l}} c_{\mathbf{m}}^* c_{\mathbf{k}}^*[-\mathbf{k},-\mathbf{m}|0,\mathbf{l}] + c_{\mathbf{k}}^* c_{\mathbf{l}} c_{\mathbf{m}}[0,-\mathbf{k}|\mathbf{l},\mathbf{m}] + c_{\mathbf{l}}^* c_{\mathbf{k}} c_{\mathbf{m}}[0,-\mathbf{l}|\mathbf{k},\mathbf{m}] - c_{\mathbf{m}}^* c_{\mathbf{l}} c_{\mathbf{k}}[0,-\mathbf{m}|\mathbf{l},\mathbf{k}] - c_{\mathbf{l}}^* c_{\mathbf{m}} c_{\mathbf{k}}^*[-\mathbf{l},-\mathbf{k}|0,\mathbf{m}] + c_{\mathbf{l}} c_{\mathbf{m}}^* c_{\mathbf{k}}^*[-\mathbf{l},-\mathbf{m}|0,\mathbf{k}]\}. \quad (177)$$

We need its asymptotic when one of the momenta of the soft excitation A is small,

$$\Lambda_3^{AAO}(\mathbf{0},\mathbf{l},\mathbf{m}) = \frac{v_0}{2^2\pi^{3/2}}\delta_{\mathbf{l}+\mathbf{m}}|\gamma_{\mathbf{l}}|. \quad (178)$$

The diagram of Fig. 7(b), after integration over the field direction momenta k_z, l_z, is

$$-2^5\pi^3 L_z\int_{\mathbf{k},\mathbf{l},\mathbf{m}}\frac{\Lambda_3^{AAO}(\mathbf{k},\mathbf{l},\mathbf{m})\Lambda_3^{AAO}(-\mathbf{k},-\mathbf{l},-\mathbf{m})}{\mu_{\mathbf{k}}^A\mu_{\mathbf{l}}^A\mu_{\mathbf{m}}^O(\mu_{\mathbf{k}}^A+\mu_{\mathbf{l}}^A+\mu_{\mathbf{m}}^O)}. \quad (179)$$

The leading divergence is determined by the asymptotics of the integrand as both $\mathbf{k}$ and $\mathbf{l}$ approach zero. Consequently, it is given by the integral when the two vertex functions replaced with their values taken at $\mathbf{k}=\mathbf{l}=\mathbf{0}$ and momenta of $\mu_{\mathbf{k}}^O$ and $\mu_{\mathbf{k}}^O+\mu_{\mathbf{l}}^A+\mu_{\mathbf{m}}^A$ in the denominator also taken to zero. The $\log^2 L$ divergent part near $\mathbf{k}=\mathbf{l}=\mathbf{0}$ is therefore

$$f_{\rm div}^2 = -2^5\pi^3 L_z\int_{\mathbf{k},\mathbf{l},\mathbf{m}}\frac{\Lambda_3^{AAO}(\mathbf{0},\mathbf{l},\mathbf{m})\Lambda_3^{AAO}(0,-\mathbf{l},-\mathbf{m})}{\mu_{\mathbf{k}}^A\mu_{\mathbf{l}}^A\mu_{\mathbf{l}}^O(\mu_{\mathbf{0}}^A+\mu_{\mathbf{l}}^A+\mu_{\mathbf{l}}^O)}$$
$$= -\frac{L_zL_xL_y}{2^2\pi^2}v_0^2\int_{\mathbf{k},\mathbf{l}}\frac{2|\gamma_{\mathbf{0}}|^2}{\mu_{\mathbf{k}}^A\mu_{\mathbf{l}}^A\mu_{\mathbf{0}}^O\mu_{\mathbf{0}}^O}$$
$$= -\frac{\rm vol}{(2\pi)^2}\int_{\mathbf{k},\mathbf{l}}\frac{\beta_\Delta}{\mu_{\mathbf{k}}^A\mu_{\mathbf{l}}^A}. \quad (180)$$

d. The bubble diagrams and cancellation of the leading divergences

Diagrams given in Figs. 7(e)–7(g) can be easily evaluated,

$$\frac{f_{(e,f,g)}}{\rm vol} = \frac{1}{(2\pi)^2}\int_{\mathbf{k},\mathbf{l}}\beta_{\mathbf{k}-\mathbf{l}}\left(\frac{1}{\mu_{\mathbf{k}}^O}+\frac{1}{\mu_{\mathbf{k}}^A}\right)\left(\frac{1}{\mu_{\mathbf{l}}^O}+\frac{1}{\mu_{\mathbf{l}}^A}\right) + \frac{1}{2\beta_A}\frac{1}{(2\pi)^2}\left\{\int_{\mathbf{k}}|\gamma_{\mathbf{k}}|\left(\frac{1}{\mu_{\mathbf{k}}^O}-\frac{1}{\mu_{\mathbf{k}}^A}\right)\right\}^2. \quad (181)$$

The leading divergence is

$$\frac{f_{\rm div}^3}{\rm vol} = \frac{3}{2}\frac{1}{(2\pi)^2}\int_{\mathbf{k},\mathbf{l}}\beta_\Delta\frac{1}{\mu_{\mathbf{k}}^A\mu_{\mathbf{l}}^A}. \quad (182)$$

One observes that sum of the three leading $(\log L)^2$ divergences given in Eqs. (173), (180), and (182) cancels. There are still subleading $\log L$ divergences. They require more care since "not dangerous" momenta cannot be put to zero and are treated next.

e. Cancellation of the IR divergencies

The two-loop contribution to energy in a "standard" form

$$f = \frac{V}{(2\pi)^2}\int_{\mathbf{k},\mathbf{l}}\frac{F(\mathbf{k},\mathbf{l})}{\mu_{\mathbf{k}}^A\mu_{\mathbf{l}}^A}. \quad (183)$$

In order to demonstrate cancellation of the IR divergences we investigate the value of the numerator $F(\mathbf{k},\mathbf{l})$ at $\mathbf{k}=0$ and $\mathbf{l}=0$ and show that $F(\mathbf{k}=\mathbf{0},\mathbf{l})=0$ and $F(\mathbf{k},\mathbf{l}=\mathbf{0})=0$. The part due to nondiagrammatic terms [Eq. (172)] can be written as

$$F^1(\mathbf{k},\mathbf{l}) = -\frac{1}{2\beta_\Delta}\left[\frac{2\beta_{\mathbf{k}}+|\gamma_{\mathbf{k}}|}{\mu_{\mathbf{k}}^O}\mu_{\mathbf{k}}^A + 2\beta_{\mathbf{k}} - |\gamma_{\mathbf{k}}|\right] \times\left[\frac{2\beta_{\mathbf{l}}+|\gamma_{\mathbf{l}}|}{\mu_{\mathbf{l}}^O}\mu_{\mathbf{l}}^A + 2\beta_{\mathbf{l}} - |\gamma_{\mathbf{l}}|\right], \quad (184)$$

$$F^1(0,\mathbf{l}) = -\frac{\mu_{\mathbf{l}}^A}{2}\left[\frac{2\beta_{\mathbf{l}}+|\gamma_{\mathbf{l}}|}{\mu_{\mathbf{l}}^O}+\frac{2\beta_{\mathbf{l}}-|\gamma_{\mathbf{l}}|}{\mu_{\mathbf{l}}^A}\right],$$

similarly, the setting sun diagram

$$F^2(\mathbf{0},\mathbf{l}) = -\frac{v_0^2 2|\gamma_{\mathbf{l}}|^2}{\mu_{\mathbf{l}}^O(\mu_{\mathbf{l}}^A+\mu_{\mathbf{l}}^O)} = -\frac{\beta_\Delta v_0^2|\gamma_{\mathbf{l}}|}{\mu_{\mathbf{l}}^O(\mu_{\mathbf{l}}^A+\mu_{\mathbf{l}}^O)}\frac{(\mu_{\mathbf{l}}^O)^2-(\mu_{\mathbf{l}}^A)^2}{|a_T|} = -\mu_{\mathbf{l}}^A|\gamma_{\mathbf{l}}|\left(\frac{1}{\mu_{\mathbf{l}}^A}-\frac{1}{\mu_{\mathbf{l}}^O}\right), \tag{185}$$

according to Eq. (180). The divergent part of the bubble diagrams can be written as

$$F^3(\mathbf{0},\mathbf{l}) = \frac{\mu_{\mathbf{l}}^A}{2}\left[|\gamma_{\mathbf{l}}|\left(\frac{1}{\mu_{\mathbf{l}}^A}-\frac{1}{\mu_{\mathbf{l}}^O}\right)+2\beta_{\mathbf{l}}\left(\frac{1}{\mu_{\mathbf{l}}^A}-\frac{1}{\mu_{\mathbf{l}}^O}\right)\right]. \tag{186}$$

One explicitly observes that $F^1(\mathbf{0},\mathbf{l})+F^2(\mathbf{0},\mathbf{l})+F^3(\mathbf{0},\mathbf{l})=0$. The same happens for $F^1(\mathbf{k},\mathbf{0})+F^2(\mathbf{k},\mathbf{0})+F^3(\mathbf{k},\mathbf{0})=0$. Therefore all IR divergences, e.g., the $\log L$ and $(\log L)^2$, canceled. Similar cancellations of all the logarithmic IR divergencies occur in scalar models with Goldstone bosons in $D=2$ and $D=3$ [where the divergencies are known as spurious (Jevicki, 1977; David, 1981)].

f. Vortex lattice energy

For the finite result for the Gibbs free energy to two loops, finite parts of the integrals were calculated numerically. Up to two loops the calculation (Li and Rosenstein, 2002a, 2002b, 2002c) [extending the one carried in Rosenstein (1999) to umklapp processes) gives

$$f_d(a_T) = \frac{f}{\text{vol}} = -\frac{a_T^2}{2\beta_\Delta}+2.848|a_T|^{1/2}+\frac{2.4}{a_T}. \tag{187}$$

In regular units the free energy density is

$$\frac{\mathcal{F}}{\text{vol}} = \frac{H_{c2}^2}{2\pi\kappa^2}\left(\frac{\sqrt{\text{Gi}}bt}{4\pi}\right)^{4/3}\left(-\frac{a_T^2}{2\beta_\Delta}+2.848|a_T|^{1/2}+\frac{2.4}{a_T}\right). \tag{188}$$

Below we use this expression to determine the melting line and various thermal and magnetic properties of the vortex solid: magnetization, entropy, and specific heat. Near the melting point $a_T\approx -9.5$ the precision becomes of order 0.1% allowing comparison with the free energy of vortex liquid, which is much harder to get. Eventually the (asymptotic) expansion becomes inapplicable near the spinodal point at which the crystal is unstable due to thermal "softening." This is considered using the Gaussian approximation in Sec. III.D.

4. Correlators of the U(1) phase and the structure function

a. Correlator of the U(1) phase and helicity modulus

The correlator of the order parameter is finite at all distances in the absence of thermal fluctuations,

$$C_{\text{mf}}(r,r') = \psi^*(r)\psi(r') = v_0^2\varphi^*(r)\varphi(r'), \tag{189}$$

where $v_0^2=|a_T|/\beta_\Delta$ is finite exhibiting the phase long range order in the vortex lattice (despite periodic modulation). However, the order is expected to be disturbed by thermal fluctuations. Leading order perturbation theory gives an early indication of the loss of the order in directions perpendicular to the field. The leading correction consists of the α correction to the shift v [Eq. (169)] and sum of two propagators,

$$C(r,r') = \int_{k,l}\varphi_k^*(r)\varphi_l(r')\left\langle\left[v\,\delta_k+\frac{c_{\mathbf{k}}^*}{\sqrt{2}(2\pi)^{3/2}}(O_k-iA_k)\right]\times\left[v\,\delta_l+\frac{c_{\mathbf{l}}}{\sqrt{2}(2\pi)^{3/2}}(O_l+iA_l)\right]\right\rangle = C^{(0)}(r,r')+\alpha\left\{v_1^2\varphi^*(r)\varphi(r')+\frac{1}{2(2\pi)^3}\times\int_k[G_0^A(k)+G_0^O(k)]\varphi_k^*(r)\varphi_k(r')\right\}+O(\alpha^2). \tag{190}$$

One observes that the logarithmic divergences of the second and the third terms cancel but that the correlator in the x-y plane depends on the large distance $\mathbf{r}-\mathbf{r}'$ as a log,

$$C(\mathbf{r},z=0,\mathbf{r}',z'=0) \sim v_0^2\varphi^*(\mathbf{r})\varphi(\mathbf{r}')\left\{1+\frac{\alpha}{2\pi}\int_{\mathbf{k}}[e^{i\mathbf{k}\cdot(\mathbf{r}-\mathbf{r}')}-1]\frac{1}{\mu_{0\mathbf{k}}^A}\right\} = v_0^2\varphi^*(\mathbf{r})\varphi(\mathbf{r}')[1+\alpha c\log|\mathbf{r}-\mathbf{r}'|]. \tag{191}$$

It is expected that exactly as the expectation value v dependence on IR cutoff, the actual correlator is not growing logarithmically but rather decreasing as a power $|\mathbf{r}-\mathbf{r}'|^{-c}$. This is an example of the Berezinsky-Kosterlitz-Thouless phenomenon (Itzykson and Drouffe, 1991). It appears, however, at rather high dimensionality $D=3$. Note that the LLL constraint (large magnetic fields) effectively reduces dimensionality, enhancing the role of thermal fluctuations.

In the direction parallel to the field the correlations are still long range. Indeed the helicity modulus is

$$C(\mathbf{r}=\mathbf{0},z,\mathbf{r}'=\mathbf{0},z') \sim v_0^2\left\{1+\frac{\alpha 4\pi\sqrt{2}}{2(2\pi)^3}\int_k[e^{ik_z(z-z')}-1]\frac{1}{(\mu_{0\mathbf{k}}^A)^2+k_z^2/2}\right\} \sim v_0^2. \tag{192}$$

b. Structure function: Definitions

The superfluid density correlator, defined by

$$\tilde{S}(r) = \frac{1}{\mathrm{vol}} \int_{r'} \langle |\psi(r')|^2 |\psi(r'+r)|^2 \rangle, \tag{193}$$

quantifies spontaneous breaking of the translational and rotational symmetries only as in both locations the superfluid density is invariant under the U(1) gauge transformations. This is different from the phase correlator $\langle \psi^*(r)\psi(r') \rangle$ discussed in the previous section, which decays as a power as indicated by the IR divergences. As in the case of the U(1) phase correlations, it is easier to consider the Fourier transform of the correlator, the structure function. Since translational symmetry is not broken along the field direction, one can restrict the discussion to the lateral correlations and consider partial Fourier transform,

$$S(\mathbf{q},0) = \int d\mathbf{r} e^{i\mathbf{q}\cdot\mathbf{r}} \tilde{S}(\mathbf{r}, r_z = 0). \tag{194}$$

In this section the structure function is calculated to leading order in thermal fluctuation strength (harmonic approximation) within the LLL, namely, neglecting higher a_H corrections. We discuss these corrections later.

c. Structure function of the vortex crystal without thermal fluctuations

Substituting the LLL mean field solution [Eq. (61)] into the definition of structure function one obtains

$$\begin{aligned} S_{\mathrm{mf}}(\mathbf{q},0) &\equiv \frac{1}{L_x L_y} \left(\frac{a_T}{\beta_A}\right)^2 \int_{\mathbf{r}} e^{i\mathbf{q}\cdot\mathbf{r}} \int_{\mathbf{r}'} |\varphi(\mathbf{r}')|^2 |\varphi(\mathbf{r}'+\mathbf{r})|^2 \\ &= \left(\frac{a_T}{\beta_A}\right)^2 \frac{1}{2\pi} \int_{\mathrm{cell}} |\varphi(\mathbf{r}')|^2 e^{-i\mathbf{q}\cdot\mathbf{r}'} \int_{\mathbf{r}} |\varphi(\mathbf{r})|^2 e^{i\mathbf{q}\cdot\mathbf{r}} \\ &= \left(\frac{a_T}{\beta_A}\right)^2 4\pi^2 \sum_{\mathbf{K}} \delta(\mathbf{q}-\mathbf{K}) e^{-\mathbf{q}^2/2}, \end{aligned} \tag{195}$$

where we made use of formulas in Appendix A and delta function peaks are located at vectors of the reciprocal lattice. The height of the peak decreases rapidly beyond the reciprocal magnetic length (which is our unit). When mesoscopic thermal fluctuations are significant, they might broaden the peaks far below the temperature at which the lattice becomes unstable (the spinodal point).

d. Leading order corrections to thermal broadening of Bragg peaks

The calculation of the structure function closely follows that of free energy. The correlator is calculated using the Wick contractions,

$$\begin{aligned} \tilde{S}(\mathbf{r}, z=0) = \frac{1}{L_x L_y} \int_{k,l,k',l',\mathbf{r}'} & \varphi^*_{\mathbf{k}}(\mathbf{r}') \varphi_{\mathbf{l}}(\mathbf{r}') \varphi^*_{\mathbf{k}'}(\mathbf{r}'+\mathbf{r}) \\ & \times \varphi_{\mathbf{l}'}(\mathbf{r}'+\mathbf{r}) \left[v\delta_k + \frac{c^*_{\mathbf{k}}}{\sqrt{2}(2\pi)^{3/2}} (O_k - iA_k) \right] \\ & \times \left[v\delta_l + \frac{c_{\mathbf{l}}}{\sqrt{2}(2\pi)^{3/2}} (O_l + iA_l) \right] \\ & \times \left[v\delta_{k'} + \frac{c^*_{\mathbf{k}'}}{\sqrt{2}(2\pi)^{3/2}} \times (O_{k'} - iA_{k'}) \right] \\ & \times \left[v\delta_{l'} + \frac{c_{\mathbf{l}'}}{\sqrt{2}(2\pi)^{3/2}} (O_{l'} + iA_{l'}) \right]. \end{aligned} \tag{196}$$

The leading order (α^0) term is the mean field part [Eq. (195)], while the first order term is the harmonic fluctuation part.

The fluctuation part contains v_1 correction term $S_4(\mathbf{q},0)$, same in structure as the leading order but with (IR diverging) coefficient $2(a_T/\beta_A)v_1^2 4\pi^2$ instead of $(a_T/\beta_A)^2 4\pi^2$ and four contractions (diagrams),

$$\begin{aligned} & \frac{v_0^2}{L_x L_y [\sqrt{2}(2\pi)^{3/2}]^2} \int_{k,l,k',l',\mathbf{r}'} \varphi^*_{\mathbf{k}}(\mathbf{r}') \varphi_{\mathbf{l}}(\mathbf{r}') \\ & \quad \times \varphi^*_{\mathbf{k}'}(\mathbf{r}'+\mathbf{r}) \varphi_{\mathbf{l}'}(\mathbf{r}'+\mathbf{r}) \{ c^{*2}_{\mathbf{k}} (G^O_{0k} - G^A_{0k}) \delta_l \delta_{l'} \delta_{k+k'} \\ & \quad + c^2_{\mathbf{l}} (G^O_{0l} - G^A_{0l}) \delta_k \delta_{k'} \delta_{l+l'} + 2(G^O_{0k} + G^A_{0k}) \delta_{k'} \delta_{l'} \delta_{k+l} \\ & \quad + 2(G^O_{0k} + G^A_{0k}) \delta_l \delta_{k'} \delta_{k+l'} \}. \end{aligned} \tag{197}$$

Performing integrations and Fourier transforms using methods described in Appendix A the first two contributions are

$$\begin{aligned} S_1(\mathbf{q},0) = \frac{4\pi a_T}{\beta_A} \cos(k_x k_y + \mathbf{k}\times\mathbf{Q} + \theta_{\mathbf{k}}) e^{-\mathbf{q}^2/2} [(\mu^O_{0\mathbf{k}})^{-1} \\ - (\mu^A_{0\mathbf{k}})^{-1}], \end{aligned} \tag{198}$$

where $\mathbf{Q}$ and $\mathbf{k}$ are the "integer" and the "fractional" parts of $\mathbf{q}$ in a sense $\mathbf{q}=\mathbf{k}+\mathbf{Q}$ for $\mathbf{k}$ inside Brillouin zone and $\mathbf{Q}$ on the reciprocal lattice. The third term is

$$S_2(\mathbf{q},0) = \frac{4\pi a_T}{\beta_A} e^{-\mathbf{q}^2/2} [(\mu^O_{0\mathbf{k}})^{-1} + (\mu^A_{0\mathbf{k}})^{-1}], \tag{199}$$

while the last is

$$\begin{aligned} S_3(\mathbf{q},0) = \frac{4\pi a_T}{\beta_A} \delta_n(\mathbf{q}) e^{-\mathbf{q}^2/2} \int_{\mathbf{k}} \cos(\mathbf{k}\times\mathbf{Q}) [(\mu^O_{0\mathbf{k}})^{-1} \\ + (\mu^A_{0\mathbf{k}})^{-1}]. \end{aligned} \tag{200}$$

e. Cancellation of the infrared divergences

Although all of the four terms S_1, S_2, S_3, and S_4 are divergent as any of the peaks is approached, $\mathbf{k}\to 0$, the sums S_1, S_2 and S_3, S_4 are not. We start with the first two,

TABLE I. Values of $f_2(\mathbf{Q})$ with small n_1,n_2.

n_1,n_2	(0, 1), (1, 0), (1, 1)	(1, 2), (0, 2), (2, 2)	(1, 3)
$f_2(\mathbf{Q})/(2\pi)$	−5.20	−7.11	−8.31

$$S_1 + S_2 = (4\pi a_h/\beta_A)e^{-\mathbf{q}^2/2} f_1(\mathbf{q}), \tag{201}$$

where

$$f_1(\mathbf{q}) = [1 + \cos(k_x k_y + \mathbf{k}\times\mathbf{Q} + c_k)](\mu^O_{0\mathbf{k}})^{-1} + [1 - \cos(k_x k_y + \mathbf{k}\times\mathbf{Q} + c_{\mathbf{k}})](\mu^A_{0\mathbf{k}})^{-1}. \tag{202}$$

When $\mathbf{k}\to 0$, it can be shown that $k_x k_y + c_k = O(\mathbf{k}^{2\cdot 2})$, thus $(k_x k_y + \mathbf{k}\times\mathbf{Q} + c_k \to \mathbf{k}\times\mathbf{Q}$ and $1-\cos(k_x k_y + \mathbf{k}\times\mathbf{Q} + c_k) \to (\mathbf{k}\times\mathbf{Q})^2$. Hence it will cancel the $1/k^2$ singularity coming from $1/\mu^A_{0\mathbf{k}}$. Thus $f_1(\mathbf{q})$ approaches const+const $\times(\mathbf{k}\times\mathbf{Q})^2/k^2$ when $\mathbf{Q}\neq 0$ and approaches const+const $\times k^6$ when $\mathbf{Q}=0$. Similarly the sum of $S_4(\mathbf{q},0)$ and $S_3(\mathbf{q},0)$ is not divergent, although separately they are. Their sum is

$$S_3(\mathbf{q},0) + S_4(\mathbf{q},0) = (4\pi a_T^{1/2}/\beta_A)\delta_n(\mathbf{q})e^{-\mathbf{q}^2/2}[f_2(\mathbf{Q}) + f_3], \tag{203}$$

with

$$f_2(\mathbf{Q}) = \int_{\mathbf{k}} [-1 + \cos(\mathbf{k}\times\mathbf{Q})][(\mu^O_{0\mathbf{k}})^{-1} + (\mu^A_{0\mathbf{k}})^{-1}],$$
$$f_3 = -\int_{\mathbf{k}} (\mu^O_{0\mathbf{k}} + \mu^A_{0\mathbf{k}}) = -8.96. \tag{204}$$

f. Supersoft phonons and the "halo" shape of the Bragg peaks

The sum of all four terms can be cast in the following form:

$$S(\mathbf{q},0) = \frac{4\pi^2}{\beta_A}\frac{a_T^2}{\beta_A}\delta_n(\mathbf{q})e^{-\mathbf{q}^2/2} + \frac{4\pi a_T^{1/2}}{\beta_A} \times e^{-\mathbf{q}^2/2}[f_1(\mathbf{q}) + \delta_n(\mathbf{q})f_2(\mathbf{Q}) + \delta_n(\mathbf{q})f_3]. \tag{205}$$

The results were compared (Li and Rosenstein, 2002a) with numerical simulation of the LLL system in Sasik and Stroud (1995). For reciprocal lattice vectors close to origin the value of $f_2(\mathbf{Q})$ is shown in Table I.

The correction to the height of the peak at $\mathbf{Q}$, $[c_1\Delta(\mathbf{q})/(1+c_1 f_3)]f_2(\mathbf{Q})$, is quite small. The theoretical prediction has roughly the same characteristic saddle shape halos around the peaks as in MC simulation (Sasik and Stroud, 1995) and experiment (Kim *et al.*, 1999). Conversely, MC simulation result provides the nonperturbative evidence $\mu^A_{0\mathbf{k}}\to|k|^2$ for small k_x, k_y. In Eq. (205), if $\mu^A_{0\mathbf{k}}\to|k|$, we get a contribution from the most singular term const+const$\times\frac{(\mathbf{k}\times\mathbf{Q})^2}{k}$. This term will become constant when $k\to 0$, and we will not get the same characteristic saddle shape halos around the peaks as in Sasik and Stroud (1995). Consequently, the $\mu^A_{0\mathbf{k}}\to|k|^2$ asymptotics for $k\to 0$ is crucial for such characteristic shape and thus the MC simulation result provides a nonperturbative evidence for it.

g. Magnetization profile

Another quantity which can be measured is the magnetic field distribution. In addition to constant magnetic field background there are $1/\kappa^2$ magnetization corrections due to field produced by supercurrent. To leading order in $1/\kappa^2$ magnetization is given by Eq. (123). The superfluid density $\langle|\psi(r)|^2\rangle$ is calculated as in Eq. (190),

$$\langle|\psi(\mathbf{r},z=0)|^2\rangle = \frac{a_T}{\beta_A}|\varphi(\mathbf{r})|^2 + \frac{1}{2\pi}\int_{\mathbf{k}}|\varphi_{\mathbf{k}}(x)|^2 \times\left(\frac{1}{\mu^A_{0\mathbf{k}}} + \frac{1}{\mu^O_{0\mathbf{k}}}\right) - \frac{1}{2\pi}\int_{\mathbf{k}}\left(\frac{2\beta_{\mathbf{k}} + |\gamma_{\mathbf{k}}|}{\beta_\Delta\mu^O_{0\mathbf{k}}} + \frac{2\beta_k - |\gamma_k|}{\beta_\Delta\mu^A_{0\mathbf{k}}}\right)|\varphi(\mathbf{r})|^2. \tag{206}$$

Its Fourier transform $\rho(\mathbf{q})\equiv\int d\mathbf{r}e^{i\mathbf{q}\cdot\mathbf{r}}\langle|\psi(\mathbf{r},z=0)|^2\rangle$ can be easily calculated,

$$\rho(\mathbf{q}) = 4\pi^2\delta_n(\mathbf{q})\left\{\frac{a_T}{\beta_A} + \frac{1}{2\pi}\int_{\mathbf{k}}\left[\left(e^{i\mathbf{k}\times\mathbf{q}} - \frac{2\beta_{\mathbf{k}} + |\gamma_{\mathbf{k}}|}{\beta_\Delta}\right)\times(\mu^O_{0\mathbf{k}})^{-1} + \left(e^{i\mathbf{k}\times\mathbf{q}} - \frac{2\beta_{\mathbf{k}} - |\gamma_{\mathbf{k}}|}{\beta_\Delta}\right)\times(\mu^A_{0\mathbf{k}})^{-1}\right]\right\}e^{-\mathbf{q}^2/4 + i\pi n_1(n_2+1)}. \tag{207}$$

Performing integrals, one obtains

$$\rho(\mathbf{q}) = 4\pi^2\delta_n(\mathbf{q})e^{-\mathbf{q}^2/4 + i\pi n_1(n_2+1)} \times\left\{\frac{a_T}{\beta_A} + \frac{1}{2\pi}[f_3 + f_2(\mathbf{Q})]a_T^{-1/2}\right\}. \tag{208}$$

The function $f_2(\mathbf{Q})$ and constant f_3 appeared in Eq. (204).

C. Basic properties of the vortex liquid: Gaussian approximation

1. The high temperature perturbation theory and its shortcomings

a. The loop expansion

Unlike the perturbation theory in the crystalline state, in which various translational, rotational, and gauge U(1) symmetries are spontaneously broken, the perturbation theory at high temperature is quite straightforward. One directly uses the quadratic and the quartic terms in the Boltzmann factor [Eq. (117)] as a "large" part K and a "perturbation" V,

$$K = \frac{1}{2^{5/2}\pi}f_0, \quad V = \frac{1}{2^{5/2}\pi}f_{\text{int}}. \tag{209}$$

Again the "parameter" α is actually 1 but is regarded as small and the actual expansion parameter will become

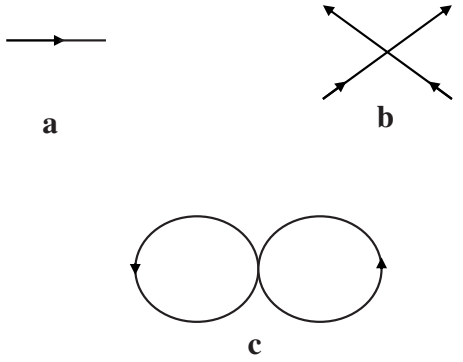

FIG. 8. Feynman rules and the diagrams in the homogeneous phase: (a) propagator, (b) vertex, (c) the two loop energy correction.

apparent shortly. The Feynman rules for a field ψ, namely, the propagator

$$G_0(k) = \frac{2^{5/2}\pi}{k_z^2/2 + a_T} \tag{210}$$

and the four-point vertex, are shown in Figs. 8(a) and 8(b), respectively, which is defined in Eq. (142). Since ψ is a complex field, we use an arrow to indicate the "orientation" of the propagator.

The leading contribution to the LLL scaled free energy, that of the quadratic theory, is

$$f_1 = 2^{5/2}\pi \,\mathrm{Tr}\log D^{-1}(k) = \frac{\mathrm{vol}}{2^{1/2}\pi^2}\int_k \log G(k)$$
$$= \frac{\mathrm{vol}}{2^{1/2}\pi^2}\int_{k_z} \log\frac{k_z^2/2 + a_T}{2^{5/2}\pi} = \mathrm{vol}\; 4a_T^{1/2} + \mathrm{const}. \tag{211}$$

The const in the last line is ultraviolet divergent but unimportant for our purposes and will be generally suppressed. Corrections can be conveniently presented as Feynman diagrams.

The next, "two-loop," correction is the diagram in Fig. 8(c), which reads

$$f_2 = \frac{1}{(2\pi)^6}\int_{k,l} \Lambda(k,l,k,l)G_0(k)G_0(l) = \mathrm{vol}\; 4a_T^{-1} \tag{212}$$

One observes that the k_z integrations can be reduced to corresponding integrations in quantum mechanics of the anharmonic oscillator (Thouless, 1975; Ruggeri and Thauless, 1976; Ruggeri, 1978), so that the series resemble a dimensionally reduced $D-2=1$ field theory or quantum mechanics.

b. Actual expansion parameter and the applicability range

This expansion can be carried to a high order after several simple tricks are learned (Thouless, 1975; Ruggeri and Thouless, 1976; Ruggeri, 1978; Hu and MacDonald, 1993; Hu *et al.*, 1994). The result to four loops is

$$f_d = 4a_T^{1/2} + 4/a_T - 17/2a_T^{5/2} + 907/24a_T^4. \tag{213}$$

One observes that the small parameter is $a_T^{-3/2}$ although coefficients grow and series are asymptotic. The difference with analogous expansion in the crystalline phase is that the sign of a_T is opposite and the leading order is $\sqrt{a_T}$ rather than a_T^2. Phenomenologically the region of positive large a_T is not very interesting since at that point, for example, magnetization is already small. Also higher Landau level effects become significant as discussed in Sec. III.E, where HLL effects (Prange, 1969) are considered.

Therefore attempts were made to extend the series to smaller temperatures. One of the simplest methods is to perform a Hartree-Fock-type resummation order by order. We first describe in some detail a certain variant of this type of approximation called generally Gaussian since it will be extensively used to treat thermal fluctuations as well as disorder effects in the following sections. It will be shown in Sec. III.D that the approximation is not just a variational scheme but constitutes a first approximant in a convergent series of approximants (which however are not series in an external parameter) called "optimized perturbation theory" (OPT).

2. General Gaussian approximation

a. Variational principle

We start from the simplest one parameter version of the Gaussian approximation which is quite sufficient to describe the basic properties of the vortex liquid well below the mean field transition point $a_T=0$. Within this approximation one introduces a variational parameter μ (which is physically an excitation energy of the vortex liquid) adding and subtracting a simple quadratic expression $\mu^2|\psi|^2$ from the Boltzmann factor,

$$f(\mu) = K + \alpha V, \tag{214}$$

$$K = \frac{1}{2^{5/2}\pi}\int_r \left(\mu^2|\psi|^2 + \frac{1}{2}|\partial_z\psi|^2\right) = \int_k \psi_k^* G^{-1}\psi_k,$$
$$V = \frac{1}{2^{5/2}\pi}\left[a_T\int_k |\psi_k|^2 + \frac{1}{2}\int_k \Lambda(k,l,k',l')\psi_k^*\psi_l\psi_{k'}^*\psi_{l'}\right], \tag{215}$$

where the constant a was defined by

$$a \equiv a_T - \mu^2. \tag{216}$$

Now one considers K as an "unperturbed" part and αV as a small perturbation. This is a different partition than the one we used previously to develop a perturbation theory. Despite the fact that $\alpha=1$, we develop perturbation theory as before. To first order in α, the scaled free energy is

$$f_{\text{Gauss}} = -2^{5/2}\pi \log\left\{\int_{\psi} e^{-K+\alpha V}\right\}$$
$$= -2^{5/2}\pi \log\left\{\int_{\psi} e^{-K+\alpha V}\right\}$$
$$\approx -2^{5/2}\pi \log\left\{\int_{\psi_k} e^{-K}[1+\alpha V]\right\}$$
$$= -2^{5/2}\pi \log\left\{Z_\mu + \alpha\int_{\psi_k} e^{-K} V\right\}$$
$$\approx -2^{5/2}\pi[\log Z_\mu - \alpha\langle V\rangle_\mu], \quad (217)$$

where Z_μ is the Gaussian partition function $Z_\mu = \int_{\psi_k} e^{-K}$ and thermal averages denoted by $\langle\cdots\rangle$ are made in this quadratic theory.

Collecting terms, one obtains

$$f_{\text{Gauss}}/\text{vol} = 2\mu + \alpha[2\mu + 2a/\mu + 4/\mu^2]. \quad (218)$$

Now comes the improvement. One optimizes the solvable quadratic large part by minimizing energy for $\alpha = 1$ with respect to μ. The optimization condition is called "gap equation,"

$$\mu^3 - a_T\mu - 4 = 0, \quad (219)$$

since the BCS approximation is one application of the general Gaussian approximation.

b. Existence of a metastable homogeneous state down to zero temperature: Pseudocritical fixed point

It is clear that the overheated solid becomes unstable at some finite temperature. It is not clear, however, whether overcooled liquid becomes unstable at some finite temperature (like water) or exists all the way down to $T=0$ as a metastable state. It was shown by (a) variety of methods that liquid (gas) phase of the classical one component Coulomb plasma exists as a metastable state down to zero fluctuation temperature with energy gradually approaching that of the Madelung solid and excitation energy diminishing (Leote de Carvalho *et al.*, 1999). It seems plausible that the same would happen with any system of particles repelling each other with sufficiently long range forces. In fact the vortex system in the London approximation becomes a sort of repelling particles with the force even more long range than Coulombic.

Note that there always exists one solution of this cubic equation for positive μ for all values of a_T, negative as well as positive. The excitation energy in the liquid decreases asymptotically as

$$\mu_{a_T\to-\infty} \sim -4/a_T \quad (220)$$

at temperatures approaching zero. Importantly it becomes small at the melting point located at $a_T = -9.5$ (see below). The Gaussian energy is shown in Fig. 9 (marked as the $T0$ line). The existence of the solution means that the homogeneous phase exists all the way down to $T=0$ albeit as a metastable state below the melting point at which the free energy of the solid is smaller (see Fig. 11). Physically this rather surprising fact is intimately related to repulsion of the vortex lines. It is well known that if in addition to repulsion there exists an attraction such as a long range attractive forces between atoms and molecules, they will lead to a spinodal point of the liquid (Lovett, 1977). However, if the attractive part is absent like in, for instance, electron liquid, one component plasma etc., the spinodal point is pushed down to zero temperature. It becomes a "pseudocritical" point, namely, exhibits criticality, but globally unstable due to existence of a lower energy state (Compagner, 1974). Scaled LLL free energy density diverges as a power as well,

$$f(a_T \to -\infty) \sim -a_T^2/2 \quad (221)$$

(see Fig. 9).

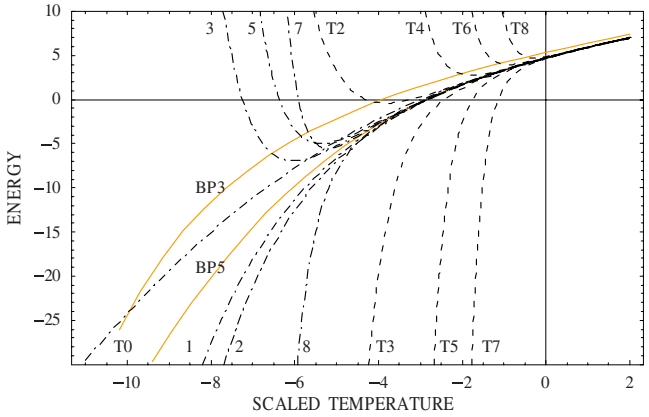

FIG. 9. (Color online) Free energy in liquid. The curve $T0$ is the Gaussian approximation, while $T1$,… are higher order renormalized perturbation theory results. Optimized perturbation theory gives curves 1,2,… and finally BP lines are the Borel-Pade results.

Assuming absence of singularities on the liquid branch allows us to develop an essentially precise theory of the LLL GL model in vortex liquid (even including overcooled liquid) using the Borel-Pade (BP) (Baker, 1990) method at any temperature. This calculation is carried out in Sec. III.D.3. The Gaussian liquid state can be used as a starting point of "renormalized" perturbation theory around it. Such an expansion was first developed by Ruggeri and Thouless (Thouless, 1975; Ruggeri and Thouless, 1976; Ruggeri, 1978) for the GL model.

D. More sophisticated theories of vortex liquid

1. Perturbation theory around the Gaussian state

After the variational spectrum μ was fixed, one can expand in presumably small terms in Eq. (214) multiplied by α up to a certain order. Here we summarize the Feynman rules.

a. Feynman diagrams

The propagator in the quasimomentum space,

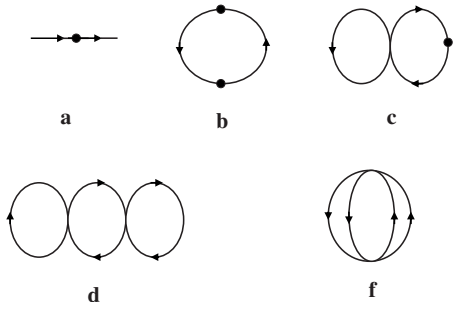

FIG. 10. Additional diagram of the renormalized perturbation theory shown in (a). Bubbles or cacti diagrams summed by the optimized expansion are shown in (b)–(d). A diagram which is not of that type is shown in (f).

$$G_k = 2^{5/2}\pi/(\mu^2 + k_z^2/2), \tag{222}$$

is the same as in usual perturbation theory [Fig. 8(a)] but with Gaussian mass μ. The four-leg interaction vertex is also the same as Fig. 8(b), but there is an additional two-leg term. It has a factor α and treated as a vertex and can be represented by a dot on a line [Fig. 10(a)], with a value of $(\alpha/2^{5/2}\pi)a$. The second term is a four line vertex [Fig. 8(b)], with a value of $\alpha/2^{7/2}\pi$.

To calculate the effective energy density $f = -2^{5/2}\pi \ln Z$, one draws all the connected vacuum diagrams. To the three loop order one has

$$\frac{f_1}{\text{vol}} = -\frac{1}{2\mu^5}(17 + 8a\mu + a^2\mu^2),$$
$$\frac{f_2}{\text{vol}} = \frac{1}{24\mu^8}(907 + 510a\mu + 96a^2\mu^2 + 6a^3\mu^3). \tag{223}$$

The liquid LLL (scaled) free energy is generally written as (using the gap equation)

$$f/\text{vol} = 4\mu[1 + g(x)]. \tag{224}$$

The function g can be expanded as

$$g(x) = \sum_{n=1} c_n x^n, \tag{225}$$

where the high temperature small parameter is $x = \frac{1}{2}\mu^{-3}$. The coefficients c_n were calculated to sixth order in (Thouless, 1975; Ruggeri and Thouless, 1976; Ruggeri, 1978) and extended to ninth order in (Brézin *et al.*, 1990; Herbut *et al.*, 1991). The consecutive approximants are shown in Fig. 6 ($T1-T9$).

b. Applicability range and ways to improve it

One clearly sees that the series are asymptotic and can be used only at $a_T > -2$. Therefore the great effort invested in these high order evaluations still falls short of a required values to describe the melting of the vortex lattice. One can improve on this by optimizing the variational parameter μ at each order instead of fixing it at the first order calculation. This will lead in the following sections to a convergent series instead of the asymptotic one. The radius of convergence happens to be around $a_T = -5$ short of melting and roughly at the spinodal point of the vortex solid (see next section).

Another direction is to capitalize on the "pseudocritical fixed point" at zero temperature. Indeed, the excitation energy, for example, behaves as a power $\mu \propto a_T^{-1}$, other physical quantities are also "critical," at least according to Gaussian approximation. It is therefore possible to consider supercooled liquid or liquid above the melting line but at low enough temperature as being in the neighborhood of a pseudocritical point. To this end the experience with critical phenomena is helpful. One generally develops an expansion around a weak coupling unstable fixed point (high temperature in our case) and "flows" toward a strong coupling stable fixed point (zero temperature in our case) (Itzykson and Drouffe, 1991). Practically, when higher order expansions are involved, one makes use of the renormalization group methods in a form of the Pade-Borel resummation (Baker, 1990). This route will be followed in Sec. III.D.3 and will lead to a theory valid for arbitrarily low temperature. The OPS will serve as a consistency check on the upper range of applicability of the resummation, which is generally hard to predict.

2. Optimized perturbation theory

a. General idea of the optimized Gaussian perturbation theory

We use a variant of OPT, the optimized Gaussian series (Kleinert, 1990), to study the vortex liquid (Li and Rosenstein, 2001, 2002a, 2002b, 2002c). It is based on the "principle of minimal sensitivity" idea (Stevenson, 1981; Okopinska, 1987) first introduced in quantum mechanics. Any perturbation theory starts from dividing the Hamiltonian into a solvable "large" part and a perturbation. Since we can solve any quadratic Hamiltonian, we have a freedom to choose "the best" such quadratic part. Quite generally such an optimization converts an asymptotic series into a convergent one [see a comprehensive discussion, references, and a proof in Kleinert (1990)]. The free energy is divided into the large quadratic part and a perturbation introducing variational parameter μ like for Gaussian approximation [Eq. (214)], although now the minimization will be made on orders of α higher than the first.

Expanding the logarithm of the statistical sum to order α^{n+1},

$$Z = \int_\psi \exp(-K)\exp(-\alpha V) = \int_\psi \sum_{j=0} \frac{1}{j!}(\alpha V)^j \exp(-K),$$
$$\tilde{f}_n[\mu] = -2^{5/2}\pi \log Z = -2^{5/2}\pi\left\{\log\left[\int_\psi e^{-K}\right] - \sum_{j=1}^{n+1} \frac{(-\alpha)^j}{j!}\langle V^i\rangle_K\right\}, \tag{226}$$

where $\langle\ \rangle_K$ denotes the sum of all the connected Feynman diagrams with G as a propagator and then taking

$\alpha \to 1$, we obtain a functional of G. To define the nth order OPT approximant f_n one minimizes $\tilde{f}_n[G]$ with respect to G,

$$f_n = \min_{\mu} \tilde{f}_n[\mu]. \tag{227}$$

Until now the method has been applied and comprehensively investigated in quantum mechanics only (Kleinert, 1990, and references therein) although attempts in field theory have been made (Duncan and Jones, 1993; Bender *et al.*, 1994; Guida *et al.*, 1995, 1996; Bellet *et al.* 1996a, 1996b).

b. Implementation and the convergence radius in GL

We can obtain all OPT diagrams which do not appear in the Gaussian theory by insertions of bubbles and the additional vertex [Fig. 1(c)] insertions from the diagrams contributing to the nonoptimized theory. Bubbles or "cacti" diagrams (see Fig. 8) are effectively inserted into energy by a technique known in field theory (Kleinert, 1990). One writes f in the following form:

$$f = 4\mu_1 + 4\mu_1 f(x), \tag{228}$$

where $x = \alpha/2\varepsilon_1^{3/2}$ and μ_1 is given by a solution of cubic equation

$$\mu_1^3 - \mu_2^2\mu_1 - 4\alpha = 0. \tag{229}$$

Summing up all insertions of the mass vertex, which now has a value of $(\alpha/2^{5/2}\pi)a$, is achieved by

$$\varepsilon_2 = \varepsilon + \alpha a. \tag{230}$$

We then expand f to order α^{n+1}, and then taking $\alpha = 1$, to obtain f_n. The solution of Eq. (229) can be obtained perturbatively in α,

$$\mu_1 = \mu_2 + \frac{2\alpha}{\mu_2^2} - \frac{6\alpha^2}{\mu_2^5} + \frac{32\alpha^3}{\mu_2^8} - \frac{210\alpha^4}{\mu_2^{11}} + \cdots. \tag{231}$$

The nth OPT approximant f_n is obtained by minimization of $\tilde{f}_n(\mu)$ with respect to μ,

$$\left[\frac{\partial}{\partial(\mu^2)} - \frac{\partial}{\partial a}\right]\tilde{f}_n(\mu, a) = 0. \tag{232}$$

The above equation is equal to $\mu^{-(3n+4)}$ times a polynomial $g_n(z)$ of order n in $z \equiv a\mu$. That Eq. (232) is of this type can be seen by noting that the function f depends on combination $\alpha/(\mu^2 + \alpha a_H)^2$ only. We were unable to prove this rigorously but have checked it to the 40th order in α. This property simplifies greatly the task: one has to find roots of polynomials rather than solving transcendental equations. There are n (real or complex) solutions for $g_n(z) = 0$. However [as in the case of anharmonic oscillator (Kleinert, 1990)] the best root is the real root with the smallest absolute value.

We then obtain μ by solving the cubic equation, $z_n = a\mu = (a_T - \mu^2)\mu$, explicitly,

$$\mu = 2^{1/3} a_T (-27z + \sqrt{-108a_T^3 + 729z^2})^{-1/3} + \frac{1}{32^{1/3}}(-27z + \sqrt{-108a_T^3 + 729z^2})^{1/3}. \tag{233}$$

For $z_0 = -4$, we obtain the Gaussian result, dashed line marked $T0$ in Fig. 9.

Feynman rules undergo minor modifications. The mass insertion vertex now has a value of $(\alpha/2^{5/2}\pi)a_H$, while the four line vertex is $\alpha/2^{5/2}\pi$. However, since the propagator in the field direction z and perpendicular factorizes, the k_z integrations can be reduced to corresponding integrations in quantum mechanics of the anharmonic oscillator, as explained in Sec. III.B. Expanding f in α to order $n+1$, then one then sets $\alpha = 1$ to obtain $\tilde{f}_n$. We list here first few OPT approximants $\tilde{f}_n$,

$$\tilde{f}_0 = 4\mu + \frac{2a_H}{\mu} + \frac{4}{\mu^2},$$

$$\tilde{f}_1 = \tilde{f}_0 - \frac{1}{2\mu^5}(17 + 8a_H\mu + a_H^2\mu^2), \tag{234}$$

$$\tilde{f}_2 = \tilde{f}_1 + \frac{1}{24\mu^8}(907 + 510a_H\mu + 96a_H^2\mu^2 + 6a_H^3\mu^3),$$

with higher orders given by Li and Rosenstein (2002b).

c. Rate of convergence of OPT

The remarkable convergence of OPS in simple models was investigated in numerous works (Duncan and Jones, 1993; Bender *et al.*, 1994; Guida *et al.*, 1995, 1996; Bellet *et al.*, 1996a, 1996b). It was found that at high orders the convergence of partition function of simple integrals [similar to the "zero-dimensional GL" studied by Wilkin and Moore (1993)]

$$Z = \int_{-\infty}^{\infty} d\varphi e^{-(a\varphi^2 + \varphi^4)} \tag{235}$$

is exponentially fast. The reminder in bound by (Duncan and Jones, 1993; Bender *et al.*, 1994; Guida *et al.*, 1995, 1996; Bellet *et al.*, 1996a, 1996b)

$$r_N = |Z - Z_N| < c_1 \exp[-c_2 N]. \tag{236}$$

For quantum mechanical anharmonic oscillator (both positive and negative quadratic terms) it is just a bit slower,

$$R_N = |E - E_N| < c_1 \exp[-c_2 N^{1/3}], \tag{237}$$

where E is the ground state energy. We follow here the convergence proof of Duncan and Jones (1993), Bender *et al.* (1994), Guida *et al.* (1995, 1996), Bellet *et al.*, (1996a, 1996b). The basic idea is to construct a conformal map from the original coupling g to a coupling of bounded range and isolate a nonanalytic prefactor. Suppose we have a perturbative expansion (usually asymptotic, sometimes non-Borel summable),

$$E(g) = \sum_{n=0}^{\infty} c_n g^n. \tag{238}$$

One defines a set of conformal maps dependent on parameter ρ of coupling g onto new coupling β,

$$\bar{g}(\beta,\rho) = \rho\beta/(1-\beta)^{\kappa}. \tag{239}$$

While range of g is the cut complex plane the range of β is compact. The value of parameter ρ for each approximant will be defined later. Then one defines a "scaled" energy,

$$\Omega(\beta,\rho) = (1-\beta)^{\sigma} E(\bar{g}(\beta,\rho)), \tag{240}$$

where the prefactor $(1-\beta)^{\sigma}$ is determined by strong coupling limit so that $\Omega(\beta,\rho)$ is bounded everywhere. Approximants to Ω are expansion to Nth order in β,

$$\Omega_N(\beta,\bar{\rho}) = \sum_{n=0}^{N} \frac{1}{n!}\frac{\partial^n}{\partial\beta^n}\{(1-\beta)^{\alpha} E(\bar{g}(\beta,\bar{\rho}))\}, \tag{241}$$

with parameter $\bar{\rho}$ substituted by $\bar{\rho}=(g/\beta)(1-\beta)^{\kappa}$. The energy approximant becomes

$$E_N(\beta) = \Omega_N(\beta)/(1-\beta)^{\sigma}. \tag{242}$$

Two exponents, $\sigma=\frac{1}{2}$ and $\kappa=\frac{3}{2}$, for example, are anharmonic oscillator and 3D GL model. OPS is equivalent to choosing β which minimizes $E_N(\beta)$. It can be shown quite generally [see Appendix C of Bender *et al.* (1994) and Kleinert (1990)] that the minimization equation is a polynomial one in ρ. This is in line with our observation in the previous section that minimization equations are polynomial in z with ρ identified as $-1/z$.

The remainder $R_N=|E-E_N|$ using dispersion relation is bounded by

$$R_N < c_1 g^{\sigma/\kappa}(\bar{\rho}N^b)^N + c_2 \exp[-N(\bar{\rho}/g)^{1/\kappa}], \tag{243}$$

where exponent b is determined by discontinuity of $E(g)$ at small negative g,

$$\mathrm{disc}\, E(g) \sim \exp[-\mathrm{const}/(-g)^{1/b}]. \tag{244}$$

The constants are $b=1$ for anharmonic oscillator and $b=3/4$ for 3D GL model (Thouless, 1975; Ruggeri and Thouless, 1976; Ruggeri, 1978). For 3D GL model, we found that $R_N < c_1 \exp(-c_2 N^{1/3})$ as in anharmonic oscillator.

3. Overcooled liquid and the Borel-Pade interpolation

a. Borel-Pade resummation

We have already observed using the Gaussian approximation that there exists a pseudocritical fixed point at zero fluctuation temperature $\alpha_T \to -\infty$. One can therefore attempt to use the RG "flow" from the weak coupling point, the perturbation at high temperature, to this strongly couple fixed point. This procedure always has an element of interpolation. It should be consistent with the perturbation theory but goes far beyond it. Technically it is achieved by the Borel-Pade (BP) approximants. We will not attempt to describe the method in detail [see Baker (1990)] and concentrate on application.

The procedure is not unique. One starts from the renormalized perturbation series of $g(x)$, calculated in Sec. III.B [Eq. (225)], $g(x)=\Sigma c_n x^n$. We denote by $g_k(x)$ the $[k,k-1]$ BP transform of $g(x)$ (other BP approximants clearly violate the correct low temperature asymptotics and are not considered). The BP transform is defined as

$$\int_0^{\infty} g_k'(xt)\exp(-t)dt, \tag{245}$$

where g_k' is the $[k,k-1]$ Pade transform of the better convergent series,

$$\sum_{n=1}^{2k-1} \frac{c_n x^n}{n!}. \tag{246}$$

The $[k,k-1]$ Pade transform of a function is defined as a rational function of the form

$$\frac{\sum_{i=0}^{k} h_i x^i}{\sum_{i=0}^{k-1} d_i x^i}, \tag{247}$$

whose expansion up to order $2k-1$ coincides with that of the function of the series [Eq. (246)].

The results are shown in Fig. 9 as solid lines for $k=3,4$, and 5. The lines for $k=4,5$ are practically indistinguishable on the plot. The energy converges therefore even at low temperatures below melting. It describes therefore the metastable liquid up to zero temperature. Due to inherent nonunique choice of the BP approximants it is crucial to compare the results with convergent series (within the range of convergence). This is achieved by comparison with the OPT results of the previous section.

b. Comparison with other results

As shown in Fig. 9, the two highest available BP approximants are consistent with the converging OPT series described above practically in the whole range of α_T. One can compare the results with existing (not very extensive) Monte Carlo simulation and agreement is well within the MC precision. Moreover, similar method was applied to the 2D GL model which was simulated extensively (Tešanović and Xing, 1991; Hu and MacDonald, 1993; Kato and Nagaosa, 1993; O'Neill and Moore, 1993; Hu *et al.*, 1994) and for which longer series are available (Brézin *et al.*, 1990; Hikami *et al.*, 1991) and agreement is still perfect. We conclude that the method is precise enough to study the melting problem.

Now we mention several issues, which prevented its use and acceptance early on. Ruggeri and Thouless (Thouless, 1975; Ruggeri and Thouless, 1976; Ruggeri, 1978) tried to use BP to calculate the specific heat without much success because their series were too short

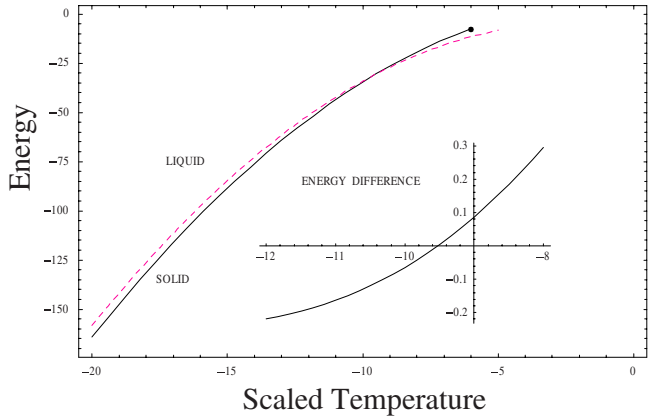

FIG. 11. (Color online) The melting point and the spinodal point of the crystal. The free energies of the crystalline and the liquid states are equal at melt, while metastable crystal becomes unstable at spinodal point.

(Wilkin and Moore, 1993). In addition, they tried to force it to conform to the solid expression at low temperatures, which is impossible. Attempts to use BP for calculation of melting also ran into problems. Hikami *et al.* (Brézin *et al.*, 1990; Hikami *et al.*, 1991) tried to find the melting point by comparing the BP energy with the one loop solid energy and obtained $a_T=-7$. However, their one loop solid energy was incorrect (by factor $\sqrt{2}$) and in any case it was not precise enough since the two loop contribution is essential.

To conclude, the BP method and the OPT are precise enough to quantitatively determine thermodynamic properties of the vortex liquid, including the supercooled one. The precision is good enough in order to determine the melting line. We therefore turn to the physical consequences of the analytical methods for both the crystalline and the melted liquid states.

c. Magnetization and specific heat in vortex liquids

As long as the free energy is known, one differentiates it to other calculated physical quantities such as entropy, magnetization, and specific heat using general LLL formulas. Since the BP formulas, although analytical, are quite bulky (and can be found in MATHEMATICA file) we will not provide them. The magnetization curves were compared to those in fully oxidized YBCO of Li and Rosenstein (2002a) to data of Nishizaki *et al.* (2000) and with Nb (after correction to a rather small κ) to data of Salem-Sugui *et al.* (2002), while the specific heat data were compared with experimental in $SnNb_3$ of Lortz *et al.* (2006) and in Nb (also after the finite κ correction).

E. First order melting and metastable states

1. The melting line and discontinuity at melt

a. Location of the melting line

Comparing solid two-loop free energy given by Eq. (188) and liquid BP energy (Fig. 11), we find that they intersect at $a_T^m=-9.5$ (see inset for the difference). The available 3D Monte Carlo simulations (Sasik and Stroud, 1995) unfortunately are not precise enough to provide an accurate melting point since the LLL scaling is violated and one gets values $a_T^m=-14.5$, -13.2, and -10.9 at magnetic fields of 1, 2, and 5 T, respectively. This is perhaps due to small sample size ($\sim$100 vortices). The situation in two dimensions is better since the sample size is much larger. We performed a similar calculation to that in three dimensions for the 2D LLL GL liquid free energy, combined it with the earlier solid energy calculation (Rosenstein, 1999; Li and Rosenstein, 2002a),

$$\frac{f_{\rm sol}}{\rm vol}=-\frac{a_T^2}{2\beta_A}+2\log\frac{|a_T|}{4\pi^2}-\frac{19.9}{a_T^2}-2.92, \tag{248}$$

and find that the melting point obtained $a_T^m=-13.2$. It is in good agreement with numerous MC simulations (Hu and MacDonald, 1993; Kato and Nagaosa, 1993; Hu *et al.*, 1994; Li and Nattermann, 2003).

b. Comparison with phenomenological Lindemann criterion and experiments

Phenomenologically the melting line can be located using the Lindemann criterion or its more refined version using the Debye-Waller factor. The more refined definition is required since vortices are not pointlike. It was found numerically for a Yukawa gas (Stevens and Robbins, 1993) that the Debye-Waller factor e^{-2W} (ratio of the structure function at the second Bragg peak at melting to its value at $T=0$) is about 60%. To one loop order one gets using the methods of Li and Rosenstein (1999b) to calculate the Debye-Waller factor at the melting line obtained here using the nonperturbative method

$$e^{-2W}=0.50. \tag{249}$$

The higher loop correction to this factor is supposed to be positive and the total value might be equal to a value around 0.6 (we did not undertake this calculation due to the complexity). However, we apply a "one loop" criterion (the Debye-Waller factor is 0.5 calculated to one loop), and this method was applied to the layered superconductor based on Lawrence-Doniach-Ginzburg-Landau model and the rotating Bose-Einstein condensate by Wu *et al.* (2007) and Feng *et al.* (2009) and the results were both in surprisingly good agreement with numerical calculations by Hu and MacDonald (1997) and Cooper *et al.* (2001).

The melting line is in accord with numerous experiments in both clean low T_c materials such as $NbSe_2$ (Kokubo *et al.*, 2004, 2005 2007; Xiao *et al.*, 2004; Thakur *et al.*, 2005; Adesso *et al.*, 2006) and Nb_3Sn (Lortz *et al.*, 2006), in which the line can be inferred from the peak effect (see below) and various dynamical effects, or high T_c such as the fully oxidized $YBa_2Cu_3O_7$ (Nishizaki *et al.*, 2000) [see fit of Li and Rosenstein (2002a)]. The fully oxidized YBCO is best suited for the application of the present theory since pinning on the mesoscopic scale is negligible. For example, the melting line is extended beyond 30 T as shown by Li and Rosenstein (2002a).

TABLE II. Parameters of high T_c superconductors deduced from the melting line.

Material	T_c	H_{c2}	Gi	κ	γ_a
$YBCO_{7-\delta}$	93.07	167.53	1.9×10^{-4}	48.5	7.76
$YBCO_7$	88.16	175.9	7.0×10^{-5}	50	4
$DyBCO_{6.7}$	90.14	163	3.2×10^{-5}	33.77	5.3

Melting lines of optimally doped untwined (Welp *et al.*, 1991, 1996; Schilling *et al.*, 1996, 1997; Willemin *et al.*, 1998; Bouquet *et al.*, 2001) $YBa_2Cu_3O_{7-\delta}$ and $DyBa_2Cu_3O_7$ (Roulin *et al.*, 1996, 1996; Revaz *et al.*, 1998) are also fitted extremely well (Li and Rosenstein, 2003). More recently both $NbSe_2$ and thick films of Nb_3Ge were fitted by Kokubo *et al.* (2007) in which disorder is significant but the pristine melting line is believed to be clearly seen in dynamics via peak effect. In Table II parameters inferred from these fits are given where the data for $YBCO_{7-\delta}$, $DyBCO_{6.7}$, and $YBCO_7$ are taken from Schilling *et al.* (1996), Roulin, Junod, and Walter (1996), Roulin, Junod, *et al.* (1996), and Nishizaki *et al.* (2000), respectively. Parameters such as Gi characterizing the strength of thermal fluctuations differ a bit from the often mentioned (Blatter *et al.*, 1994). Similar fits were made in two dimensions for an organic superconductor (Fruchter *et al.*, 1997). Unlike the Lindemann criterion, the quantitative calculation allows determination of various discontinuities across the melting line (since we have energies of both phases) to which we turn next.

2. Discontinuities at melting

a. Magnetization jump

The scaled magnetization, which is defined by $m(a_T) = -df(a_T)/da_T$, can be calculated in both phases and the difference $\Delta m = m_s - m_l$ at the melting point $a_T^m = -9.5$ is

$$\Delta M/M_s = \Delta m/m_s = 0.018. \tag{250}$$

This was compared by Li and Rosenstein (2003) with experimental results on fully oxidized $YBa_2Cu_3O_7$ (Nishizaki *et al.*, 2000) and optimally doped untwined $YBa_2Cu_3O_{7-\delta}$ (Welp *et al.*, 1991, 1996). These samples probably have the lowest degree of disorder not included in calculations.

b. Specific heat jump

In addition to the delta-function-like spike at melting following from the magnetization jump discussed above experiment shows also a specific heat jump (Schilling *et al.*, 1996, 1997; Bouquet *et al.*, 2001; Lortz *et al.*, 2006). The theory allows us to quantitatively estimate it. The specific heat jump is

$$\Delta c = 0.0075\left(\frac{2-2b+t}{t}\right)^2 - 0.20\mathrm{Gi}^{1/3}(b-1-t)\left(\frac{b}{t^2}\right)^{2/3}. \tag{251}$$

It was compared by Li and Rosenstein (2003) with the experimental values of Willemin *et al.* (1998). See also the comparison with specific heat in $NbSn_3$ of Lortz *et al.* (2006).

In addition the value of the specific heat jump in the 2D GL model is in good agreement with MC simulations (Hu and MacDonald, 1993; Kato and Nagaosa, 1993; Hu *et al.*, 1994), while the 3D MC result is still unavailable.

3. Gaussian approximation in the crystalline phase and the spinodal line

a. Gaussian variational approach with shift of the field

The Gaussian variational approach in the phase exhibiting spontaneously broken symmetry is quite a straightforward, albeit more cumbersome, extension of the method to include the "shift" $v(r)$. In our case of one complex field one should consider the most general quadratic form,

$$K = \int_{r,r'} [\psi^*(r) - v^*(r)]G^{-1}(r,r')[\psi(r') - v(r')] + [\psi(r) - v(r)]H^*(r,r')[\psi(r') - v(r')] + \text{c.c.} \tag{252}$$

To obtain the shift v and "width of the Gaussian" which is a matrix containing G and H, one minimizes the Gaussian effective free energy (Cornwall *et al.*, 1974), which is an upper bound on the energy. Assuming hexagonal symmetry, the shift should be proportional to the zero quasimomentum function, $v(r) = v\varphi(r)$, with a constant v taken real, thanks to the global U(1) gauge symmetry. On LLL, as in perturbation theory, we use the phonon variables O_k and A_k defined in quasimomentum basis Eqs. (139) and (143) instead of $\psi(r)$,

$$\psi(r) = v\varphi(\mathbf{r}) + \frac{1}{\sqrt{2}(2\pi)^{3/2}}\int_k e^{ik_z z}c_{\mathbf{k}}\varphi_{\mathbf{k}}(\mathbf{r})(O_k + iA_k). \tag{253}$$

The phase defined after Eq. (148) is quite important for simplification of the problem and was introduced for future convenience. The most general quadratic form in these variables is

$$K = \int_k O_k G_{OO}^{-1}(k) O_{-k} + A_k G_{AA}^{-1}(k) A_{-k} + O_k G_{OA}^{-1}(k) A_{-k} + A_k G_{OA}^{-1}(k) O_{-k}, \quad (254)$$

with matrix of functions to be determined together with the constant v by the variational principle. The Gaussian free energy is

$$\begin{aligned}\frac{f_{\text{gauss}}}{\text{vol}} &= a_T v^2 + \frac{\beta_\Delta}{2} v^4 + \frac{2^{5/2}\pi}{2(2\pi)^3}\int_{\mathbf{k}} \log\det(G^{-1}) \\ &+ \frac{1}{2(2\pi)^3}\int_{\mathbf{k}} \left\{ \left(\frac{k_z^2}{2} + a_T\right)[G_{OO}(k) + G_{AA}(k)] \right. \\ &+ v^2[(2\beta_{\mathbf{k}} + |\gamma_{\mathbf{k}}|)G_{OO}(k) \\ &\left. + (2\beta_{\mathbf{k}} - |\gamma_{\mathbf{k}}|)G_{AA}(k)] \right\} + \frac{1}{2\beta_\Delta}\left[\frac{1}{2(2\pi)^3}\int_{\mathbf{k}} |\gamma_{\mathbf{k}}| \right. \\ &\left. \times [G_{OO}(k) - G_{AA}(k)]\right]^2 + \frac{2}{\beta_\Delta}\left[\frac{1}{2(2\pi)^3}\int_{\mathbf{k}} |\gamma_{\mathbf{k}}| \right. \\ &\left. \times [G_{OA}(k)]\right]^2 + \frac{1}{4(2\pi)^6}\int_{\mathbf{k},l} \beta_{\mathbf{k}-\mathbf{l}}[G_{OO}(k) \\ &+ G_{AA}(k)][G_{OO}(l) + G_{AA}(l)], \end{aligned} \quad (255)$$

leading to the following minimization equations:

$$\begin{aligned} v^2 + \frac{a_T}{\beta_A} &= -\frac{1}{2(2\pi)^3\beta_\Delta}\int_k (2\beta_{\mathbf{k}} + |\gamma_{\mathbf{k}}|)G_{OO}(k) \\ &+ (2\beta_{\mathbf{k}} - |\gamma_{\mathbf{k}}|)G_{AA}(k), \end{aligned} \quad (256)$$

$$\begin{aligned} 2^{5/2}\pi[G(k)^{-1}]_{OO} &= k_z^2/2 + a_T + v^2(2\beta_{\mathbf{k}} + |\gamma_{\mathbf{k}}|) + \frac{1}{2(2\pi)^3}\int_l \left(2\beta_{\mathbf{k}-\mathbf{l}} \right. \\ &\left. + \frac{|\gamma_{\mathbf{k}}||\gamma_{\mathbf{l}}|}{\beta_\Delta}\right)G_{OO}(l) + \left(2\beta_{\mathbf{k}-\mathbf{l}} - \frac{|\gamma_{\mathbf{k}}||\gamma_{\mathbf{l}}|}{\beta_\Delta}\right)G_{AA}(l) \end{aligned}$$

and

$$\begin{aligned} 2^{5/2}\pi[G(k)^{-1}]_{AA} &= \frac{k_z^2}{2} + a_T + v^2(2\beta_k - |\gamma_{\mathbf{k}}|) + \frac{1}{2(2\pi)^3} \\ &\times \int_l \left(2\beta_{\mathbf{k}-\mathbf{l}} + \frac{|\gamma_{\mathbf{k}}||\gamma_{\mathbf{l}}|}{\beta_\Delta}\right)G_{AA}(l) \\ &+ \left(2\beta_{\mathbf{k}-\mathbf{l}} - \frac{|\gamma_{\mathbf{k}}||\gamma_{\mathbf{l}}|}{\beta_\Delta}\right)G_{OO}(l)2^{5/2}\pi[G(k)^{-1}]_{OA} \\ &= -\frac{2^{5/2}\pi G_{OA}(k)}{G_{OO}(k)G_{AA}(k) - G_{OA}(k)^2} \\ &= 4\frac{|\gamma_{\mathbf{k}}|}{\beta_\Delta}\frac{1}{2(2\pi)^3}\int_l |\gamma_{\mathbf{l}}| G_{OA}(l). \end{aligned} \quad (257)$$

These equations look quite intractable, however, they can be simplified.

b. How to eliminate the off-diagonal terms

The crucial observation is that after we have inserted the phase $c_{\mathbf{k}} = \sqrt{\gamma_{\mathbf{k}}/|\gamma_{\mathbf{k}}|}$ in Eq. (255) using our experience with perturbation theory, G_{AO} appears explicitly only on the right hand side of the last equation. It also implicitly appears on the left hand side due to a need to invert the matrix G. Obviously $G_{OA}(k)=0$ is a solution and in this case the matrix diagonalizes. However, the general solution can be shown to differ from this simple one just by a global gauge transformation. Subtracting the OO equation from the AA equation above [Eq. (256)] and using the OA equation, we observe that matrix G^{-1} has a form

$$\begin{aligned} G^{-1} &\equiv \begin{pmatrix} G_{OO}^{-1}(k) & G_{AO}^{-1}(k) \\ G_{AO}^{-1}(k) & G_{AA}^{-1}(k) \end{pmatrix} \\ &= \frac{1}{2^{5/2}\pi}\begin{pmatrix} k_z^2/2 + \mu_{O\mathbf{k}}^2 & \mu_{AO\mathbf{k}}^2 \\ \mu_{AO\mathbf{k}}^2 & k_z^2/2 + \mu_{A\mathbf{k}}^2 \end{pmatrix}, \end{aligned} \quad (258)$$

with

$$\begin{aligned} &\mu_{O\mathbf{k}}^2 = E_{\mathbf{k}} + \Delta_1|\gamma_{\mathbf{k}}|, \quad \mu_{A\mathbf{k}}^2 = E(k) - \Delta_1|\gamma_{\mathbf{k}}|, \\ &\mu_{AO\mathbf{k}}^2 = \Delta_2|\gamma_{\mathbf{k}}|, \end{aligned} \quad (259)$$

where Δ_1, Δ_2 are constants. Substituting this into the Gaussian energy one finds that it depends on Δ_1, Δ_2 via the combination $\Delta = \sqrt{\Delta_1^2 + \Delta_2^2}$ only. Therefore without loss of generality we can set $\Delta_2 = 0$, thereby returning to the $G_{OA}=0$ case.

Using this observation, the gap equations significantly simplify. The function $E_{\mathbf{k}}$ and the constant Δ satisfy

$$E_{\mathbf{k}} = a_T + 2v^2\beta_k + 2\left\langle \beta_{\mathbf{k}-\mathbf{l}}\left(\frac{1}{\mu_{O\mathbf{l}}} + \frac{1}{\mu_{A\mathbf{l}}}\right)\right\rangle_{\mathbf{l}}, \quad (260)$$

$$\beta_\Delta\Delta = -a_T - 2\left\langle \beta_{\mathbf{l}}\left(\frac{1}{\mu_{O\mathbf{l}}} + \frac{1}{\mu_{A\mathbf{l}}}\right)\right\rangle_{\mathbf{l}} \quad (261)$$

and the shift equation

$$v^2 + \frac{a_T}{\beta_A} = -\left\langle \frac{2\beta_{\mathbf{k}} + |\gamma_{\mathbf{k}}|}{\mu_{O\mathbf{k}}} + \frac{2\beta_{\mathbf{k}} - |\gamma_{\mathbf{k}}|}{\mu_{A\mathbf{k}}}\right\rangle_{\mathbf{k}}. \quad (262)$$

The Gaussian energy (after integration over k_z) becomes

$$\begin{aligned} &\frac{f}{\text{vol}} = v^2 a_T + \frac{\beta_A}{2}v^4 + f_1 + f_2 + f_3, \\ &f_1 = \langle \mu_{O\mathbf{k}} + \mu_{A\mathbf{k}}\rangle_{\mathbf{k}}, \\ &f_2 = a_T\langle(\mu_{O\mathbf{k}}^{-1} + \mu_{A\mathbf{k}}^{-1}) + v^2[(2\beta_k + |\gamma_k|)\mu_{O\mathbf{k}}^{-1} \\ &\quad + (2\beta_k - |\gamma_k|)\mu_{A\mathbf{k}}^{-1}]\rangle_{\mathbf{k}}, \\ &f_3 = \langle \beta_{\mathbf{k}-\mathbf{l}}(\mu_{O\mathbf{k}}^{-1} + \mu_{A\mathbf{k}}^{-1})(\mu_{O\mathbf{l}}^{-1} + \mu_{A\mathbf{l}}^{-1})\rangle_{\mathbf{k},\mathbf{l}} \\ &\quad + \frac{1}{2\beta_\Delta}[\langle|\gamma_k|(\mu_{O\mathbf{l}}^{-1} - \mu_{A\mathbf{l}}^{-1})\rangle_{\mathbf{k}}]^2. \end{aligned} \quad (263)$$

The problem becomes quite manageable numerically after one spots an unexpected small parameter.

TABLE III. Mode expansion.

a_T	−30	−20	−10	−5.5
f	−372.2690	−159.5392	−33.9873	−6.5103

c. The mode expansion

Using formula (A18)

$$\beta_{\mathbf{k}} = \sum_{n=0}^{\infty} \chi^n \beta_n(\mathbf{k}),$$
$$\beta_n(\mathbf{k}) \equiv \sum_{|\mathbf{X}|^2 = n a_\Delta^2} \exp[i\mathbf{k}\cdot\mathbf{X}], \tag{264}$$

derived in Appendix A and the hexagonal symmetry of the spectrum, one deduces that $E_{\mathbf{k}}$ can be expanded in "modes,"

$$E_{\mathbf{k}} = \sum E_n \beta_n(\mathbf{k}). \tag{265}$$

The integer n determines the distance of a points on reciprocal lattice from the origin, and $\chi \equiv \exp[-a_\Delta^2/2] = \exp[-2\pi/\sqrt{3}] = 0.0265$. One estimates that $E_n \simeq \chi^n a_T$; therefore the coefficients decrease exponentially with n. Note that for some integers, for example, $n=2,5,6$, $\beta_n = 0$. Retaining only first s modes will be called the s mode approximation. We minimized numerically the Gaussian energy by varying v, Δ, and first few modes of $E_{\mathbf{k}}$.

The sample results of free energy density for various a_T with three modes are given in Table III. In practice two modes are also quite enough. We see that in the interesting region of not very low temperatures the energy converges extremely fast. In practice two modes are quite enough.

d. Spinodal point

One can show that above

$$a_T^{\text{spinodal}} = -5.5 \tag{266}$$

there is no solution for the gap equations. The corresponding value in two dimensions is $a_T^{\text{spinodal}} = -7$ and is consistent with the relaxation time measured in Monte Carlo simulations (Kato and Nagaosa, 1993). The spinodal point was observed in $NbSb_2$ (Xiao *et al.*, 2004; Thakur *et al.*, 2005; Adesso *et al.*, 2006) at the position consistent with the theoretical estimate.

e. Corrections to the Gaussian approximation

The lowest order correction to the Gaussian approximation (sometimes called the post-Gaussian correction) was calculated by Li and Rosenstein (2002a, 2002b, 2002c) to determine the precision of the Gaussian approximation. This is necessary in order to fit experiments and compare with low temperature perturbation theory and other nonperturbative methods.

A general idea behind calculating systematic corrections to the Gaussian approximation was described for liquid in Sec. III.C and modifications are quite analogous to those done for the Gaussian approximation. Results for the specific heat were compared by Li and Rosenstein (2002c). Generally the post-Gaussian result is valid until $a_T = -7$ and rules out earlier approximations, as the one of Tešanović *et al.* (1992) and Tešanović and Andreev (1994) (dotted line).

IV. QUENCHED DISORDER AND THE VORTEX GLASS

In any superconductor there are impurities present either naturally or systematically produced using the proton or electron irradiation. The inhomogeneities on both the microscopic and the mesoscopic scales greatly affect thermodynamic and especially dynamic properties of type II superconductors in a magnetic field. The field penetrates the sample in a form of Abrikosov vortices, which can be pinned by disorder. In addition, in high T_c superconductors thermal fluctuations also greatly influence the vortex matter, for example, in some cases thermal fluctuations will effectively reduce the effects of disorder. As a result the T-H phase diagram of the high T_c superconductors is very complex due to the competition between thermal fluctuations and disorder, and it is still far from being reliably determined even in the best studied superconductor, the optimally doped YBCO superconductor.

It is the purpose of this section to describe the glass transition and static and thermodynamic properties of both the disordered reversible and the irreversible glassy phases. The disorder is represented by the random component of the coefficients of the GL free energy [Eq. (20)] and the main technique used is the replica formalism. The most general so-called hierarchical homogeneous (liquid) ansatz (Mezard and Parisi, 1991) and its stability are considered to obtain the glass transition line and to determine the nature of the transition for various values of the disorder strength of the GL coefficients. In most cases the glassy phase exhibits the phenomenon of replica symmetry breaking when ergodicity is lost due to trapping of the system in multiple metastable states. In this case physical quantities do not possess a unique value but rather have a distribution. We start with the case of negligible thermal fluctuations.

A. Quenched disorder as a perturbation of the vortex lattice

1. The free energy density in the presence of pinning potential

a. GL model with δT_c disorder

We start with space variations of the coefficient of $|\Psi|^2$ [Eq. (20)] distributed as white noise [Eq. (21)]. It can be regarded as a local variation of T_c. As mentioned in Sec. I other types of disorder are present and might be important, however, as will be shown later are more complicated.

Since a pointlike disorder breaks the translational symmetry in all directions including that of the magnetic

field z, one has to consider configurations dependent on all three coordinates and take into account anisotropy. We restrict to the case $m_a^*=m_b^*\equiv m^*$,

$$F[W]=\int_r \frac{\hbar^2}{2m^*}|\mathbf{D}\Psi|^2+\frac{\hbar^2}{2m_c^*}|\partial_z\Psi|^2 + \alpha(T-T_c)[1+W(r)]|\Psi|^2+\frac{\beta}{2}|\Psi|^4, \quad (267)$$

where $W(r)$ is the δT_c random disorder (real) field, which we assume to be white noise with variance that can be written in the following form:

$$\overline{W(r)W(r')}=n\xi^2\xi_c\delta^3(r-r'). \quad (268)$$

The dimensionless parameter n is proportional to the density of pinning centers and a single pin's strength, while $\xi_c\equiv\xi(m^*/m_c^*)^{1/2}$ is the coherence length in the field direction. The units used here are the same as before with the addition of ξ_c as the unit of length in the z direction. As in previous sections, we confined ourselves mainly to the region in parameter space described well by the lowest Landau level approximation (LLL) defined next.

b. The disordered LLL GL free energy in the quasimomentum basis

In the units and the field normalization described in Sec. II.A the LLL energy becomes

$$F[W]=\int_r\left[\frac{1}{2}|\partial_z\Psi|^2-a_H|\Psi|^2+\frac{1-t}{2}W(r)|\Psi|^2+\frac{1}{2}|\Psi|^4\right], \quad (269)$$

where $a_H=\frac{1}{2}(1-b-t)$ and

$$\overline{W(r)W(r')}=n\delta^3(r-r') \quad (270)$$

in the new length unit. The order parameter field on LLL can be expanded in the quasimomentum basis defined in Sec. III.A as

$$\Psi(r)=\frac{1}{(2\pi)^{3/2}}\int_k\varphi_k(r)\Psi_k, \quad (271)$$

where $k\equiv(\mathbf{k},k_z)$, functions are defined in Eqs. (134) and (137), and the integration measure was defined in Sec. III.A to be the Brillouin zone in the x-y plane and the full range of momenta in the z direction. We consider the hexagonal lattice, although modifications required to consider a different lattice symmetry are minor. Using the quasimomentum LLL functions of Eq. (134), the disorder term becomes

$$F_{\rm dis}=\frac{1-t}{2}\int_r W(r)|\Psi(r)|^2=\int_{k,l}w_{k,l}\Psi_k^*\Psi_l \quad (272)$$

with

$$w_{k,l}=\frac{1-t}{2(2\pi)^3}\int_r W(r)\varphi_k^*(r)\varphi_l(r). \quad (273)$$

The remaining terms can be written as

$$F_{\rm clean}=\int_k(k_z^2/2-a_H)\Psi_k^*\Psi_k+\frac{1}{2(2\pi)^3}\int_{k,k',l,l'}[k,k'|l,l']\Psi_k^*\Psi_{k'}^*\Psi_l\Psi_{l'}\times\sum_Q\delta(k+k'-l-l'-Q), \quad (274)$$

with $[k,l|k'l']=(1/\mathrm{vol})\int_r\varphi_k^*(r)\varphi_l(r)\varphi_{k'}^*(r)\varphi_{l'}(r)$ and where $Q=(\vec{\mathbf{Q}},0)$ and $\vec{\mathbf{Q}}$ is the reciprocal lattice vectors as k,l,k',l' satisfy the momentum conservation up to a reciprocal lattice vector. $[k,l|k'l']$ will be equal to zero if $k+k'-l-l'\neq Q$.

2. Perturbative expansion in disorder strength

a. Expansion around the Abrikosov solution

The GL equations derived from the free energy in the quasimomentum basis are

$$(k_z^2/2-a_H)\Psi_k+\alpha\int_l w_{k,l}\Psi_l+\int_{k'l,l'}\sum_Q\delta(k+k'-l-l'-Q)\times\frac{[k,k'|l,l']}{(2\pi)^3}\Psi_{k'}^*\Psi_l\Psi_{l'}=0. \quad (275)$$

The parameter $\alpha=1$ inserted here will help with counting orders. The expansion in orders of the disorder strength α reads

$$\Psi=\Psi^{(0)}+\alpha\Psi^{(1)}+\alpha^2\Psi^{(2)}+\cdots. \quad (276)$$

The clean case Abrikosov solution of Sec. II is defined as the quasimomentum zero. Therefore

$$\Psi^{(0)}=(2\pi)^{3/2}\sqrt{a_H/\beta_\Delta}\,\delta_k. \quad (277)$$

The delta function appears due to its long-range translational order. Now Eq. (275) can be solved order by order in α. Since contributions linear in disorder potential will average to zero, in order to get the leading contribution of disorder one should calculate the free energy to the second order in α. Multiplying the exact equation [Eq. (275)] by Ψ_k^* and integrating over k, one can express the order 4 in Ψ term via simpler quadratic ones,

$$F=\frac{1}{2}\int_k(k_z^2/2-a_H)|\Psi_k|^2+\frac{\alpha}{2}\int_{k,l}\Psi_k^*w_{k,l}\Psi_l. \quad (278)$$

Substituting the expansion [Eq. (276)] and using delta functions of $\Psi^{(0)}$ of Eq. (277) one gets the following α^2 terms:

$$F^{(2)} = -\frac{a_H^{3/2}(2\pi)^{3/2}}{2\beta_\Delta^{1/2}}[\Psi_0^{(2)*} + \Psi_0^{(2)}] + \frac{1}{2}\int_k (k_z^2/2 - a_H) \times |\Psi_k^{(1)}|^2 + \frac{a_H^{1/2}(2\pi)^{3/2}}{2\beta_\Delta^{1/2}}\int_k [w_{0,k}\Psi_k^{(1)} + \Psi_k^{(1)*}w_{k,0}]. \quad (279)$$

Therefore the second order correction to Ψ is needed only for zero quasimomentum.

b. First order elastic response of the vortex lattice

To order α one obtains the following equation:

$$(k_z^2/2 - a_H)\Psi_k^{(1)} + w_{k,0}(2\pi)^{3/2}\sqrt{\frac{a_H}{\beta_\Delta}} + 2\frac{a_H}{\beta_\Delta}\beta_{\mathbf{k}}\Psi_k^{(1)} + \frac{a_H}{\beta_\Delta}\gamma_{\mathbf{k}}\Psi_{-k}^{(1)*} = 0 \quad (280)$$

as $Q=0$ because of the conservation of quasimomentum in this case. This equation and its complex conjugate lead to a system of two linear equations for two variables, $\Psi_k^{(1)}$ and $\Psi_{-k}^{(1)*}$. The solution, not surprisingly, involves the spectrum of harmonic excitations of the vortex lattice already familiar from the perturbative corrections due to thermal fluctuations (Sec. III.A),

$$\Psi_k^{(1)} = -\frac{(2\pi)^{3/2}}{\varepsilon_k^A\varepsilon_k^O}\frac{a_H^{1/2}}{\beta_\Delta^{1/2}}\left[\left(k_z^2/2 - a_H + 2\frac{a_H}{\beta_\Delta}\beta_{\mathbf{k}}\right)w_{k,0} - \frac{a_H}{\beta_\Delta}\gamma_{\mathbf{k}}w_{-k,0}^*\right], \quad (281)$$

where ε_k^A, ε_k^O are defined in Eq. (150).

c. Disorder average of the pinning energy to leading order

The relevant equation (zero quasimomentum) at second order in α is

$$-a_H\Psi_0^{(2)} + \int_k w_{0,k}\Psi_k^{(1)} + \frac{a_H}{\beta_\Delta}[2\beta_\Delta\Psi_0^{(2)} + \beta_\Delta\Psi_0^{(2)*}] + \frac{a_H^{1/2}}{\beta_\Delta^{1/2}(2\pi)^{3/2}}\int_l [2\beta_{\mathbf{k}}\Psi_k^{(1)*} + \gamma_{\mathbf{k}}^*\Psi_k^{(1)}]\Psi_k^{(1)} = 0 \quad (282)$$

leading to

$$a_H[\Psi_0^{(2)} + \Psi_0^{(2)*}] = -\int_k \Psi_k^{(1)}\left\{w_{0,k} + \frac{a_H^{1/2}}{\beta_\Delta^{1/2}(2\pi)^{3/2}} \times [2\beta_{\mathbf{k}}\Psi_k^{(1)*} + \gamma_{\mathbf{k}}^*\Psi_{-k}^{(1)}]\right\}. \quad (283)$$

Substituting this into Eq. (279) and simplifing the equation using Eq. (280), we obtain the energy expressed via $\Psi_k^{(1)}$,

$$F^{(2)} = \frac{a_H^{1/2}(2\pi)^{3/2}}{2\beta_\Delta^{1/2}}\int_k \{w_{0,k}\Psi_k^{(1)} + \Psi_k^{(1)*}w_{k,0}\}, \quad (284)$$

and using the expression for $\Psi_k^{(1)}$ [Eq. (281)] one obtains various terms quadratic in disorder w. The disorder averages are

$$\overline{w_{k,l}w_{k',l'}} = \frac{(1-t)^2nV}{4}[k,k'|l,l'],$$

$$\overline{w_{k,l}w_{k',l'}^*} = \frac{(1-t)^2nV}{4}[k,l'|l,k'], \quad (285)$$

$$\overline{w_{k,l}^*w_{k',l'}^*} = \frac{(1-t)^2nV}{4}[l,l'|k,k'],$$

and the pinning energy becomes after some algebra

$$\frac{\overline{F^{(2)}}}{\mathrm{vol}} = -\frac{(1-t)^2na_H}{8\beta_\Delta(2\pi)^3}\int_k\left(\frac{\beta_{\mathbf{k}} + |\gamma_{\mathbf{k}}|}{\epsilon_k^O} + \frac{\beta_{\mathbf{k}} - |\gamma_{\mathbf{k}}|}{\epsilon_k^A}\right). \quad (286)$$

Integrating over k_z, one finally obtains

$$\frac{\overline{F^{(2)}}}{\mathrm{vol}} = -\frac{(1-t)^2na_Hb}{2^{5/2}4\pi\beta_\Delta}\left\langle\frac{\beta_{\mathbf{k}} + |\gamma_{\mathbf{k}}|}{\mu_{O\mathbf{k}}} + \frac{\beta_{\mathbf{k}} - |\gamma_{\mathbf{k}}|}{\mu_{A\mathbf{k}}}\right\rangle_{\mathbf{k}}, \quad (287)$$

where $\mu_{\mathbf{k}}^{A,O}$ are given in Eq. (150).

The second term of the above expression is potentially divergent at $\mathbf{k}\to 0$, since $\mu_{A\mathbf{k}} \propto \mathbf{k}^2$ for small $\mathbf{k}$. Using an expansion for small $\mathbf{k}$ of the functions $\beta_{\mathbf{k}}$ and $\gamma_{\mathbf{k}}$ derived in Appendix A, one can see that the second term is finite, since for small $\mathbf{k}$ the numerator of the integral in Eq. (288) behaves as

$$\beta_{\mathbf{k}} - |\gamma_{\mathbf{k}}| \propto \mathbf{k}^2. \quad (288)$$

Numerically

$$\left\langle\frac{\beta_{\mathbf{k}} + |\gamma_{\mathbf{k}}|}{\mu_{O\mathbf{k}}} + \frac{\beta_{\mathbf{k}} - |\gamma_{\mathbf{k}}|}{\mu_{A\mathbf{k}}}\right\rangle_{\mathbf{k}} \approx \frac{1.4837}{\sqrt{a_H}} \quad (289)$$

d. Stronger disorder: 2D GL and columnar defects

The same calculation can be performed in two dimensions with the result

$$\frac{\overline{F^{(2)}}}{\mathrm{vol}} = -\frac{(1-t)^2na_H}{4\beta_\Delta(2\pi)^2}\int_k\left(\frac{\beta_{\mathbf{k}} + |\gamma_k|}{\mu_{O\mathbf{k}}^2} + \frac{\beta_{\mathbf{k}} - |\gamma_{\mathbf{k}}|}{\mu_{A\mathbf{k}}^2}\right). \quad (290)$$

This is logarithmically IR divergent at any value of the disorder strength since at small $\mathbf{k}$

$$\frac{\beta_{\mathbf{k}} - |\gamma_{\mathbf{k}}|}{\mu_{A\mathbf{k}}^2} \propto 1/\mathbf{k}^2. \quad (291)$$

Therefore either the dependence is not analytic or (more probably) disorder significantly modifies the structure of the solution. Generalization in another direction, that of long-range correlated disorder, can also be easily performed; one replaces the white noise variance by a general one,

$$\overline{W(r)W(r')} = K(r-r'). \quad (292)$$

For columnar defects the variance is independent of z,

$$K(r-r') = n\delta(\mathbf{r}-\mathbf{r}'), \tag{293}$$

and one again obtains a logarithmic divergence,

$$\frac{\overline{F^{(2)}}}{\text{vol}} \propto \left\langle \frac{\beta_{\mathbf{k}}+|\gamma_k|}{\mu^2_{O\mathbf{k}}} + \frac{\beta_{\mathbf{k}}-|\gamma_{\mathbf{k}}|}{\mu^2_{A\mathbf{k}}} \right\rangle_{\mathbf{k}}. \tag{294}$$

3. Disorder influence on the vortex liquid and crystal: Shift of the melting line

a. Disorder correction to free energy

Thermal fluctuations in the presence of quenched are still described by the partition function

$$Z = -\frac{1}{\omega_t}\left[F[\Psi] + \frac{1-t}{2}\int_r W(r)|\Psi(r)|^2\right]. \tag{295}$$

If W is small, we can calculate Z by perturbation theory in W. To second order the free energy $-T\ln Z$ is

$$G = G_{\text{clean}} + \frac{1-t}{2}\int_r W(r)\langle|\Psi(r)|^2\rangle - \frac{1}{8\omega_t}(1-t)^2 \times \int_{r,r'} W(r)W(r')[\langle|\Psi(r)|^2|\Psi(r')|^2\rangle - \langle|\Psi(r)|^2\rangle \times \langle|\Psi(r')|^2\rangle], \tag{296}$$

where $\langle\,\rangle$ and f_{clean} denote the thermal average and free energy of the clean system. Averaging now over disorder one obtains

$$\Delta G_{\text{dis}} = G - G_{\text{clean}} = -\frac{n}{8\omega_t}(1-t)^2\int_r [\langle|\Psi(r)|^4\rangle - \langle|\Psi(r)|^2\rangle^2]. \tag{297}$$

Therefore one has to calculate the superfluid density thermal correlator. In LLL approximation and LLL units,

$$\Delta G_{\text{dis}}/V = -r(t)\,\triangle f,$$

$$\Delta f = \tfrac{1}{2}[\langle|\Psi_{\text{LLL}}(r)|^4\rangle_r - \langle|\Psi_{\text{LLL}}(r)|^2\rangle_r^2], \tag{298}$$

$$r(t) = \frac{n}{4\omega_t}(1-t)^2 = \frac{n_0(1-t)^2}{t}, \quad n_0 = \frac{n}{4\sqrt{2\pi\text{Gi}}}.$$

Calculations of this kind in both solid and liquid were the subject of the previous section.

b. Correlators in the crystalline and the liquid states

Within LLL (and using the LLL units introduced in Sec. III) the one loop disorder correction to the crystal's energy is

$$\Delta f_{\text{crystal}} = 2.14|a_T|^{1/2}. \tag{299}$$

An explicit expression for $f_{\text{liq}}(a_T)$, obtained using the Borel-Pade resummation of the renormalized high temperature series (confirmed by optimized Gaussian series and Monte Carlo simulation), is rather bulky and can be found in Li and Rosenstein (2002a). One can derive an expression for the disorder correction in liquid by differentiating the "clean" partition function with respect to parameters

$$\Delta f_{\text{liq}} = \tfrac{1}{3}(f_{\text{liq}} - 2a'_T f'_{\text{liq}})/3 - \tfrac{1}{2}(f'_{\text{liq}})^2. \tag{300}$$

These two results enable us to find the location of the transition line and, in addition, to calculate discontinuities of various physical quantities across the transition line.

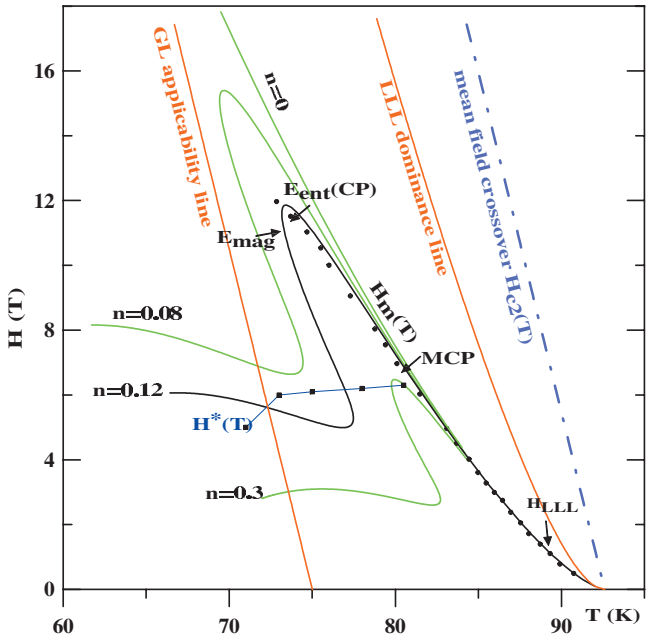

FIG. 12. (Color) Phase diagram for YBCO.

c. The "downward shift" of the first order transition line in the T-H plane

It was noted in Sec. III that in a clean system a homogeneous state exists as a metastable overcooled liquid state all the way down to zero temperature (not just below the melting temperature corresponding to $a_T = -9.5$; see the $n=0$ line in Fig. 12). This is important since the interaction with disorder can convert the metastable state into a stable one. Indeed generally a homogeneous state gains more than a crystalline state from pinning since it can easier adjust itself to the topography of the pinning centers. At large $|a_T|$ in particular $\Delta f_{\text{liq}} \propto a_T^2$ compared to just $\Delta f_{\text{sol}} \propto |a_T|^{1/2}$. As a result in the presence of disorder the transition line shifts to lower fields. The equation for the melting line is

$$d(a_T) \equiv (f_{\text{liq}} - f_{\text{sol}})/(\Delta f_{\text{liq}} - \Delta f_{\text{sol}}) = n(t). \tag{301}$$

The universal function $d(a_T)$, plotted in Fig. 13, turns out to be nonmonotonic. This is an important fact. Since $n(t)$ is a monotonic function of t, one obtains the transition lines for various n in Fig. 12 by "sweeping" Fig. 13. A peculiar feature of $d(a_T)$ is that it has a local minimum at $a_T \approx -17.2$ and a local maximum at $a_T \approx -12.1$ (before crossing zero at $a_T \approx -9.5$). Therefore between these two

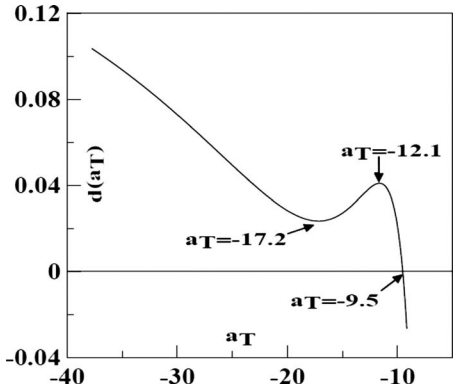

FIG. 13. Universal function $d(a_T)$ determining the shift of the melting line due to disorder.

points there are three solutions to the melting line equation. As a result, starting from the zero field at T_c, the transition field $H(T)$ reaches a maximum at $E_{\rm ent}$ beyond which the curve sharply turns down [this feature was called "inverse melting" by Avraham *et al.* (2001)] and at $E_{\rm mag}$ backward. Then it reaches a minimum and continues as the Bragg glass-vortex glass line roughly parallel to the T axis.

The temperature dependence of the disorder strength $n(t)$, as any parameter in the GL approach, should be derived from a microscopic theory or fitted to experiment. The general dependence near T_c is $n(t)=n(1-t)^2/t$. The extra factor $(1-t)^2$, not appearing in a phenomenological derivation (Blatter *et al.*, 1994), is due to the fact that near H_{c2} order parameter is small, $|\psi|^2\propto(1-t)$, and disorder (oxygen deficiencies) locally destroys superconductivity rather than perturbatively modifies the order parameter. The curves in Fig. 12 correspond to the disorder strengths $n_0=0.08,0.12,0.3$. The best fit for the low field part of the experimental melting line $H_m(T)$ of the optimally doped YBCO [data taken from Schilling *et al.* (1996), $T_c=92.6$, $\gamma=8.3$] gives $\mathrm{Gi}=2.0\times10^{-4}$, $H_{c2}=190$ T, and $\kappa=\lambda/\xi=50$ (consistent with other experiments, for example, Deligiannis *et al.* (2000) and Shibata *et al.* (2002). This part is essentially independent of disorder. The upper part of the melting curve is very sensitive to disorder: both the length of the "finger" and its slope depend on n_0. The best fit is $n_0=0.12$. This value is of the same order of magnitude as the one obtained phenomenologically using Eq. (3.82) of Blatter *et al.* (1994). We speculate that the low temperature part of the "unified" line corresponds to the solid-vortex glass transition $H^*(T)$ observed in numerous experiments (Schilling *et al.*, 1996, 1997; Kokkaliaris *et al.*, 2000; Bouquet *et al.*, 2001; Pal *et al.*, 2001, 2002; Radzyner *et al.*, 2002; Shibata *et al.*, 2002) [see data (squares in Fig. 12) from Shibata *et al.* (2002)]. A complicated shape of the "wiggling" line has been observed (Pal *et al.*, 2001, 2002). Now we turn to a more detailed characteristics of the phase transition.

d. Discontinuities across the transition and the Kauzmann point: Absence of a second order transition

Magnetization and specific heat of both solid and liquid can be calculated from the above expressions for free energy. Magnetization of liquid along the melting line $H_m(T)$ is larger than that of solid. The magnetization jump is compared in Li and Rosenstein (2003) with SQUID experiments (Schilling *et al.*, 1997) in the range of 80–90 K (triangles) and with torque experiments [stars (Willemin *et al.*, 1998) and circles (Shibata *et al.*, 2002)]. One observes that the results of the torque experiments compare surprisingly well above 83 K, but those of Shibata *et al.* (2002) vanish abruptly below 83 K unlike the theory and are inconsistent with the specific heat experiments (Schilling *et al.*, 1996; Deligiannis *et al.*, 2000) discussed below. The SQUID data are lower than theoretical (same order of magnitude though). We predict that at lower temperatures (somewhat beyond the range investigated experimentally so far) magnetization reaches its maximum and changes sign at the point $E_{\rm mag}$ (at which the magnetization of liquid and solid are equal).

Li and Rosenstein (2003) calculated the entropy jump using the Clausius-Clapeyron relation $\partial H_m(T)/\partial T=-\Delta S/\Delta M$ and compared with an experimental one deduced from the spike of the specific heat [Schilling *et al.* (1996) and an indirect measurement from the magnetization jumps by Shibata *et al.* (2002)]. At high temperatures the theoretical values are a bit lower than the experimental and both seem to approach a constant at T_c. The theoretical entropy jump and the experimental one of Schilling *et al.* (1996) vanish at $E_{\rm ent}$ (Fig. 12) near 75 K. Such points are called Kauzmann points. Below this temperature the entropy of the liquid becomes smaller than that of the solid. Note that the equal magnetization point $E_{\rm mag}$ is located at a slightly lower field than the equal entropy point $E_{\rm ent}$. Experimentally a Kauzmann point was established in BSCCO as a point at which the inverse melting appears (Avraham *et al.*, 2001). The Kauzmann point observed at a lower temperature in YBCO by Radzyner *et al.* (2002) is different from $E_{\rm ent}$ since it is a minimum rather than a maximum of magnetic field. It is also located slightly outside the region of applicability of our solution. The point $E_{\rm ent}$ is observed in Pal *et al.* (2001, 2002) in which the universal line is continuous.

In addition to the spike, the specific heat jump has also been observed along the melting line $H_m(T)$ (Schilling *et al.*, 1996, 1997; Deligiannis *et al.*, 2000). Theoretically the jump does not vanish at either $E_{\rm ent}$ or $E_{\rm mag}$ but is rather flat in a wide temperature range. Our results are larger than the experimental jumps of Schilling *et al.* (1996) (which are also rather insensitive to temperature) by a factor of 1.4–2 (Li and Rosenstein, 2003). In many experimental papers there appears a segment of the second order phase transition continuing the first order melting line beyond a certain point. Bouquet *et al.* (2001) showed that at that point the specific heat profile shows "rounding." We calculated the specific heat profile

above the universal first order transition line. It exhibits a rounding feature similar to that displayed by the data of Schilling *et al.* (1996, 1997, 2002) and Bouquet *et al.* (2001) with no sign of the criticality. The height of the peak is roughly the size of the specific heat jump. We therefore propose not to interpret this feature as evidence for a second order transition above the first order line.

e. Limitations of the perturbative approach

The perturbative approach of course is limited to small couplings only. In fact, when the correction is compared to the main part of the lattice energy the range becomes too narrow for practical applications in low temperature superconductors. For high T_c superconductors thermal fluctuations cannot be neglected at higher temperatures since it "melts" the lattice and even at low temperatures provides thermal depinning. On the conceptual side, it is clear that disorder contributes to destruction of the translational and rotational order. Therefore at certain disorder strength, vortex matter might restore the translation and rotation symmetries even without help of thermal fluctuations. It is possible to use the perturbation theory in disorder with the liquid state as a starting point in the case of large thermal fluctuations, however it fails to describe the most interesting phenomenon of the vortex glass introduced by Fisher (Fisher, 1989; Fisher *et al.*, 1991). Therefore one should try to develop nonperturbative methods to describe disorder. This is the subject the following sections.

B. The vortex glass

When thermal fluctuations are significant the efficiency of imperfections to pin the vortex matter is generally diminished. This phenomenon is known as "thermal depinning." In addition, as discussed in Sec. III, the vortex lattice becomes softer and eventually melts via a first order transition into the vortex liquid. The interdependence of pinning, interactions, and thermal fluctuations is complex and one needs an effective nonperturbative method to evaluate the disorder averages. Such a method, using the replica trick, was developed initially in the theory of spin glasses. It is more difficult to apply it in a crystalline phase, so we start from a simpler homogeneous phase (the homogeneity might be achieved by both the thermal fluctuations and disorder) and return to the crystalline phase in the following section.

1. Replica approach to disorder

a. The replica trick

The replica method is widely used to study disordered electrons in metals and semiconductors, spin glasses, and other areas of condensed matter physics and far beyond it (Itzykson and Drouffe, 1991). It was applied to vortex matter in the elastic medium approximation (Nattermann, 1990; Korshunov, 1993; Giamarchi and Le Doussal, 1994, 1995a, 1995b, 1996, 1997; Bogner *et al.*, 2001). In the following we describe the method in some detail.

The main problem in calculation of disorder averages is that one typically has to take the average of nonpolynomial functions of the statistical sum [Eq. (18)],

$$Z = \int \mathcal{D}\Psi\mathcal{D}\Psi^* \exp\left\{-1/\omega_t\left[F[\Psi] + \frac{1-t}{2}\int_r W(r) \times|\Psi(r)|^2\right]\right\}. \tag{302}$$

Most interesting physical quantities are calculated by taking derivatives of the free energy which is a logarithm of Z. Applying a simple mathematical identity to represent the logarithm as a small power, $\log(z) = \lim_{n\to 0}(1/n)(z^n-1)$, the average over the free energy is written as

$$\bar{\mathcal{F}} = -\omega_t \lim_{n\to 0}\frac{1}{n}\overline{(Z^n-1)}. \tag{303}$$

The quantity Z^n can be looked upon as a statistical sum over n identical replica fields Ψ_a, $a=1,\ldots,n$,

$$Z^n[W] = \prod_b \int_{\Psi_b} \exp\left\{-\sum_{a=1}^{n}\left[\frac{F[\Psi_a]}{\omega_t} + \frac{1-t}{2\omega_t}\int_r W(r) \times|\Psi_a(r)|^2\right]\right\}, \tag{304}$$

where $F[\Psi_a]$ is the free energy (in physical unit meantime) without disorder. Note that the disorder potential enters in the exponent. The disorder measure, consistent with variance in Eq. (268) is Gaussian. Therefore disorder average is a Gaussian integral which can be readily performed,

$$\overline{Z^n} = \frac{1}{\text{norm}}\int \mathcal{D}W \exp\left[-1/2n\int_r W^2(r)\right] Z^n[W] = \int_{\Psi_a} e^{-(1/\omega_t)F_n}, \tag{305}$$

where

$$F_n \equiv \sum_a F[\Psi_a] + \frac{1}{2}r(t)\sum_{a,b}\int_r |\Psi_a|^2|\Psi_b|^2. \tag{306}$$

After the disorder average different replicas are no longer independent. In the LLL limit and units,

$$\overline{Z^n} = \int_{\Psi_a} e^{-(1/4\pi\sqrt{2})F_n}, \qquad F_n \equiv \sum_a F[\Psi_a] + \frac{r(t)}{2}\sum_{a,b}\int_r |\Psi_a|^2|\Psi_b|^2. \tag{307}$$

This statistical physics model is a type of scalar field theory and the simplest nonperturbative scheme commonly used to treat such a model is Gaussian approximation already introduced in Sec. III.B. Its validity and precision can be checked only by calculating corrections.

b. Correlators and distributions

Correlators averaged over both the thermal fluctuations and disorder can be generated by the usual trick of introducing an external "source" into statistical sum [Eq. (302)],

$$Z[W,S^*,S]=\int_{\Psi,\Psi^*}\exp\left\{-\frac{1}{\omega_t}\left[F[\Psi]+\frac{1}{2}(1-t)\int_r W(r)|\Psi(r)|^2+\int_r \Psi(r)S^*(r)+\Psi^*(r)S(r)\right]\right\}$$
$$=\int_{\Psi,\Psi^*} e^{-(1/\omega_t)F[\Psi,W(r),S(r),S^*(r)]} \tag{308}$$

and taking functional derivatives of the free energy in the presence of sources

$$\mathcal{F}[W,S^*,S]=-\omega_t \log Z[W,S^*,S]. \tag{309}$$

The first two thermal correlators are

$$\langle\Psi(r)\rangle=\frac{1}{Z[W,S^*,S]}\int_{\Psi,\Psi^*}\Psi(r)e^{-(1/\omega_t)F[\Psi,W(r),S(r),S^*(r)]}-\frac{\omega_t}{Z[W,0,0]}\frac{\delta}{\delta S^*(r)}Z[W,S^*,S]|_{S,S^*=0}$$
$$=\frac{\delta}{\delta S^*(r)}\mathcal{F}[W,S^*,S]|_{S,S^*=0},$$
$$\langle\Psi^*(r)\Psi(r')\rangle_c=\langle\Psi^*(r)\Psi(r')\rangle-\langle\Psi^*(r)\rangle\langle\Psi(r')\rangle=\frac{\delta^2}{\delta S(r)\delta S^*(r')}\mathcal{F}[W,S^*,S]|_{S,S^*=0}. \tag{310}$$

Now the disorder averages of these quantities are calculated using the replica trick,

$$\overline{\langle\Psi(r)\rangle}=-\omega_t\frac{\delta}{\delta S^*(r)}\lim_{n\to 0}\frac{1}{n}\overline{(Z[S,S^*]^n-1)}$$
$$=-\omega_t\lim_{n\to 0}\frac{1}{n}\frac{\delta}{\delta S^*(r)}\int_{\Psi_a}\exp\left\{-1/\omega_t\left[F_n[\Psi_a]+S^*(r)\sum_a\Psi^a(r)\right]\right\}\Big|_{S^*=0}$$
$$=\lim_{n\to 0}\frac{1}{n}\int_{\Psi_a}\sum_a\Psi^a(r)e^{-(1/\omega_t)F_n[\Psi_a]}$$
$$=\frac{1}{n}\sum_a\langle\Psi^a(r)\rangle. \tag{311}$$

A similar calculation for the two field correlator results in

$$\overline{\langle\Psi^*(r)\Psi(r')\rangle_c}=\lim_{n\to 0}\frac{1}{n}\sum_{a,b}\langle\Psi^{*a}(r)\Psi^b(r')\rangle. \tag{312}$$

In disorder physics it is of interest to know the disorder distribution of physical quantities such as magnetization [which within LLL is closely related to the correlator (see Sec. III.B)]. The simplest example is the second moment of the order parameter distribution $\overline{\langle\Psi^*(r)\rangle\langle\Psi(r')\rangle}$. This is harder to evaluate due to two thermal averages. One still uses Eq. (310) twice,

$$\langle\Psi^*(r)\rangle\langle\Psi(r')\rangle=\frac{1}{Z^2[W]}\int_{\Psi_1\Psi_2}\Psi_1(r)\Psi_2(r')\times e^{-(1/\omega_t)F[\Psi_1,W(r)]-(1/\omega_t)F[\Psi_2,W(r)]}$$
$$=\lim_{n\to 0}\int_{\Psi_1\Psi_2}\Psi_1(r)\Psi_2(r')\times e^{-(1/\omega_t)F[\Psi_1,W(r)]-(1/\omega_t)F[\Psi_2,W(r)]}Z^{n-2}[W]$$
$$=\lim_{n\to 0}\int_{\Psi_1\Psi_2}\Psi_1(r)\Psi_2(r')\times\exp\left\{-1/\omega_t\sum_{i=1}^{n}F[\Psi_i,W(r)]\right\}. \tag{313}$$

The disorder average leads to (Mezard *et al.*, 1987)

$$\overline{\langle\Psi^*(r)\rangle\langle\Psi(r')\rangle}=\lim_{n\to 0}\int_{\Psi_1\Psi_2}\Psi_1(r)\Psi_2(r')e^{-(1/\omega_t)F_n}$$
$$=\lim_{n\to 0,a\neq b}\int_{\Psi_a\Psi_b}\Psi_a(r)\Psi_b(r')e^{-(1/\omega_t)F_n}$$
$$=Q_{a,b}. \tag{314}$$

In case of replica symmetry breaking, Eq. (314) shall be written as

$$\overline{\langle\Psi^*(r)\rangle\langle\Psi(r')\rangle}=\lim_{n\to 0,a\neq b}\frac{1}{n(n-1)}\sum_{a\neq b}Q_{a,b}. \tag{315}$$

Therefore

$$\overline{\langle\Psi^*(r)\Psi(r')\rangle}=\overline{\langle\Psi^*(r)\Psi(r')\rangle_c}+\overline{\langle\Psi^*(r)\rangle\langle\Psi(r')\rangle}$$
$$=\lim_{n\to 0}\frac{1}{n}\sum_a\langle\Psi^{*a}(r)\Psi^a(r')\rangle. \tag{316}$$

c. Disordered LLL theory

Restricting the order parameter to LLL [Eq. (112)] by expanding it in quasimomentum LLL functions [Eq. (271)] one obtains the disordered LLL theory. We also rewrite the model in the same units we have used in Sec. III. The resulting Boltzmann factor is $\frac{1}{2^{5/2}\pi}f$,

$$f=\sum_a\{\psi_k^{a*}(k_z^2/2+a_T)\psi_k^a+f_{\rm int}[\psi_a]\}+f_{\rm dis}, \tag{317}$$

with the disorder term

$$f_{\rm dis}=\sum_{a,b}\frac{r(t)L_xL_y}{2(2\pi)^5}\int_{k,l,k',l'}\delta(k_z-l_z+k'_z-l'_z)\times[\mathbf{k},\mathbf{k}'|\mathbf{l},\mathbf{l}']\psi^{a*}_k\psi^a_l\psi^{b*}_{l'}\psi^c_{k'}, \tag{318}$$

in which $[\mathbf{k},\mathbf{k}'|\mathbf{l},\mathbf{l}']$ was defined in Eq. (142).

2. Gaussian approximation

a. Gaussian energy in homogeneous (amorphous) phase

One can recover the perturbative results of the previous section and even generalize them to finite temperatures by expanding in r, however, the replica method's advantage is more profound when nonperturbative effects are involved. We now apply the Gaussian approximation, which has been used in vortex physics in the framework of the elastic medium approach (Korshunov, 1990, 1993; Giamarchi and Le Doussal, 1994, 1995a, 1995b, 1996, 1997) following its use in polymer and disordered magnets' physics (Mezard and Parisi, 1991). As usual, homogeneous phases are simpler than the crystalline phase considered in the previous section, so we start from the case in which both the translational and the U(1) symmetries are respected by the variational correlator,

$$\overline{\langle\psi^{a*}_k\psi^b_k\rangle}=G_{ab}(k_z)=\left[\frac{2^{5/2}\pi}{(k_z^2/2)I+\mu^2}\right]_{a,b}. \tag{319}$$

Since the Gaussian approximation in the vortex liquid within the GL approach was described in Sec. III, here we just generalize various expressions to the case of n replicas. The Gaussian effective free energy is expressed via the variational parameter (Mezard and Parisi, 1991; Li and Rosenstein, 2002a, 2002b, 2002c) μ_{ab} which in the present case is a matrix in the replica space. The bubble and the trace log integrals appearing in the free energy are very simple,

$$\frac{1}{(2\pi)^3}\int_k\left[\frac{2^{5/2}\pi}{\frac{k_z^2}{2}I+\mu^2}\right]_{a,b}=2[\mu^{-1}]_{ab}\equiv 2u_{ab},$$
$$\frac{2^{5/2}\pi}{(2\pi)^3}\int_k[\log G^{-1}(k_z)]_{aa}=4\mu_{aa}+\text{const}, \tag{320}$$

where the "inverse mass" matrix u_{ab} was defined. As a result the Gaussian effective free energy density can be written in a form

$$nf_{\rm Gauss}=\sum_a-\frac{2^{5/2}\pi}{(2\pi)^3}\int_k[\log G^{-1}(k_z)]_{aa}+\frac{1}{(2\pi)^3}\int_k[(k_z^2/2+a_T)G(k_z)-I]_{aa}+4(u_{aa})^2-2r\sum_{a,b}|u_{ab}|^2$$
$$=2\sum_a\{\mu_{aa}+a_Tu_{aa}+2(u_{aa})^2\}-2r\sum_{a,b}|u_{ab}|^2, \tag{321}$$

where we discarded a (ultraviolet divergent) constant and higher order in n, and for simplicity $r(t)$ is denoted by r.

b. Minimization equations

It is convenient to introduce a real (not necessarily symmetric) matrix Q_{ab}, which is in one-to-one linear correspondence with the Hermitian (generally complex) matrix u_{ab} via

$$Q_{ab}=\text{Re}[u_{ab}]+\text{Im}[u_{ab}]. \tag{322}$$

Unlike u_{ab}, all the matrix elements of Q_{ab} are independent. In terms of this matrix the free energy can be written as

$$\frac{n}{2}f_{\rm Gauss}=\sum_a(u^{-1})_{aa}+a_TQ_{aa}+2(Q_{aa})^2-r\sum_{a,b}Q^2_{ab}. \tag{323}$$

Taking the derivative with respect to independent variables Q_{ab} gives the saddle point equation for this matrix element,

$$\frac{n}{2}\frac{\delta f}{\delta Q_{ab}}=-\frac{1}{2}[(1-i)(u^{-2})_{ab}+\text{c.c.}]+a_T\delta_{ab}+4Q_{aa}\delta_{ab}-2rQ_{ab}=0. \tag{324}$$

Since the electric charge (or the superconducting phase) U(1) symmetry is assumed, we consider only solutions with real u_{ab}. In this case $u_{ab}=Q_{ab}$ is a symmetric real matrix.

c. The replica symmetric matrice ansatz and the Edwards-Anderson order parameter

Experience with very similar models in the theory of disordered magnets indicates that solutions of these minimization equations are most likely to belong to the class of hierarchical matrices, which will be described in the next section. We limit ourselves here to most obvious of those, namely, to matrices which respect the Z_n replica permutation symmetry,

$$Q_{ab}\to Q_{p(a)p(b)} \tag{325}$$

for any of $n!$ permutations $a\to p(a)$. If we also include disorder in $|\psi(r)|^4$ term, one will find in the low temperature region that replica symmetry is spontaneously breaking as soon as the Edwards-Anderson (EA) order parameter is nonzero. However, we limit our discussion to replica symmetric solution [not considering disorder in $|\psi(r)|^4$] and think that the glass transition appears when the EA order parameter is nonzero. This transition line from zero EA to nonzero EA obtained in the following is very near to the replica symmetry breaking transition line considering weak disorder in $|\psi(r)|^4$ (Li, Rosenstein, and Vinokur, 2006). We also believe that

even without disorder in $|\psi(r)|^4$ term, the replica symmetry is breaking if we can solve the model nonperturbatively.

The most general matrix of the replica symmetric solution has the form

$$Q_{ab} = u_{ab} = \delta_{ab}\tilde{u} + (1 - \delta_{ab})\lambda. \tag{326}$$

The off-diagonal elements are equal to the EA order parameter λ. A nonzero value for this order parameter signals that the annealed and the quenched averages are generally different. We calculate $\overline{\langle\psi^*(r)\rangle\langle\psi(r)\rangle}$ starting from Eq. (314). Using Eq. (319), one obtains with the Gaussian approximation

$$\overline{\langle\psi^*(r)\rangle\langle\psi(r)\rangle}_r = 2\lambda, \tag{327}$$

where $\langle\ \rangle_r$ also contains space average.

One can visualize this phase as a phase with locally broken U(1) symmetry with various directions of the phase at different locations with zero average $\overline{\langle\psi(r)\rangle}=0$ but a distribution of nonzero value of characteristic width λ. The distribution of more complicated quantities will be discussed in Sec. IV.B.4. Here we refer to this state as glass, although in Sec. IV.B.4 it will be referred to as the "ergodic pinned liquid" (EPL) distinguished from the "nonergodic pinned liquid" (NPL) in which, in addition, the ergodicity is broken. Broken ergodicity is related to "replica symmetry breaking," however, as we show there, in the present model of the δT_c disorder and within the Gaussian approximation RSB does not occur. If the EA order parameter is zero, disorder does not have a profound effect on the properties of the vortex matter. We refer to this state as "liquid."

The dynamic properties of such phase are generally quite different from those of the nonglassy λ (zero EA order parameter) phase. In particular it is expected to exhibit infinite conductivity (Fisher, 1989; Fisher *et al.*, 1991; Dorsey *et al.*, 1992). However, if u_{ab} is replica symmetric, pinning does not results in the multitude of time scales. Certain time scale sensitive phenomena such as various memory effects (Paltiel, Zeldov, Myasoedov, Rappaport, *et al.*, 2000; Paltiel, Zeldov, Myasoedov, Shtrikman, *et al.*, 2000; Xiao *et al.*, 2002) and the responses to "shaking" (Beidenkopf *et al.*, 2005) are expected to be different from the case when u_{ab} breaks the replica permutation symmetry.

We show in the following section that within the Gaussian approximation and the limited disorder model that we consider (the δT_c inhomogeneity only) RSB does not occur. Then we can consider the remaining problem without using the machinery of hierarchical matrices.

d. Properties of the replica symmetric matrices

It is easy to work with the RS matrices like u_{ab} in Eq. (326). It has two eigenvalues. A replica symmetric eigenvector

$$u\begin{pmatrix}1\\1\\\cdots\\1\end{pmatrix} = \Delta'\begin{pmatrix}1\\1\\\cdots\\1\end{pmatrix}, \quad \Delta' \equiv \tilde{u} + (n-1)\lambda \simeq \tilde{u} - \lambda, \tag{328}$$

where subleading terms at small n were omitted in the last line and the rest of the space (replica asymmetric vectors) which is $n-1$ times degenerate. For example,

$$u\begin{pmatrix}1\\-1\\0\\\cdots\end{pmatrix} = \Delta\begin{pmatrix}1\\-1\\0\\\cdots\end{pmatrix}, \quad \Delta \equiv \tilde{u} - \lambda \simeq \tilde{u} - \lambda. \tag{329}$$

The counting seems strange but mathematically can be defined and works. Numerous attempts to discredit replica calculations on these grounds were proven baseless. Note that the two eigenvalues differ by order n terms only. Projectors on these spaces are

$$P_S = \frac{1}{n}\begin{pmatrix}1 & 1 & \cdots & 1\\ 1 & 1 & \cdots & 1\\ \cdots & \cdots & \cdots & \cdots\\ 1 & 1 & \cdots & 1\\ 1 & 1 & & 1\end{pmatrix}, \quad P_A = \mathcal{I} - P_s,$$
$$u = \Delta' P_S + \Delta P_A. \tag{330}$$

Here $\mathcal{I}$ is the unit matrix δ_{ab}. It is easy to invert RS matrices and multiply them using this form. For example,

$$u^{-1} = \Delta'^{-1} P_S + \Delta^{-1} P_A. \tag{331}$$

3. The glass transition between the two replica symmetric solutions

a. The unpinned liquid and the "ergodic glass" replica symmetric solutions of the minimization equations

The minimization equation [Eq. (324)] for RS matrices takes the form

$$-\Delta'^{-2} P_S - \Delta^{-2} P_A + (a_T + 4\tilde{u})\mathcal{I} - 2r(\Delta' P_S + \Delta P_A) = 0. \tag{332}$$

Expressing it via independent matrices I and P_s one obtains

$$[\Delta^{-2} - \Delta'^{-2} - 2r(\Delta' - \Delta)]P_S + (-\Delta^{-2} + a_T + 4\tilde{u} - 2r\Delta)\mathcal{I} = 0. \tag{333}$$

To leading order in n (first) the P_s equation is

$$\lambda(\Delta^{-3} - r) = 0. \tag{334}$$

This means that there exists a RS symmetric solution λ =0. In addition there is a nondiagonal one. It turns out that there is a third order transition between them.

The second equation,

$$-\Delta^{-2}+a_T+4\tilde{u}-2r\Delta=0, \tag{335}$$

for the diagonal (liquid) solution, $\Delta_l=\tilde{u}_l$, is just a cubic equation,

$$-\tilde{u}_l^{-2}+a_T+4\tilde{u}_l-2r\tilde{u}_l=0. \tag{336}$$

For the nondiagonal solution the first equation [Eq. (334)] gives $\Delta=r^{1/3}$, which when plugged into the first equation gives

$$\tilde{u}_g=\tfrac{1}{4}(3r^{2/3}-a_T),\quad \lambda=\tfrac{1}{4}(3r^{2/3}-a_T)-r^{-1/3}. \tag{337}$$

The matrix u therefore is

$$u^g_{ab}=r^{-1/3}\delta_{ab}+\lambda. \tag{338}$$

The two solutions coincide when $\lambda_g=0$ leading to the glass line equation

$$a^g_T=r^{-1/3}(3r-4). \tag{339}$$

b. Free energy and its derivatives: The third order glass line

We now calculate the energies of the solutions. The energy of such a RS matrix is given, using Eq. (331), by

$$\begin{aligned}\frac{n}{2}f_{\text{Gauss}}&=\sum_a\{(\Delta'^{-1}P_S+\Delta^{-1}P_A)_{aa}+a_T\tilde{u}+2\tilde{u}^2\\&\quad-r(\Delta'^2P_S+\Delta^2P_A)_{aa}\}\\&\simeq n\{2\Delta^{-1}-\Delta^{-2}\lambda+a_T\tilde{u}+2\tilde{u}^2\\&\quad-r(\Delta^2+2\Delta\lambda)\},\end{aligned} \tag{340}$$

where leading order in small n was kept. The RS energy is

$$f_l=2\tilde{u}_l^{-1}+2a_T\tilde{u}_l+2(4-2r)\tilde{u}_l^2, \tag{341}$$

which can be further simplified using Eq. (336),

$$f_l=4\tilde{u}_l^{-1}. \tag{342}$$

The glass free energy is even simpler,

$$f_g=6r^{1/3}-\tfrac{1}{4}(3r^{2/3}-a_T)^2. \tag{343}$$

Since in addition to the energy, the first derivative of the scaled energy, the scaled entropy,

$$df/da_T=2r^{-1/3}, \tag{344}$$

and the second derivative, the specific heat,

$$d^2f/da_T^2=-\tfrac{1}{2}, \tag{345}$$

both coincide for solution on the transition line defined by Eq. (339). The third derivatives are different so that the transition is a third order one.

c. Hessian and the stability domain of a solution

Up to now we have found two homogeneous solutions of the minimization equations. There might be more and the solutions might not be stable when considered on the wider set of Gaussian states. In order to prove that a solution is stable beyond the set of replica symmetric matrices u, one has to calculate the second derivative of free energy (so called Hessian) with respect to arbitrary real matrix Q_{ab} defined in Eq. (322),

$$\begin{aligned}H_{(ab)(cd)}&\equiv\frac{n}{2}\frac{\delta^2 f_{\text{eff}}}{\delta Q_{ab}\delta Q_{cd}}\\&=\left\{\frac{1}{2}[(u^{-2})_{ac}(u^{-1})_{db}-i(u^{-2})_{ad}(u^{-1})_{cb}]\right.\\&\quad\left.+\frac{1}{2}[(u^{-1})_{ac}(u^{-2})_{db}-i(u^{-1})_{ad}(u^{-2})_{cb}]+\text{c.c.}\right\}\\&\quad+4\delta_{ac}\delta_{bd}\delta_{ab}-2r\delta_{ac}\delta_{bd}.\end{aligned} \tag{346}$$

The Hessian matrix should be considered as a matrix in a space, which itself is a space of matrices, so that Hessian's index contains two pairs of indices of u. We use a simplified notation for the product of the Kronecker delta functions with more than two indices: $\delta_{ac}\delta_{bd}\delta_{ab}\equiv\delta_{abcd}$. It is not trivial to define what is meant by "positive definite" when the number of components approaches zero. It turns out that the correct definition consists in finding all eigenvalues of the Hessian "supermatrix."

d. Stability of the liquid solution

For the diagonal solution the Hessian matrix is a very simple operator on the space of real symmetric matrices,

$$H_{(ab)(cd)}=c_I I_{abcd}+c_J J_{abcd}, \tag{347}$$

where the operators I (the identity in this space) and J are defined as

$$I\equiv\delta_{ac}\delta_{bd},\quad J=\delta_{abcd} \tag{348}$$

and their coefficients in the liquid phase are

$$c_I=2(\tilde{u}_l^{-3}-r),\quad c_J=4, \tag{349}$$

with $\tilde{u}_l$ a solution of Eq. (336). The corresponding eigenvectors in the space of symmetric matrices are

$$v_{(cd)}\equiv A\,\delta_{cd}+B. \tag{350}$$

To find eigenvalues h of H we apply the Hessian matrix on a vector v. The result is (dropping terms vanishing in the limit $n\to 0$)

$$\begin{aligned}H_{(ab)(cd)}v_{cd}&=A(c_I+c_J)\delta_{ab}+B(c_I+c_J\delta_{ab})\\&=h(A\,\delta_{ab}+B).\end{aligned} \tag{351}$$

Then the two eigenvalues are therefore $h^{(1)}=c_I$ and $h^{(2)}=c_I+c_J$. Since $c_J=4>0$, the sufficient condition for stability is

$$c_I=2(\tilde{u}^{-3}-r)>0; \tag{352}$$

it is satisfied everywhere below the transition line of Eq. (339).

e. The stability of the glass solution

The analysis of stability of the nondiagonal solution is slightly more complicated. The Hessian matrix for the nondiagonal solution is

$$H_{(ab)(cd)} = c_V V + c_U U + c_J J, \tag{353}$$

where the new operators are

$$V_{(ab)(cd)} = \delta_{ac} + \delta_{bd}, \quad U_{(ab)(cd)} = 1 \tag{354}$$

and the coefficients are

$$c_V = -3\lambda r^{2/3}, \quad c_U = 4\lambda^2 r^{1/3}, \quad c_J = 4. \tag{355}$$

In the present case, one obtains three different eigenvalues (de Alameida and Thouless, 1978; Fischer and Hertz, 1991; Dotsenko, 2001),

$$h^{(1.2)} = 2(1 \pm \sqrt{1 - 4\lambda r^{2/3}}) \tag{356}$$

and $h^{(3)}=0$. Note that the eigenvalues of the Hessian matrix on the antisymmetric matrices are degenerate with eigenvalue $h^{(1)}$ in this case. For $\lambda<0$ the solution is unstable due to negative $h^{(2)}$. For $\lambda>0$, both eigenvalues are positive and the solution is stable. The line $\lambda=0$ coincides with the third order transition line, hence the nondiagonal solution is stable when the diagonal is unstable and vice versa. We conclude that one of the two RS solutions is stable for any value of external parameters (here represented by a_T and r). There still might be a replica asymmetric solution with first order transition to it, but this possibility will be ruled out within the Gaussian approximation and in the homogeneous phase without the $|\psi|^4$ disorder term in the next section. Therefore the transition does not correspond to RSB. Despite this in the phase with nonzero EA order parameter there are Goldstone bosons corresponding to $h^{(3)}$ in the replica limit of $n\to 0$. The criticality and the zero modes due to disorder (pinning) in this phase might lead to a variety of interesting phenomena in both statics and dynamics.

f. Generalizations and comparison with experimental irreversibility line

The glass line resembles typical irreversibility lines in both low T_c and high T_c materials (see Fig. 14), where the irreversibility line of $NbSe_2$ is fitted. The theory can be generalized to 2D GL model describing thin films or very anisotropic layered superconductors. The glass line is given in two dimensions,

$$a_T^g = 2\sqrt{2}(R-1)/\sqrt{R}. \tag{357}$$

Examples of organic superconductor (Shibauchi *et al.*, 1998) were given by Li, Rosenstein, and Vinokur (2006). The data of BSCCO (Beidenkopf *et al.*, 2005) are compared to the theoretical results in Fig. 15.

4. The disorder distribution moments of the LLL magnetization

As discussed in Sec. III, the magnetization within LLL is proportional to the superfluid density, whose average is

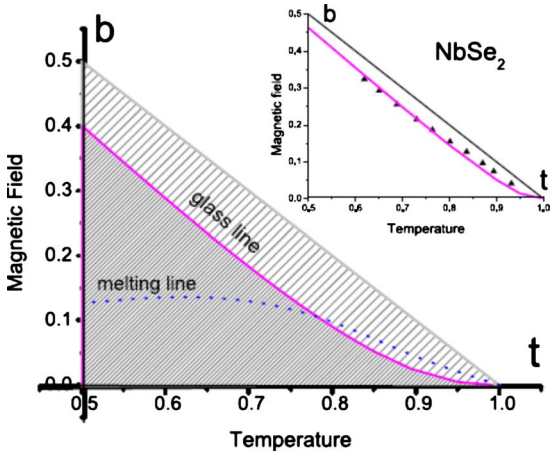

FIG. 14. (Color online) $NbSe_2$ phase diagram.

$$\overline{\langle\psi^*(r)\psi(r)\rangle_r} = \lim_{n\to 0}\frac{1}{n}\sum_a \langle\Psi^{*a}(r)\Psi^a(r)\rangle_r \frac{1}{n} \times \sum_a \frac{4\pi\sqrt{2}}{(2\pi)^3}\int_k \left[\left(\frac{k_z^2}{2}1 + \mu^{2-1}\right)\right]_{aa} = \frac{2}{n}\sum_a u_{aa} = 2\tilde{u}. \tag{358}$$

The variance of the distribution is determined from the two thermal averages, disorder average,

$$\overline{[\langle\psi^*\psi\rangle\langle\psi^*\psi\rangle]_r} = \frac{1}{n(n-1)}\sum_{a\neq b}\langle|\psi^{*a}(r)|^2|\psi^b(r)|^2\rangle_r. \tag{359}$$

Within the Gaussian approximation (Wick contractions) the correlators are

$$\overline{[\langle\psi^*\psi\rangle\langle\psi^*\psi\rangle]_r} = 4(\tilde{u}^2 + \lambda^2). \tag{360}$$

Therefore the variance of the distribution is given by λ. This variance determines the width of the magnetization loop. In turn, according to the phenomenological

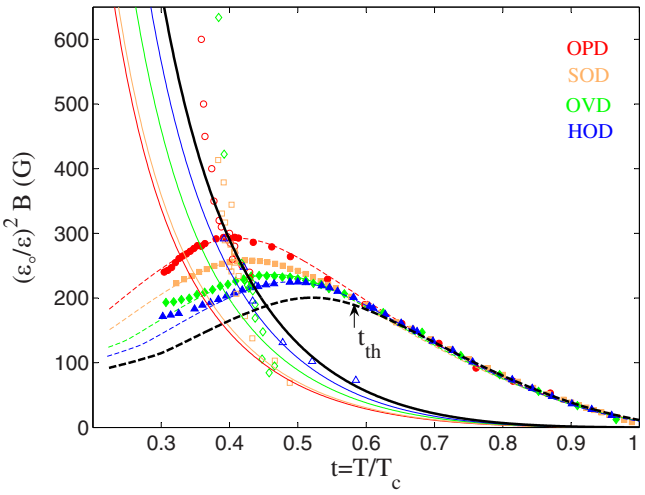

FIG. 15. (Color online) Melting line and order-disorder lines in layered superconductor BSCCO (Beidenkopf *et al.*, 2007).

Bean model (Tinkham, 1996), the width of the magnetization loop is proportional to the critical current. The distribution of magnetization is not symmetric, as the third moment shows,

$$\overline{[\langle\psi^*\psi\rangle^3]}_r = 8(\tilde{u}^3 + 3\tilde{u}\lambda^2 + \lambda^3). \tag{361}$$

Its calculation is more involved. The third irreducible cumulant is therefore nonzero,

$$\overline{[\langle\psi^*\psi\rangle^3]}_r - 3\times 2\tilde{u}\overline{[\langle\psi^*\psi\rangle^2]}_r + 2(2\tilde{u})^3 = 8\lambda^3. \tag{362}$$

In analogy to Mezard and Parisi (1991) one can define "glass susceptibility,"

$$\chi = \langle\psi^*\psi\rangle - \langle\psi^*\rangle\langle\psi\rangle = 2(\tilde{u}-\lambda), \tag{363}$$

useful in description of the glassy state. Its variance of susceptibility vanishes without RSB,

$$\overline{\chi^2} = \bar{\chi}^2. \tag{364}$$

We return to the replica symmetry breaking after considering the crystalline phase.

C. Gaussian theory of a disordered crystal

1. Replica symmetric ansatz in Abrikosov crystal

In Sec. IV.A we used perturbation theory in disorder to assess the basic properties of the vortex crystal. However, we learned in the previous section that certain properties such as the glass related phenomena cannot be captured by perturbation theory and one has to resort to simplest nonperturbative methods available. In the homogeneous phase the Gaussian approximation in the replica symmetric subspace was developed and we now generalize to a more complicated crystalline case. This is quite analogous to what we did with thermal fluctuations, so the description contains less details.

a. Replica symmetric shift of the free energy

Within the Gaussian approximation the expectation values of the fields as well as their propagators serve as variational parameters. To implement it, it is convenient to shift and "rotate" the fields according to Eq. (143),

$$\psi_a(r) = v_a\varphi(r) + \frac{1}{4\pi^{3/2}}\int_k c_{\mathbf{k}}\exp(ik_z)\varphi_{\mathbf{k}}(\mathbf{r})(O_k^a + iA_k^a), \tag{365}$$

where the factor $c_{\mathbf{k}}\equiv\gamma_k/|\gamma_k|$ was introduced for convenience and $\varphi_{\mathbf{k}}(x)$ are the quasimomentum functions. In principle the shift as well as fields are replica index dependence. However, assumption of the unbroken replica symmetry means that

$$v_a = v \tag{366}$$

is the only variational shift parameter.

To evaluate the Gaussian energy we first substitute this into free energy and write quadratic, cubic, and quartic parts in fields A and O. The quadratic terms originating from the interaction and disorder term are listed below. The OO terms coming from the interaction part are the $O_a^*O_b$ term,

$$\frac{v^2}{2^4\pi^3}\int_r|\varphi(r)|^2\int_{k,l}\varphi_{\mathbf{k}}^*(x)c_{-\mathbf{k}}c_{\mathbf{k}}\varphi_{\mathbf{l}}(\mathbf{r})O_{-k}^aO_l^b = \frac{v^2}{2}\int_k\beta_{\mathbf{k}}O_k^aO_{-k}^b, \tag{367}$$

the $O_a^*O_b^*$ term, $(2/4)\int_k|\gamma_{\mathbf{k}}|O_k^aO_{-k}^b$, and finally the O_aO_b term, $(v^2/4)\int_k|\gamma_{\mathbf{k}}|O_k^aO_{-k}^b$. Sum over all four OO terms is therefore

$$\int_k v^2(\beta_{\mathbf{k}}+|\gamma_k|)O_k^aO_{-k}^b. \tag{368}$$

Similarly the AA terms sum up to

$$\int_k v^2(\beta_{\mathbf{k}}-|\gamma_{\mathbf{k}}|)A_k^aA_{-k}^b, \tag{369}$$

while the OA terms cancel. The disorder term contributes (leading order in n as usual for replica method)

$$\frac{r}{2}v^2\left[n\int_k\beta_{\mathbf{k}}\sum_a A_k^aA_{-k}^a + \int_k(\beta_{\mathbf{k}}-|\gamma_{\mathbf{k}}|)\sum_{a,b}A_k^aA_{-k}^b\right] = \frac{r}{2}v^2\int_k\left[\sum_a(\beta_{\mathbf{k}}-|\gamma_{\mathbf{k}}|)A_k^aA_{-k}^a + \sum_{a\neq b}(\beta_{\mathbf{k}}-|\gamma_{\mathbf{k}}|)A_k^aA_{-k}^b\right] \tag{370}$$

to the A part and

$$\frac{r}{2}v^2\left[\int_k\sum_a(\beta_{\mathbf{k}}+|\gamma_{\mathbf{k}}|)O_k^aO_{-k}^a + \sum_{a\neq b}\int_k(\beta_{\mathbf{k}}+|\gamma_{\mathbf{k}}|)O_k^aO_{-k}^b\right] \tag{371}$$

to the O part. The quadratic part of the free energy therefore is

$$\begin{aligned} f_2 = \frac{1}{2}\int_k\sum_a[a_T + v^2(2\beta_{\mathbf{k}}-|\gamma_{\mathbf{k}}|) + rv^2(\beta_{\mathbf{k}}-|\gamma_{\mathbf{k}}|)]A_k^aA_{-k}^a \\ + rv^2\sum_{a\neq b}(\beta_{\mathbf{k}}-|\gamma_{\mathbf{k}}|)A_k^aA_{-k}^b + [a_T + v^2(2\beta_{\mathbf{k}}+|\gamma_{\mathbf{k}}|) \\ + rv^2(\beta_{\mathbf{k}}+|\gamma_{\mathbf{k}}|)]O_k^aO_{-k}^a + rv^2 \\ \times\sum_{a\neq b}(\beta_{\mathbf{k}}-|\gamma_{\mathbf{k}}|)O_k^aO_{-k}^b. \end{aligned} \tag{372}$$

There is no linear term and a cubic term is not needed since its contraction vanishes. The quartic term will be taken into account later. We will not need cubic terms within the Gaussian approximation, while the quartic terms are not affected by the shift of fields. We are ready therefore to write down the Gaussian variational energy.

b. Gaussian energy

Now we describe contributions to the Gaussian energy. The mean field terms (namely, containing the shift only with no pairings) are

$$f_{\rm mf}=\int_x\left[nf(\psi_a)-\frac{r}{2}n^2|\psi_a|^4\right], \tag{373}$$

which using Eq. (365) takes the form

$$f_{\rm mf}=na_T v^2+(n/2)\beta_A v^4-(r/2)n^2\beta_A v^4. \tag{374}$$

The last term can be omitted since the power of n exceeds 1. The Gaussian effective energy in addition to $f_{\rm mf}$ contains the Tr log term and the "bubble diagrams." The Tr log term comes from free Gaussian part (see Sec. III). The reference "best Gaussian (or quadratic) energy" is defined variationally as a quadratic form,

$$\frac{1}{2}\int_k(\varepsilon_k^A A_k^a A_{-k}^a+\varepsilon_k^O O_k^a O_{-k}^a)+\sum_{a\neq b}[(\bar\mu_{\mathbf k}^A)^2 A_k^a A_{-k}^b+(\bar\mu_{\mathbf k}^O)^2 O_k^a O_{-k}^b], \tag{375}$$

and

$$\varepsilon_{\mathbf k}^A=k_z^2/2+(\mu_{\mathbf k}^A)^2,\quad \varepsilon_{\mathbf k}^O=k_z^2/2+(\mu_{\mathbf k}^O)^2, \tag{376}$$

where $\mu_{\mathbf k}^A,\mu_{\mathbf k}^O,\bar\mu_{\mathbf k}^A,\bar\mu_{\mathbf k}^O$ are all variational parameters. We assumed no mixing of the A and the O modes, following the experience in the clean case and the structure of the quadratic part determined in the previous section.

In the following we keep subleading terms in n since they contribute to order n in energy. The Tr log (divided by volume) is sum of logarithms of all eigenvalues,

$$\begin{aligned}f_{\rm tr\,log}&=\frac{1}{2^{3/2}\pi^2}\int_k(n-1)\log[\varepsilon_k^A-(\bar\mu_{\mathbf k}^A)^2]\\&\quad+\log[\varepsilon_k^A+(n-1)(\bar\mu_{\mathbf k}^A)^2]\\&\quad+(n-1)\log[\varepsilon_k^O-(\bar\mu_{\mathbf k}^O)^2]\\&\quad+\log[\varepsilon_k^O+(n-1)(\bar\mu_{\mathbf k}^O)^2]\\&=\frac{1}{\pi}\int_{\mathbf k}(n-1)[(\mu_{\mathbf k}^A)^2-(\bar\mu_{\mathbf k}^A)^2]^{1/2}\\&\quad+[(\mu_{\mathbf k}^A)^2+(n-1)(\bar\mu_{\mathbf k}^A)^2]^{1/2}\\&\quad+(n-1)[(\mu_{\mathbf k}^O)^2-(\bar\mu_{\mathbf k}^O)^2]^{1/2}\\&\quad+[(\mu_{\mathbf k}^O)^2+(n-1)(\bar\mu_{\mathbf k}^O)^2]^{1/2},\end{aligned} \tag{377}$$

where the last integral is over the Brillouin zone. One observes that the order $O(n)$ terms cancel, while the relevant order is

$$\begin{aligned}f_{\rm tr\,log}&=\frac{n}{2\pi}\int_{\mathbf k}2[(\mu_{\mathbf k}^A)^2-(\bar\mu_{\mathbf k}^A)^2]^{1/2}+(\bar\mu_{\mathbf k}^A)^2[(\mu_{\mathbf k}^A)^2\\&\quad-(\bar\mu_{\mathbf k}^A)^2]^{-1/2}+2[(\mu_{\mathbf k}^O)^2-(\bar\mu_{\mathbf k}^O)^2]^{1/2}\\&\quad+(\bar\mu_{\mathbf k}^O)^2[(\mu_{\mathbf k}^O)^2-(\bar\mu_{\mathbf k}^O)^2]^{-1/2}.\end{aligned} \tag{378}$$

The diagrams are of two kinds. Those including one propagator and ones which have two propagators from the part quartic in fields. The propagators are expectation values of pair of fluctuating fields obtained by inverting the replica symmetric matrix as in the previous section. For example, for the acoustic mode one gets

$$\begin{aligned}4\pi\sqrt{2}p_k^A&=\langle A_k^a A_{-k}^a\rangle=4\pi\sqrt{2}\frac{\varepsilon_k^A-2(\bar\mu_{\mathbf k}^A)^2}{[\varepsilon_k^A-(\bar\mu_{\mathbf k}^A)^2]^2},\\4\pi\sqrt{2}\bar p_k^A&=\langle A_k^a A_{-k}^b\rangle=-\frac{4\pi\sqrt{2}(\bar\mu_{\mathbf k}^A)^2}{[\varepsilon_k^A-(\bar\mu_{\mathbf k}^A)^2]^2}.\end{aligned} \tag{379}$$

The integrals of the propagators over k_z give

$$\begin{aligned}\frac{1}{2(2\pi)^3}\int_{k_z}4\pi\sqrt{2}p_k^A&=p_{\mathbf k}^A=\frac{1}{2\pi}\Big[[(\mu_{\mathbf k}^A)^2-(\bar\mu_{\mathbf k}^A)^2]^{-1/2}\\&\quad-\frac{(\bar\mu_{\mathbf k}^A)^2}{2}[(\mu_{\mathbf k}^A)^2-(\bar\mu_{\mathbf k}^A)^2]^{-3/2}\Big],\\\frac{1}{2(2\pi)^3}\int_{k_z}4\pi\sqrt{2}\bar p_k^A&=\bar p_{\mathbf k}^A=\frac{1}{2\pi}\Big[-\frac{(\bar\mu_{\mathbf k}^A)^2}{2}[(\mu_{\mathbf k}^A)^2\\&\quad-(\bar\mu_{\mathbf k}^A)^2]^{-3/2}\Big]\end{aligned} \tag{380}$$

and similarly for O.

The contraction of the quadratic parts, after the integration and expansion to order n, results in

$$\begin{aligned}f_2&=-\frac{1}{2}f_{\rm tr\,log}+n\int_{\mathbf k}\{p_{\mathbf k}^A[a_T+v^2(2\beta_{\mathbf k}-|\gamma_{\mathbf k}|)\\&\quad-rv^2(\beta_{\mathbf k}-|\gamma_{\mathbf k}|)]+rv\bar p_k^A(\beta_{\mathbf k}-|\gamma_{\mathbf k}|)\}\\&\quad+n\int_{\mathbf k}\{p_{\mathbf k}^O[a_T+v^2(2\beta_{\mathbf k}+|\gamma_{\mathbf k}|)\\&\quad-rv^2(\beta_{\mathbf k}+|\gamma_{\mathbf k}|)]+rv\bar p_k^O(\beta_{\mathbf k}+|\gamma_{\mathbf k}|)\}.\end{aligned} \tag{381}$$

For quartic terms coming from two contractions of the interaction and the disorder part one obtains

$$f_{\rm int}=n\int_{\mathbf k,\mathbf l}(p_{\mathbf k}^A+p_{\mathbf k}^O)\beta_{\mathbf k-\mathbf l}(p_{\mathbf l}^A+p_{\mathbf l}^O)+\frac{\gamma_{\mathbf k}\gamma_{\mathbf l}}{2\beta_\Delta}(p_{\mathbf k}^A-p_{\mathbf k}^O)(p_{\mathbf l}^A-p_{\mathbf l}^O) \tag{382}$$

and

$$\begin{aligned}f_{\rm dis}&=-\frac{r}{2}\int_{\mathbf k,\mathbf l}\Big[(p_{\mathbf k}^A+p_{\mathbf k}^O)\beta_{\mathbf k-\mathbf l}(p_{\mathbf l}^A+p_{\mathbf l}^O)+\frac{\gamma_{\mathbf k}\gamma_{\mathbf l}}{\beta_\Delta}(p_{\mathbf k}^A-p_{\mathbf k}^O)\\&\quad\times(p_{\mathbf l}^A-p_{\mathbf l}^O)\Big]-(\bar p_{\mathbf k}^A+\bar p_{\mathbf k}^O)\beta_{\mathbf k-\mathbf l}(\bar p_{\mathbf l}^A+\bar p_{\mathbf l}^O)\\&\quad-\frac{\gamma_{\mathbf k}\gamma_{\mathbf l}}{\beta_\Delta}(\bar p_{\mathbf k}^A-\bar p_{\mathbf k}^O)\beta_{\mathbf k-\mathbf l}(\bar p_{\mathbf l}^A-\bar p_{\mathbf l}^O),\end{aligned} \tag{383}$$

respectively. Finally we get

$$f_{\rm Gauss}=f_{\rm mf}+f_2+f_{\rm tr\,log}+f_{\rm int}+f_{\rm dis}. \tag{384}$$

2. Solution of the gap equations

a. Gap and shift equations

The Gaussian energy is minimized with respect to the variational parameters. Differentiating with respect to v^2 one gets the shift equation,

$$0 = a_T + \beta_\Delta v^2 + \langle (2\beta_{\mathbf{k}} - |\gamma_{\mathbf{k}}|)p_{\mathbf{k}}^A - r(\beta_{\mathbf{k}} - |\gamma_{\mathbf{k}}|)(p_{\mathbf{k}}^A - \bar{p}_{\mathbf{k}}^A)\rangle_{\mathbf{k}} + \langle (2\beta_{\mathbf{k}} + |\gamma_{\mathbf{k}}|)p_{\mathbf{k}}^O - r(\beta_{\mathbf{k}} + |\gamma_{\mathbf{k}}|)(p_{\mathbf{k}}^O - \bar{p}_{\mathbf{k}}^O)\rangle_{\mathbf{k}}, \quad (385)$$

while differentiating with respect to four variational parameters in the propagator matrix gap equations are obtained,

$$E_{\mathbf{k}} = a_T + \beta_\Delta v^2 - r v^2 \beta_{\mathbf{k}} + (2-r)\langle \beta_{\mathbf{k}-\mathbf{l}}(p_{\mathbf{l}}^A - p_{\mathbf{l}}^O)\rangle_{\mathbf{l}}, \quad (386)$$

$$\Delta_{\mathbf{k}} = (1-r)v^2\eta_{\mathbf{k}} + (1-r)\eta_{\mathbf{k}}\left\langle \frac{\eta_{\mathbf{l}}}{\beta_\Delta}(p_{\mathbf{l}}^A - p_{\mathbf{l}}^O)\right\rangle_{\mathbf{l}},$$

$$\bar{E}_{\mathbf{k}} = -r\beta_\Delta v^2 - r\langle \beta_{\mathbf{k}-\mathbf{l}}(\bar{p}_{\mathbf{k}}^A + \bar{p}_{\mathbf{k}}^O)\rangle_{\mathbf{l}}, \quad (387)$$

$$\bar{\Delta}_{\mathbf{k}} = -rv^2\eta_{\mathbf{k}} + r\eta_{\mathbf{k}}\left\langle \frac{\eta_{\mathbf{l}}}{\beta_\Delta}(\bar{p}_{\mathbf{l}}^A - \bar{p}_{\mathbf{l}}^O)\right\rangle_{\mathbf{l}},$$

where

$$E_{\mathbf{k}} = \tfrac{1}{2}[(\mu_{\mathbf{k}}^O)^2 + (\mu_{\mathbf{k}}^A)^2], \quad \bar{E}_{\mathbf{k}} = \tfrac{1}{2}[(\bar{\mu}_{\mathbf{k}}^O)^2 + (\bar{\mu}_{\mathbf{k}}^A)^2], \quad (388)$$

$$\Delta_{\mathbf{k}} = \tfrac{1}{2}[(\mu_{\mathbf{k}}^O)^2 - (\mu_{\mathbf{k}}^A)^2], \quad \bar{\Delta}_{\mathbf{k}} = \tfrac{1}{2}[(\bar{\mu}_{\mathbf{k}}^O)^2 - (\bar{\mu}_{\mathbf{k}}^A)^2].$$

b. Solution by the mode expansion

One can observe that the ansatz

$$(\mu_{\mathbf{k}}^O)^2 - (\mu_{\mathbf{k}}^A)^2 = \eta_{\mathbf{k}}\Delta, \quad (\bar{\mu}_{\mathbf{k}}^O)^2 - (\bar{\mu}_{\mathbf{k}}^A)^2 = \eta_{\mathbf{k}}\bar{\Delta} \quad (389)$$

satisfies the gap equations, leading to a simpler set for two unknown functions and three unknown parameters satisfying Eqs. (385)–(387) and

$$\Delta = (1-r)\left[v^2 - \left\langle \frac{\eta_{\mathbf{l}}}{\beta_\Delta}(p_{\mathbf{l}}^A - p_{\mathbf{l}}^O)\right\rangle_{\mathbf{l}}\right], \quad (390)$$

$$\bar{\Delta} = -r\left[v^2 - \left\langle \frac{\eta_{\mathbf{l}}}{\beta_\Delta}(\bar{p}_{\mathbf{l}}^A - \bar{p}_{\mathbf{l}}^O)\right\rangle_{\mathbf{l}}\right].$$

The equation can be solved using the mode expansion,

$$\beta_k = \sum_{n=0}^{\infty} \chi^n \beta_n(k), \quad \beta_n(k) \equiv \sum_{|\mathbf{X}|^2 = n a_\Delta^2} \exp[i\mathbf{k}\cdot\mathbf{X}]. \quad (391)$$

As in Sec. III.C, The integer n determines the distance of points on a reciprocal lattice from the origin and $\chi \equiv \exp[-a_\Delta^2/2] = \exp[-2\pi/\sqrt{3}] = 0.0265$. One estimates that $E_n \simeq \chi^n a_T$, therefore the coefficients decrease exponentially with n. Note that for some integers, for example, $n = 2, 5, 6$, $\beta_n = 0$. Retaining only first s modes will be called the s mode approximation,

$$E(\mathbf{k}) = E_0 + E_1\chi\beta_1(\mathbf{k}) + \cdots + E_n\chi^n\beta_n(\mathbf{k}) + \cdots + \cdots, \quad (392)$$

$$\overline{E(\mathbf{k})} = \overline{E_0} + \overline{E_1}\chi\beta_1(\mathbf{k}) + \cdots + \overline{E_n}\chi^n\beta_n(\mathbf{k}) + \cdots + \cdots.$$

Equation (392) deviates significantly from the perturbative one, especially at low temperatures and when the 2D case is considered.

c. Generalizations and comparison to experiments

As noted in 2D disorder leads, at least perturbatively, to more profound restructuring of the vortex lattice than in three dimensions. In fact, perturbation theory becomes invalid. The gaussian methods described above remove the difficulty and allow calculation of the order-disorder line. In this case one does not encounters the "wiggle" but rather a smooth decrease of the order-disorder field when the temperature is lowered. In Fig. 15 the ODT line of strongly anisotropic high T_c superconductor BSCCO is shown.

One generally observes that there is always an off-diagonal component in the correlator of the "optical" phonon field O. However, the off-diagonal Edwards-Anderson parameter part for a more important low energy excitation "acoustic" branch appears only below a line quite similar to the glass line in the homogeneous phase.

D. Replica symmetry breaking

When thermal fluctuations are significant the efficiency of imperfections to pin the vortex matter is generally diminished. This phenomenon is known as thermal depinning. In addition, as discussed in Sec. III, the vortex lattice becomes softer and eventually melts via a first order transition into the vortex liquid. The interdependence of pinning, interactions and thermal fluctuations is very complex and one needs an effective nonperturbative method to evaluate the disorder averages. Such a method, using the replica trick, was developed initially in the theory of spin glasses. It is more difficult to apply it in a crystalline phase, so we start from a simpler homogeneous phase (the homogeneity might be achieved by both the thermal fluctuations and disorder) and return to the crystalline phase in the following section.

1. Hierarchical matrices and absence of RSB for the δT_c disorder in the Gaussian approximation

a. The hierarchical matrices and their Parisi's parametrization

Experience with similar models in the theory of disordered magnets indicates that solutions of these minimization equations are most likely to belong to the class of hierarchical matrices, which are comprehensively described, for example, by Fischer and Hertz (1991), Mezard (1991), and Dotsenko (2001). We limit ourselves here to operational knowledge of working with such matrices contained in the Appendix of Mezard and Parisi (1991) and collect several rules of using Parisi's representation in Appendix B. General hierarchical matrices u are parametrized using the diagonal elements $\tilde{u}$ and Parisi's (monotonically increasing) function u_x specifying

the off-diagonal elements with $0<x<1$ (Parisi, 1980). Physically different x represent time scales in the glass phase. In particular, the Edwards-Anderson (EA) order parameter is $u_{x=1}=\lambda>0$.

A nonzero value for this order parameter signals that the annealed and quenched averages are different. The dynamic properties of such a phase are generally quite different from those of the nonglassy $\lambda=0$ phase. In particular, it is expected to exhibit infinite conductivity (Fisher, 1989; Fisher *et al.*, 1991; Dorsey *et al.*, 1992). We refer to this phase as the EPL distinguished from the NPL in which, in addition, the ergodicity is broken. Broken ergodicity is related to replica symmetry breaking discussed below, however, as we show in the present model of the δT_c disorder and within the Gaussian approximation RSB does not occur.

In terms of the Parisi parameter $\tilde{u}$ and u_x the matrix equation [Eq. (324)] takes the form

$$-\widetilde{u^{-2}}+a_T+(4-2r)\tilde{u}=0, \tag{393}$$

$$(u^{-2})_x+2ru_x=0. \tag{394}$$

Dynamically if u_x is a constant, pinning does not results in the multitude of time scales. Certain time scale sensitive phenomena such as various memory effects (Paltiel, Zeldov, Myasoedov, Rappaport, *et al.*, 2000; Paltiel, Zeldov, Myasoedov, Shtrikman, *et al.*, 2000; Xiao *et al.*, 2002) and the responses to shaking (Beidenkopf *et al.*, 2005) are expected to be different from the case when u_x takes multiple values. If u_x takes a finite different number of n values, we call $n-1$ step RSB. On the other hand, if u_x is continuous, the continuous RSB occurs. We show below that within the Gaussian approximation and the limited disorder model that we consider (the δT_c inhomogeneity only) RSB does not occur. After that is shown, we can consider the remaining problem without using the machinery of hierarchical matrices.

b. Absence of replica symmetry breaking

In order to show that u_x is a constant, it is convenient to rewrite the second equation via the matrix μ, the matrix inverse to u,

$$(\mu^2)_x+2r(\mu^{-1})_x=0. \tag{395}$$

Differentiating this equation with respect to x one obtains

$$2[\{\mu\}_x-r(\{\mu\}_x)^{-2}]x\,d\mu_x/dx=0, \tag{396}$$

where we used a set of standard notations in the spin glass theory (Mezard and Parisi, 1991),

$$\{\mu\}_x\equiv\tilde{\mu}-\langle\mu_x\rangle-[\mu]_x,\quad \langle\mu_x\rangle\equiv\int_0^1 dx\mu_x, \tag{397}$$

$$[\mu]_x=\int_0^x dy(\mu_x-\mu_y).$$

If one is interested in a continuous monotonic part $d\mu_x/dx\neq 0$, the only solution of Eq. (395) is

$$\{\mu\}_x=r^{1/3}. \tag{398}$$

Differentiating this again and dropping the nonzero derivative $d\mu_x/dx$ again, one further gets a contradiction: $d\mu_x/dx=0$. This proves that there are, no such monotonically increasing continuous segments. One can therefore generally have either the replica symmetric solutions, namely, $u_x=\lambda$, or look for a several steplike RSB solutions (Fischer and Hertz, 1991; Dotsenko, 2001). One can show that the constant u_x solution is stable. Therefore, if a steplike RSB solution exists, it might be only an additional local minimum. We explicitly looked for a one step solution and found that there is none.

V. SUMMARY AND PERSPECTIVE

In this section we summarize and provide references to original papers, pointing out further applications and generalizations of results presented here. The bibliography of works on the GL theory of the vortex matter is so extensive that there are no doubt, many important papers and even directions missed in this outline. Some of them, however, can be found in books (Saint-James *et al.*, 1969; Tinkham, 1996; Ketterson and Song, 1999; Kopnin, 2001; Larkin and Varlamov, 2005) and reviews (Blatter *et al.*, 1994; Brandt, 1995; Nattermann and Scheidl, 2000; Giamarchi and Bhattacharya, 2002).

A. GL equations

1. Microscopic derivations of the GL equations

Phenomenological Ginzburg-Landau equations (Ginzburg and Landau, 1950) preceded a microscopic theory of superconductivity. Soon after the BCS theory appeared Gorkov and others derived from it the GL equations. Derivations and the relations of the GL parameters to the microscopic parameters in the BCS theory are reviewed by Larkin and Varlamov (2005). The dynamical versions of the theory were derived using several methods and the parameter γ in the time dependent GL equation related no normal state conductivity (Larkin and Varlamov, 2005). Most of the methods described here can be generalized to the case when the nondissipative imaginary part of γ is also present. In particular, this leads to the Hall current (Ullah and Dorsey, 1990, 1991; Troy and Dorsey, 1993) and was used to explain the "Hall anomaly" in both low T_c and high T_c superconductors.

The δT disorder was introduced phenomenologically in statics by Larkin (1970). Other coefficients of the GL free energy may also have random components (Blatter *et al.*, 1994). How these new random variables influence the LLL model, which discussed by Li, Rosenstein, and Vinokur (2006).

2. Anisotropy

High T_c cuprates are layered superconductors which can be better described by the Lawrence-Doniach (LD) model (Lascher and Doniach, 1971) than the 3D GL model discussed in the present review. The LD model is a version of the GL model with a discretized z coordinate. However, in many cases one can use two simpler limiting cases. If anisotropy is not very large, one can use anisotropic 3D GL [Eq. (5)]. The requirement that the GL can be effectively used therefore limits us to optimally doped $YBCO_{7-\delta}$ and similar materials for which the anisotropy parameter is not very large: $\gamma_a = \sqrt{m_c^*/m_{a,b}^*} = 4-8$. Effects of a layered structure are dominant in BSCCO or Tl based compounds ($\gamma_a > 80$) and noticeable for cuprates with anisotropy of order $\gamma_a = 50$, like LaBaCuO or Hg1223. Anisotropy effectively reduces dimensionality leading to stronger thermal fluctuations according to Eq. (19). Very anisotropic layered superconductors can be described by the 2D GL model,

$$F = L_z \int d^2\mathbf{r}\left[\frac{\hbar^2}{2m^*}|\mathbf{D}\psi|^2 + a'|\psi|^2 + \frac{b'}{2}|\psi|^4\right], \qquad (399)$$

which can be approached by the methods presented here. For the LD model analytical methods become significantly more complicated. The Gaussian approximation study of thermal fluctuations was, however, performed (Ikeda, 1995; Larkin and Varlamov, 2005) and used to explained the so-called crossing point of the magnetization curves, as well as crossover between the 3D to the 2D behavior (Tešanović *et al.*, 1992; Baraduc *et al.*, 1994; Salem-Sugui and Dasilva, 1994; Junod *et al.*, 1998; Rosenstein *et al.*, 2001; Huh and Finnemore, 2002; Lin and Rosenstein, 2005). In many simulations this model rather than GL was adopted (Ryu *et al.*, 1996; Wilkin and Jensen, 1997). The GL model can also be extended in direction of introducing anisotropy in the a-b plane, like the fourfold symmetric anisotropy leading to transition from the rhombic lattice to the square lattice (Chang *et al.*, 1998a, 1998b; Park and Huse, 1998; Rosenstein and Knigavko, 1999; Klironomos and Dorsey, 2003) observed in many high T_c and low T_c type II superconductors alike (Eskildsen *et al.*, 2001; Li, Lin, *et al.*, 2006).

3. Dynamics

Dynamics of vortex matter can be described by a time dependent generalization of the GL equations (Larkin and Varlamov, 2005). The bifurcation method presented here can be extended to a moving vortex lattice (Thompson and Hu, 1971; Li *et al.*, 2004). The extension is nontrivial since the linear operator appearing in the equations is non-Hermitian.

One can also consider thermal transport (Ullah and Dorsey, 1990, 1991), for example, the Nernst effect (Ussishkin *et al.*, 2002; Ussishkin, 2003; Mukerjee and Huse, 2004; Tihn and Rosenstein, 2009), measured recently in experiments (Wang *et al.*, 2002, 2006; Pourret *et al.*, 2006).

B. Theory of thermal fluctuations in GL model

Here we list alternative approaches to those described in the present review. It is important to mention an unorthodox opinion concerning the very nature of the crystalline state and melting transition. Although many recent experiments indicate that the transition is first order [for alternative interpretation see Nikulov (1995) and Nikulov *et al.* (1995)], some doubted the existence of a stable solid phase (Moore, 1989, 1992; Kienappel and Moore, 1997) and therefore of the transition all together.

1. Functional renormalization group for the LLL theory

While applying the renormalization group (RG) on the one loop level, Brézin *et al.* (1985) found no fixed points of the (functional) RG equations and thus concluded that the transition to the solid phase, if it exists, is not continuous. The RG method therefore cannot provide a quantitative theory of the melting transition. It is widely believed, however, that the finite temperature transition exists and is first order [see, however, Newman and Moore (1996), who found another solution of functional RG equations].

2. Large number of components limit

The GL theory can be generalized (in several different ways) to an N component order parameter field. The large N limit of this theory can be computed in a way similar to that in the N component scalar models widely used in theory of critical phenomena (Itzykson and Drouffe, 1991). The most straightforward generalization has been studied by Affleck and Brézin (1985) in the homogeneous phase leading to a conclusion that there is no instability of this state in the 3D GL. However, since there are other ways to extend the theory to the N component case, it was shown by Moore *et al.* (1998) that the state in which only one component has a nonzero expectation value (similar to the one component Abrikosov lattice) is not the ground state of the most straightforward generalization. Subsequently it was found (Lopatin and Kotliar, 1999; Li and Rosenstein, 2004) that there exists a generalization for which this is in fact the case.

3. Diagrams resummation

In many body theories one can resum various types of diagrams. In fact, one can consider Hartree-Fock, $1/N$, and even one loop RG methods as types of the diagram resummation. Moore and Yeo (Yeo and Moore, 1996a, 1996b, 2001) and more recently Yeo and co-workers (Yeo *et al.*, 2006; Park and Yeo, 2008) followed a strategy used in strongly coupled electron systems to resum all the parquet diagrams. The thermal fluctuation in GL model had been studied using various analytic methods (Koshelev, 1994), but in the vortex liquid region near the melting point, or overcooled liquid, the nonperturbative method must be used, for example, the Borel-Pade resummation method to obtain density-density correlation was carried out in Hu *et al.* (1994).

4. Numerical simulations

The LLL GL model was studied numerically in both three (Sasik and Stroud, 1995) and two dimensions (Tešanović and Xing, 1991; Kato and Nagaosa, 1993; O'Neill and Moore, 1993; Li and Nattermann, 2003). The melting was found to be first order. The results serve as an important check on the analytic theory described in this review. In many simulations the XY model is employed (Ryu *et al.*, 1996; Hu *et al.*, 1997; Wilkin and Jensen, 1997). It is believed that results are closely related to that of the Ginzburg-Landau model. The methods allows consideration of disorder and dynamics (Nonomura and Hu, 2001; Olsson and Teitel, 2001; Chen and Hu, 2003; Olsson, 2007) and fluctuations of the magnetic field (Nguyen and Sudbø, 1998).

5. Density functional

The density functional theory is a general method to tackle a strongly coupled system. The method crucially depends on the choice of the functional. It was applied to the GL model by Herbut and Tešanović (1994) and was employed by Menon and Dasgupta (1994), Menon *et al.* (1999), and Menon (2002) to study the melting and by Hu *et al.* (2005) to the layered systems.

6. Vortex matter theory

Elastic moduli were first calculated from the GL model by Brandt (1977a, 1977b, 1986) by considering an infinitesimal shift of zeros of the order parameter. He found that the compression and the shear moduli are dispersive. This feature is important in phenomenological applications such as the Lindemann criterion for both the melting and the orderdisorder lines (considered different) (Houghton *et al.*, 1989; Ertas and Nelson, 1996; Kierfeld and Vinokur, 2000; Mikitik and Brandt, 2001, 2003) as well to estimates of the critical current and the collective pinning theory [see Blatter *et al.* (1994) and Brandt (2005), and references therein]. The dispersion, however, is ignored in most advanced applications of the elasticity theory to statics (Giamarchi and Le Doussal, 1994, 1995a, 1995b, 1996, 1997; Nattermann and Scheidl, 2000) or dynamics (Giamarchi and Le Doussal, 1996, 1998; Chauve *et al.*, 2000; Giamarchi and Bhattacharya, 2002). Recently a phase diagram of strongly type II superconductors was discussed using a modified elasticity theory taking into account dislocations of the vortex lattice (Dietel and Kleinert, 2006, 2007, 2009).

Tešanović and co-workers (Tešanović *et al.*, 1992; Tešanović and Andreev, 1994) noted a remarkable fact that most fluctuation effects are due to condensation energy. The lateral correlation parts are around 2% and therefore can be neglected. The theory explains an approximate intersection of the magnetization curves and is used to analyze data (Zhou *et al.*, 1993; Pierson *et al.*, 1995, 1996; Pierson, Valls, *et al.*, 1998; Pierson and Walls, 1998).

7. Beyond LLL

To quantitatively describe vortex matter higher Landau levels (HLLs) corrections are sometimes required. For example, in an optimally doped YBCO superconductor one can establish the LLL scaling for fields above 3 T and temperature above 70 K [see, for example, Sok *et al.* (1995)]. A glance at the data, however, shows that above T_c the scaling is generally unconvincing: the LLL magnetization is much larger that the experimental one above T_c. Naively, on the solid side, when the distance from the mean field transition line is smaller than the inter-Landau level gap, one expects that the higher Landau modes can be neglected. More careful examination of the mean field solution presented in Sec. II.B reveals that a weaker condition should be used for a validity test of the LLL approximation. However, the fluctuation corrections involving HLL in strongly fluctuating superconductors might be important. Ikeda and co-workers calculated the fluctuation spectrum in solid including HLL (Ikeda *et al.*, 1990; Ikeda, 1995). In the vortex liquid the HLL contribution has been studied by Lawrie (1994) in the framework of the Gaussian (Hartree-Fock) approximation. He found the region of validity of the LLL approximation. The leading (Gaussian) contribution of HLL was combined with more refined treatment of the LLL modes recently resulting in reasonably good agreement with experimental data (Li and Rosenstein, 2003).

8. Fluctuations of magnetic field and the dual theory approach

Although it was understood that fluctuations of the magnetic field in strongly type II superconductors are strongly suppressed (Halperin *et al.*, 1974; Lobb, 1987), they still play an important role when κ is not large and magnetic field away from $H_{c2}(T)$ (the situation mostly not covered in the present review). The main methods are the numerical simulations (Dasgupta and Halperin, 1981; Nguyen and Sudbø, 1998; Olsson and Teitel, 2003) and the dual theory approach (Kovner and Rosenstein, 1992; Kovner *et al.*, 1993; Tešanović, 1999), which were efficient in describing the Kosterlitz-Thouless transition in superconducting thin film and layered materials (Oganesyan *et al.*, 2006). Vortex lines and loops are interpreted as a signal of "inverted U(1)" or the "magnetic flux" symmetry. The symmetry is spontaneously broken in the normal phase (with a photon as a Goldstone boson) while restored in the superconductor. Vortices are the worldlines of the flux symmetry charges.

C. The effects of quenched disorder

1. Vortex glass in the frustrated XY model

The original idea of the vortex glass and the continuous glass transition exhibiting the glass scaling of conductivity diverging in the glass phase appeared early in the framework of the so-called frustrated XY model (the gauge glass) (Fisher, 1989; Fisher *et al.*, 1991; Nattermann and Scheidl, 2000). In this approach one fixes the

amplitude of the order parameter retaining the magnetic field with random component added to the vector potential. It was studied by the RG and variational methods and has been extensively simulated numerically (Nonomura and Hu, 2001; Olsson and Teitel, 2001; Chen and Hu, 2003; Kawamura, 2003; Olsson, 2007; Chen, 2008). In analogy to the theory of spin glass the replica symmetry is broken when crossing the GT line. The model ran into several problems [see Giamarchi and Bhattacharya (2002) for a review]: for finite penetration depth λ it has no transition (Bokil and Young, 1995) and there was a difficulty to explain sharp Bragg peaks observed in experiment at low fields.

2. Disordered elastic manifolds: Bragg glass and replica symmetry breaking

To address the last problem another simplified model had been proven to be more convenient: the elastic medium approach to a collection of interacting linelike objects subject to both the pinning potential and the thermal bath Langevin force (Cha and Fertig, 1994a, 1994b; Faleski *et al.*, 1996; Reichhardt *et al.*, 1996, 2000; van Otterlo *et al.*, 1998; Dodgson *et al.*, 2000; Fangohr and Cox, 2001; Olson *et al.*, 2001; Fangohr *et al.*, 2003). The resulting theory was treated again using the Gaussian approximation (Korshunov, 1993; Giamarchi and Le Doussal, 1994, 1995a, 1995b, 1996, 1997) and RG (Nattermann, 1990; Nattermann and Scheidl, 2000; Bogner *et al.*, 2001). The result was that in $2<D<4$ there is a transition to a glassy phase in which the replica symmetry is broken following the "hierarchical pattern" (in $D=2$ the breaking is "one step"). The problem of the fast destruction of the vortex lattice by disorder was solved with the vortex matter in the replica symmetry broken (RSB) phase and it was termed "Bragg glass" (Giamarchi and Le Doussal, 1994, 1995a, 1995b, 1996, 1997). A closely related approach was developed recently for both 3D and layered superconductors in which effects of dislocations were incorporated (Dietel and Kleinert, 2006, 2007, 2009).

3. Density functional for a disordered system: Supersymmetry

Generalized replicated density functional theory (Menon, 2002) was also applied resulting in a one step RSB solution. Although the above approximations to the disordered GL theory are useful in more "fluctuating" superconductors such as BSCCO, a problem arises with their application to YBCO at temperature close T_c (where most of the experiments mentioned above are done): vortices are far from being linelike and even their cores significantly overlap. As a consequence, the behavior of the dense vortex matter is expected to be different from that of a system of linelike vortices and of the XY model although the elastic medium approximation might still be meaningful (Brandt, 1995).

One should note the work by Tešanović and Herbut (1994) on columnar defects in layered materials, which utilizes supersymmetry, as an alternative to replica or dynamics, to incorporate disorder nonperturbatively.

4. Dynamical approach to disorder in the Ginzburg-Landau model

The statics and the linear response within disordered GL model has been discussed in numerous theoretical, numerical, and experimental works. The glass line was first determined, to our knowledge using the Martin-Siggia-Rose dynamical approach in Gaussian approximation (Dorsey *et al.*, 1992) and was claimed to be obtained using resummation of a diagram in Kubo formula of Ikeda *et al.* (1990). The glass transition line for the ΔT_c disorder was obtained using the replica formalism (within a similar Gaussian approximation) by Lopatin (2000) and the result is identical to be presented in the present review. He also extended the discussion beyond the Gaussian approximation employing the Cornwall-Jackiw-Tomboulis variational method described. This was generalized to other types of disorder (the mean free path disorder) of Li, Rosenstein, and Vinokur (2006). The common wisdom is that the replica symmetry is generally broken in the glass (either via "steps" or via "hierarchical" continuous process) as in most spin glass theories (Fischer and Hertz, 1991; Dotsenko, 2001). The divergence of conductivity on the glass line was obtained by Rosenstein and Zhuravlev (2007) [it was assumed by Dorsey *et al.* (1992) and linked phenomenologically to the general scaling theory of the vortex glass proposed by Fisher (1989) and Fisher *et al.* (1991)]. The results are consistent with the replica ones presented in the present review. In this work I-V curves and critical current were derived in an improved Gaussian approximation and several physical questions related to the peak effect addressed.

5. Numerical simulation of the disordered Ginzburg-Landau model

The theory can be generalized to the 2D case appropriate for description of thin films or strongly layered superconductors and compared to experiments. The comparison for organic superconductor κ-$(BEDTTF)_2Cu[N(CN)_2]Br$ (Bel *et al.*, 2007) and BSCCO (Beidenkopf *et al.*, 2005) of the static glass line is quite satisfactory. There exist, to our knowledge, two Monte Carlo simulations of the disordered GL model (Kienappel and Moore, 1997; Li and Nattermann, 2003), both in two dimensions, in which no clear irreversibility line was found. However, the frustrated XY model was recently extensively simulated (Nonomura and Hu, 2001; Olsson and Teitel, 2001, 2003; Chen and Hu, 2003; Kawamura, 2003; Olsson, 2007; Chen, 2008) including the glass transition line and I-V curves. It shares many common features with the GL model although disorder is introduced in a different way, so that it is difficult to compare the dependence of pinning. The I-V curves and the glass line resemble the Ginzburg-Landau results.

6. Finite electric fields

Finite electric fields (namely, transport beyond linear response) were also considered analytically by Blum and

Moore (1997) and our result in the clean limit agrees with theirs. The elastic medium and the vortex dynamics within the London approximation were discussed beyond linear response in numerous analytic and numerical works. Although qualitatively the glass lines obtained here resemble the ones in phenomenological approaches based on comparison of disorder strength with thermal fluctuations and interaction (Ertas and Nelson, 1996; Kierfeld and Vinokur, 2000; Mikitik and Brandt, 2001, 2003; Radzyner *et al.*, 2002), the detailed form is different.

D. Other fields of physics

There are several physical systems in which the methods described here, in a slightly modified form, can be applied and indeed appeared under different names. Two areas are the superfluidity and the BEC condensate physics [Pethick and Smith (2008), and references therein]. The magnetic field is analogous to the rotation of the superfluid. One can observe lattice of vortices with properties somewhat reminiscent of those of the Abrikosov vortices (Madison *et al.*, 2000; Abo Shaeer *et al.*, 2001; Cooper *et al.*, 2001; Engels *et al.*, 2002; Sivona *et al.*, 2002; Baym, 2003; Sonin, 2005; Wu *et al.*, 2007). Another closely related field is the physics of the 2D electron gas in a strong magnetic field (Monarkha and Kono, 2004). In some cases the problem can be formulated in a way similar to the present case with the Wigner crystal analogous to the Abrikosov liquid (with time playing the role of the z direction of the fluxon), while quenched disorder appears in a way similar to the columnar defects in the vortex physics. Some aspects of the liquid crystal physics can also be formulated in a form similar to the GL equations in magnetic field.

ACKNOWLEDGMENTS

We are grateful to many people, who either actively collaborated with us or discussed various issues related to vortex physics. Collaborators, colleagues, and students include G. Bel, E. H. Brandt, B. Feng, P. J. Lin, P. Lipavsky, R. Lortz, Z. S. Ma, B. Ya. Shapiro, I. Shapiro, A. Shaulov, B. Tinh, V. Vinokur, T. J. Yang, Y. Yeshurun, Z. G. Wu, E. Zeldov, and V. Zhuravlev. We are indebted to G. Blatter, A. T. Dorsey, T. Giamarchi, B. Horowitz, X. Hu, A. E. Koshelev, T. Maniv, G. Menon, R. Mint, T. Nattermann, P. Olsson, C. Reichhardt, Z. Tešanović, and S. Teitel, for discussions, E. Andrei, H. Beidenkopf, C. C. Chi, M. R. Eskildsen, E. M. Forgan, A. Grover, K. Hirata, J. Juang, P. H. Kes, N. Kokubo, J. Kolacek, M. Konczykowski, J. J. Lin, J. Y. Lin, T. Nishizaki, S. Salem-Sugui, C. J. van der Beek, C. Villard, H. H. Wen, and M. K. Wu for discussions and sending experimental results, sometimes prior to publications. This work was supported by NSC of R.O.C. Grant No. 98N0978907384 and MOE ATU program and National Science Foundation of China (Grant No. 10774005). D.L. is grateful to National Chiao Tung University, while B.R. is grateful to NCTS and University Center of Samaria for hospitality during sabbatical leave.

APPENDIX A: INTEGRALS OF PRODUCTS OF THE QUASIMOMENTUM EIGENFUNCTIONS

In this appendix a method to calculate space averages of products of the quasimomentum eigenfunctions in both the static and dynamic cases.

1. Rhombic lattice quasimomentum functions

We specialize to a rhombic lattice with the following bases of the direct and the reciprocal lattices (see Fig. 3 for definition of the angle θ and the lattice spacing a_θ, subject to the flux quantization relation [Eq. (63)]),

$$\mathbf{d}_1 = d_\theta(1,0), \quad \mathbf{d}_2 = d_\theta(\tfrac{1}{2},\tfrac{1}{2}\tan\theta),$$
$$\tilde{\mathbf{d}}_1 = d_\theta(\tfrac{1}{2}\tan\theta,-\tfrac{1}{2}), \quad \tilde{\mathbf{d}}_2 = (0,d_\theta). \tag{A1}$$

We use here the "LLL" unit of magnetic length.

We start with static LLL functions for an arbitrary rhombic lattice,

$$\varphi_{\mathbf{k}} = \sqrt{\frac{2\sqrt{\pi}}{d_\theta}}\sum_l e^{i[(2\pi/a_\theta)(x+k_y)l+(\pi l^2/2)\tan\theta]} \times e^{-(1/2)[y-k_x-(2\pi/d_\theta)l]^2}. \tag{A2}$$

To include higher LL corrections, it is convenient to use rising and lowering operators introduced in Eq. (90) to work with the HLL functions, $\hat{a}^\dagger=(2)^{-1/2}(-i\partial_x+\partial_y-y)$, $\hat{a}=-(2)^{-1/2}(-i\partial_x+\partial_y+y)$. The following formula will be frequently used. If φ is an LLL function, then

$$\varphi^* a^{+N} f(x,y) = 2^{-N/2}(-i\partial_x+\partial_y)^n \varphi^* f(x,y). \tag{A3}$$

2. The basic Fourier transform formulas

a. Product of two functions

It can be verified by direct calculation of the Gaussian integrals that

$$\int_{\mathbf{r}} \varphi(\mathbf{r})\varphi^*_{\mathbf{k}}(\mathbf{r})e^{i\mathbf{r}\cdot\mathcal{K}} = 4\pi^2\sum_{K_1,K_2}\delta(\mathcal{K}-\mathbf{k}-\mathbf{K})F(\mathbf{k},\mathbf{K}),$$
$$F(\mathbf{k},\mathbf{K}) = e^{-\mathcal{K}^2/4+i[(\pi/2)K_1^2-(\mathcal{K}_x\mathcal{K}_y/2)+k_x\mathcal{K}_y]}, \tag{A4}$$

with decomposition of arbitrary momentum $\mathcal{K}$ into its "rational part" $\mathbf{k}$, which belongs to the Brillouin zone, and an "integer part" $\mathbf{K}$, belonging to the reciprocal lattice

$$\mathcal{K} = \mathbf{k}+\mathbf{K}, \quad \mathbf{K} = K_1\mathbf{d}_1 + K_2\mathbf{d}_2. \tag{A5}$$

Its inverse Fourier transform,

$$\varphi(\mathbf{r})\varphi^*(\mathbf{r}+\tilde{\mathbf{k}}) = e^{ixk_x}\sum_{\mathbf{K}} e^{-i\mathcal{K}\cdot\mathbf{r}}F(\mathbf{k},\mathbf{K}), \tag{A6}$$

where $\tilde{k}_i=\varepsilon_{ij}k_j$, can be generalized into

$$\varphi(\mathbf{r}+\tilde{\mathbf{l}})\varphi^*(\mathbf{r}+\tilde{\mathbf{k}}) = e^{i(x+l_y)(k-l)_x} \times \sum_{\mathbf{K}} e^{-i\mathcal{K}\cdot(\mathbf{r}+\tilde{\mathbf{l}})+(\pi i/2)(K_1^2+K_1)-i\mathcal{K}_x\mathcal{K}_y/2+i(k-l)_x\mathcal{K}_y-\mathcal{K}^2/4}, \tag{A7}$$

with $\mathcal{K}=\mathbf{K}+\mathbf{k}-\mathbf{l}$. This in turn provides a useful product representation,

$$\varphi_{\mathbf{k}}^*(\mathbf{r})\varphi_{\mathbf{l}}(\mathbf{r}) = \sum_{\mathbf{K}} e^{-i\mathcal{K}\cdot\mathbf{r}-\mathcal{K}^2/4} \times e^{i(\pi/2)K_1^2-i(\mathcal{K}_x\mathcal{K}_y/2)+ik_x\mathcal{K}_y-i\mathcal{K}_x l_y+il_y(k-l)_x}. \tag{A8}$$

b. The four-point vertex function

The relation above used twice gives the following expression for the four point vertex in the quasimomentum representation:

$$\int_{\mathbf{r}} \varphi_{\mathbf{k}}^*(\mathbf{r})\varphi_{\mathbf{l}}(\mathbf{r})\varphi_{\mathbf{l}'}^*(\mathbf{r})\varphi_{\mathbf{k}'}(\mathbf{r}) = (2\pi)^2\sum_{\mathcal{K}} \delta[\mathcal{K}-\mathcal{K}']e^{-\mathcal{K}^2/2+i[(\pi/2)K_1^2-(\pi/2)K_1'^2+(k_x-k_x')\mathcal{K}_y-\mathcal{K}_x(l_y-l_y')+l_y(k-l)_x-l_y'(k'-l')_x]}. \tag{A9}$$

The delta function $\delta[\mathcal{K}-K']$ implies that

$$K_1+k_1-l_1 = K_1'+k_1'-l_1'. \tag{A10}$$

As $0\leqslant k_1,l_1,k_1',l_1'<1$, we have only three possible integer values for each coordinate,

$$k_1-l_1-k_1'+l_1' = \mathbf{\Delta}_1 = 0,1,-1, \tag{A11}$$

$$k_2-l_2-k_2'+l_2' = \mathbf{\Delta}_2 = 0,1,-1,$$

which require $K_{1,2}-K_{1,2}'=0,-1,1$. Thus

$$\sum_{\mathcal{K},\mathcal{K}'} \delta[\mathcal{K}-\mathcal{K}'] = \sum_{\mathbf{K},\mathbf{\Delta}} \delta[\mathbf{K}-\mathbf{K}'+\mathbf{\Delta}] \times \delta[\mathbf{k}-\mathbf{l}-(\mathbf{k}'-\mathbf{l}')-\mathbf{\Delta}] \tag{A12}$$

and the product takes the form

$$\int_{\mathbf{r}} \varphi_{\mathbf{k}}^*(\mathbf{r})\varphi_{\mathbf{l}}(\mathbf{r})\varphi_{\mathbf{l}'}^*(\mathbf{r})\varphi_{\mathbf{k}'}(\mathbf{r}) = (2\pi)^2\sum_{\mathbf{\Delta}} \delta[\mathbf{k}-\mathbf{l}-(\mathbf{k}'-\mathbf{l}')-\mathbf{\Delta}]f[\mathbf{k},\mathbf{l},\mathbf{k}',\mathbf{l}',\mathbf{\Delta}]f[\mathbf{k},\mathbf{l},\mathbf{k}',\mathbf{l}',\mathbf{\Delta}] = \sum_{\mathbf{K},\mathbf{K}'=\mathbf{K}+\mathbf{\Delta}} e^{-\mathcal{K}^2/2}e^{i[(\pi/2)K_1^2-(\pi/2)K_1'^2+(k_x-k_x')\mathcal{K}_y-\mathcal{K}_x(l_y-l_y')+l_y(k-l)_x-l_y'(k'-l')_x]}, \tag{A13}$$

where $f[\mathbf{k},\mathbf{l},\mathbf{k}',\mathbf{l}',\mathbf{\Delta}]=0$ if $\mathbf{k}-\mathbf{l}-(\mathbf{k}'-\mathbf{l}')-\mathbf{\Delta}\neq\mathbf{0}$. The last exponent in function $f[\mathbf{k},\mathbf{l},\mathbf{k}',\mathbf{l}',\mathbf{\Delta}]$ can be also rearranged as

$$-\frac{\mathcal{K}^2}{2}-\frac{\pi i}{2}\mathbf{\Delta}_1(2K_1+\mathbf{\Delta}_1)+i(\mathbf{k}-\mathbf{k}')\wedge\mathcal{K} + i\mathcal{K}_x\mathbf{\Delta}_y+i(l_y-l_y')(k-l)_x+il_y'\mathbf{\Delta}_x. \tag{A14}$$

Using

$$\sum_{\mathbf{X}=n_1\mathbf{d}_1+n_2\mathbf{d}_2} e^{i\mathbf{X}\cdot\mathbf{q}} = \text{cell}\sum_{\mathbf{K}} \delta(\mathbf{q}-\mathbf{K}),$$

where cell is the volume of the unit cell and in our units equal to 2π, one obtains the Poisson resummation relation,

$$\sum_{\mathbf{K}} f(\mathbf{K}) = \frac{1}{\text{cell}}\int d\mathbf{q}\sum_{\mathbf{X}} \exp(i\mathbf{X}\cdot\mathbf{q})f(\mathbf{q}).$$

Using the Poisson resummation, one rewrites the sum as

$$f[\mathbf{k},\mathbf{l},\mathbf{k}',\mathbf{l}',\mathbf{\Delta}] = \sum_{\mathbf{X}} e^{-(1/2)[\mathbf{X}+\hat{z}\times(\mathbf{k}-\mathbf{k}')]^2-i\mathbf{X}\cdot(\mathbf{k}-\mathbf{l})} \times e^{i[(k_y-k_y')(k_x-l_x)+l_y'\mathbf{\Delta}_x-(\pi/2)\mathbf{\Delta}_1^2]}. \tag{A15}$$

3. Calculation of the $\beta_{\mathbf{k}}, \gamma_{\mathbf{k}}$ functions and their small momentum expansion

One often encounters the following space averages:

$$\beta_{\mathbf{k}}^N = \langle|\varphi|^2\varphi_{\mathbf{k}}\varphi_{\mathbf{k}}^{*N}\rangle_r, \quad \gamma_{\mathbf{k}}^N = \langle(\varphi^*)^2\varphi_{-\mathbf{k}}^N\varphi_{\mathbf{k}}\rangle_r, \tag{A16}$$

$\beta_{\mathbf{k}}=\beta_{\mathbf{k}}^0$ and $\gamma_{\mathbf{k}}=\gamma_{\mathbf{k}}^N$. Using formulas of the previous section, one can write

$$\varphi^* \varphi_{\mathbf{k}}^N = \frac{1}{2^{N/2}\sqrt{N!}}(-i\partial_x + \partial_y)^N \varphi^* \varphi_{\mathbf{k}}$$
$$= \frac{1}{2^{N/2}\sqrt{N!}} \sum_{\mathbf{Q}} (z_{\mathbf{k}} + z_{\mathbf{Q}})^N e^{i(\mathbf{k}+\mathbf{Q})\cdot\mathbf{x}} F^*(\mathbf{k},\mathbf{Q}), \tag{A17}$$
$$\varphi \varphi_{\mathbf{k}}^{*N} = (\varphi^* \varphi_{\mathbf{k}}^N)^* = \frac{1}{2^{N/2}\sqrt{N!}} \sum_{\mathbf{Q}} (z_{\mathbf{k}}^* + z_{\mathbf{Q}}^*)^N \times e^{-i(\mathbf{k}+\mathbf{Q})\cdot\mathbf{x}} F(\mathbf{k},\mathbf{Q}).$$

Therefore

$$\beta_k^N = \frac{1}{2^{N/2}\sqrt{N!}} \sum_{\mathbf{X}} (i z_{\mathbf{X}}^*)^N e^{-X^2/2 - i\mathbf{k}\cdot\mathbf{X}} \tag{A18}$$

and

$$\beta_k = \sum_{\mathbf{X}} e^{-X^2/2 - i\mathbf{k}\cdot\mathbf{X}}. \tag{A19}$$

Similarly $\gamma_{\mathbf{k}}^N$ can be obtained, for $\gamma_{\mathbf{k}}$, we have

$$\gamma_{\mathbf{k}} = e^{-ik_x k_y - k^2/2} \sum_{\mathbf{X}} e^{-X^2/2 - i z_{\mathbf{k}}^* z_{\mathbf{X}}}. \tag{A20}$$

Equation (A20) is valid for any lattice structure.

a. Small momentum expansion of the β_k, γ_k function for the general rhombic lattice

Consider the sum

$$S(N,M) = \sum_{\mathbf{X}} e^{-X^2/2} z_{\mathbf{X}}^N |\mathbf{X}|^M \tag{A21}$$

for any integers N, M. Due to reflection symmetry

$$\sum_{\mathbf{X}} e^{-X^2/2} X_x^{l_1} X_y^{l_2} = 0 \tag{A22}$$

for l_1, l_2 integers and $l_1 + l_2$ odd integer. For small $\mathbf{k}$,

$$\beta_{\mathbf{k}} = \sum_{\mathbf{X}} e^{-X^2/2} \left(1 + \sum_{l=1}^{\infty} \frac{(i\mathbf{k}\cdot\mathbf{X})^l}{l!}\right)$$
$$= \beta_\Delta - \sum_{\mathbf{X}} \frac{(k_x X_x + k_y X_y)^2}{2} e^{-X^2/2}$$
$$+ \sum_{\mathbf{X}} e^{-X^2/2} \frac{(k_x X_x + k_y X_y)^4}{24} + O(k^6). \tag{A23}$$

Similarly the function γ_k can be expanded for small k^2,

$$\gamma_k = e^{-ik_x k_y - k^2/2} \sum_{\mathbf{Q}} e^{-Q^2/2} \left[1 + \sum_{l=1}^{\infty} \frac{(\bar{k})^{2l} Q^{2l}}{(2l)!}\right], \tag{A24}$$

so that

$$|\gamma_k| = e^{-k^2/2} \left[\sum_{\mathbf{Q}} e^{-Q^2/2} \left(1 + \sum_{l=1}^{\infty} \frac{z_k^{*2l} z_{\mathbf{Q}}^{2l}}{(2l)!}\right)\right]^{1/2} \times \left[\sum_{\mathbf{Q}'} e^{-Q'^2/2} \left(1 + \sum_{l'=1}^{\infty} \frac{z_{\mathbf{k}}^{2l'} z_{\mathbf{Q}'}^{*2l'}}{(2l')!}\right)\right]^{1/2}. \tag{A25}$$

b. Small momentum expansion of the β_k, γ_k function for hexagonal lattice

When the symmetry is higher, the expressions simplify. Using the sixfold symmetry of the hexagonal lattice,

$$X_x' + iX_y' = e^{i\theta}(X_x + iX_y), \quad \theta = (\pi/3)l, \tag{A26}$$

the sum [Eq. (A21)] transforms into

$$S(N,M) = S(N,M) e^{in\theta}. \tag{A27}$$

Thus $S(N,M) = 0$ if $N \neq 6j$. Using $S(2,0) = S(4,0) = S(2,2) = 0$, one obtains several relations of different sums to simplify expansion of $\beta_{\mathbf{k}}$,

$$\beta_k = \sum_{\mathbf{X}} e^{-X^2/2} \left(1 - \frac{k^2 X^2}{4} + \frac{k^4 X^4}{64}\right). \tag{A28}$$

Similarly

$$|\gamma_k| = \beta_\Delta [1 - k^2/2 + k^4/8] + O(k^6), \tag{A29}$$

and its phase θ_k has an expansion

$$\gamma_{\mathbf{k}}/|\gamma_{\mathbf{k}}| = 1 - ik_x k_y + O(k^4), \quad \theta_k = -k_x k_y + O(k^4). \tag{A30}$$

In terms of z^* it is an analytic function:

$$\gamma_k = e^{-ik_x k_y - k^2/2} \gamma[z_{\mathbf{k}}^*], \quad \gamma[z_{\mathbf{k}}^*] = \sum_{\mathbf{X}} e^{-X^2/2 - i z_{\mathbf{k}}^* X}. \tag{A31}$$

c. Self-duality relation

If the lattice is self-dual, one can prove

$$\sum_{\mathbf{X}} X^2 e^{-X^2/2} = \beta_\Delta. \tag{A32}$$

Thus

$$\beta_{\mathbf{k}} = \beta_\Delta - \frac{\beta_A}{4} k^2 + \frac{k^4}{64} \sum_{\mathbf{X}} X^4 e^{-X^2/2}. \tag{A33}$$

Using the expansion for β_k, γ_k, one can obtain the supersoft acoustic phonon spectrum,

$$-\beta_\Delta + 2\beta_{\mathbf{k}} - |\gamma_k| = \left(\frac{1}{32} \sum_X X^4 e^{-X^2/2} - \frac{\beta_\Delta}{8}\right) k^4 + O(k^6). \tag{A34}$$

d. The small momentum expansion of the vertex function

For momentum, $\mathbf{k}, \mathbf{l}, \mathbf{k}'$ are not too big to have umklapp process,

$$\int_{\mathbf{r}} \varphi_{\mathbf{k}}^*(\mathbf{r}) \varphi_{\mathbf{l}}(\mathbf{r}) \varphi_0^*(\mathbf{r}) \varphi_{\mathbf{k}'}(\mathbf{r})$$
$$= (2\pi)^2 \delta[\mathbf{k} - \mathbf{l} - \mathbf{k}'] \times \sum_{\mathbf{K}} e^{-\mathcal{K}^2/2 + i(k_x - k_x')\mathcal{K}_y - i\mathcal{K}_x (l_y - l_y') + i(l_y)(k-l)_x}, \tag{A35}$$

where $\mathcal{K} = \mathbf{K} + \mathbf{k} - \mathbf{l}$. In this case, we define

$f[\mathbf{k},\mathbf{l},\mathbf{k}',\mathbf{l}',\mathbf{\Delta}]=[\mathbf{k},\mathbf{l}'|\mathbf{l},\mathbf{k}']$ and which has small momentum expansion,

$$[\mathbf{k},0|\mathbf{l},\mathbf{k}']=\beta_\Delta\left(1-\frac{l^2+k'^2}{4}+\frac{i}{2}(k_xk_y-l_xl_y-k_x'k_y')\right). \tag{A36}$$

e. Another useful identity

Any sixfold (D_6) symmetric function $F(\mathbf{k})$ [namely, a function satisfying $F(\mathbf{k})=F(\mathbf{k}')$, where $\mathbf{k},\mathbf{k}'$ is related by a $2\pi/6$ rotation] obeys

$$\int_{\mathbf{k}}F(\mathbf{k})\gamma_{\mathbf{k}}\gamma_{\mathbf{k},\mathbf{l}}=\frac{\gamma_{\mathbf{l}}}{\beta_\Delta}\int_{\mathbf{k}}F(\mathbf{k})|\gamma_{\mathbf{k}}|^2,\quad \gamma_{\mathbf{k},\mathbf{l}}=\langle\varphi_{\mathbf{k}}^*\varphi_{-\mathbf{k}}^*\varphi_{-\mathbf{l}}\varphi_{\mathbf{l}}\rangle. \tag{A37}$$

This identity can be proved by using the fact $[\int_{\mathbf{k}}F(\mathbf{k})\gamma_{\mathbf{k}}\gamma_{\mathbf{k},\mathbf{l}}]/\gamma_{\mathbf{l}}$ is a analytic function of $z_{\mathbf{l}}^*$ and is a periodic function of reciprocal lattice vectors, e.g.,

$$\mathbf{l}\to\mathbf{l}+m_1\tilde{\mathbf{d}}_1+m_2\tilde{\mathbf{d}}_2, \tag{A38}$$

the function is unchanged. The only solution for a analytic function with this property is a constant,

$$\int_{\mathbf{k}}F(\mathbf{k})\gamma_{\mathbf{k}}\gamma_{\mathbf{k},\mathbf{l}}/\gamma_{\mathbf{l}}=\text{const}. \tag{A39}$$

The constant can be determined by setting $\mathbf{l}=0$.

APPENDIX B: PARISI ALGEBRA FOR HIERARCHIAL MATRICES

In this appendix we collect without derivation the formulas used in calculation of disorder properties. The derivation can be found in Mezard (1991). The inverse matrix has the following Parisi parameters:

$$\widetilde{m^{-1}}=\frac{1}{\tilde{m}-\langle m\rangle}\left(1-\int_0^1\frac{du}{u}\frac{[m]_u}{\tilde{m}-\langle m\rangle-[m]_u}-\frac{m_0}{\tilde{m}-\langle m\rangle}\right);$$
$$m_x^{-1}=-\frac{1}{\tilde{m}-\langle m\rangle}\left(\frac{[m]_x}{x[\tilde{m}-\langle m\rangle-[m]_x]}+\int_0^x\frac{dv}{v^2}\frac{[m]_v}{\tilde{m}-\langle m\rangle-[m]_v}+\frac{m_0}{\tilde{m}-\langle m\rangle}\right). \tag{B1}$$

The square of the matrix can be treated similarly,

$$\widetilde{m^2_{a,b}}=(\tilde{m})^2-\langle(m_x)^2\rangle,$$
$$(m^2)_x=2(\tilde{m}-\langle m\rangle)m_x-\int_0^x dv(m_x-m_v)^2. \tag{B2}$$

REFERENCES

Abo-Shaeer, J. R., C. Raman, J. M. Vogels, and W. Ketterele, 2001, Science **292**, 476.

Abrikosov, A. A., 1957, Zh. Eksp. Teor. Fiz. **32**, 1442 [Sov. Phys. JETP **5**, 1174 (1957)].

Adesso, M. G., D. Uglietti, R. Flükiger, M. Polichetti, and S. Pace, 2006, Phys. Rev. B **73**, 092513.

Affleck, I., and E. Brézin, 1985, Nucl. Phys. B **257**, 451.

Avraham, N., B. Khaykovich, Y. Myasoedov, M. Rappaport, H. Shtrikman, D. E. Feldman, T. Tamegai, P. H. Kes, M. Li, M. Konczykowski, K. van der Beek, and E. Zeldov, 2001, Nature (London) **411**, 451.

Baker, G. A., 1990, *Quantitative Theory of Critical Phenomena* (Academic, Boston).

Baraduc, C., E. Janod, C. Ayache, and J. Y. Henry, 1994, Physica C **235**, 1555.

Baym, G., 2003, Phys. Rev. Lett. **91**, 110402.

Beidenkopf, H., N. Avraham, Y. Myasoedov, H. Shtrikman, E. Zeldov, B. Rosenstein, E. H. Brandt, and T. Tamegai, 2005, Phys. Rev. Lett. **95**, 257004.

Beidenkopf, H., T. Verdene, Y. Myasoedov, H. Shtrikman, E. Zeldov, B. Rosenstein, D. Li, and T. Tamegai, 2007, Phys. Rev. Lett. **98**, 167004.

Bel, G., D. Li, B. Rosenstein, V. Vinokur, and V. Zhuravlev, 2007, Physica C **460-462**, 1213.

Bellet, B., P. Garcia, and A. Neveu, 1996a, Int. J. Mod. Phys. A **11**, 5587.

Bellet, B., P. Garcia, and A. Neveu, 1996b, Int. J. Mod. Phys. A **11**, 5607.

Bender, C. M., A. Duncan, and H. F. Jones, 1994, Phys. Rev. D **49**, 4219.

Blatter, G., M. V. Feigel'man, V. B. Geshkenbein, A. I. Larkin, and V. M. Vinokur, 1994, Rev. Mod. Phys. **66**, 1125.

Blum, T., and M. A. Moore, 1997, Phys. Rev. B **56**, 372.

Bogner, S., T. Emig, and T. Nattermann, 2001, Phys. Rev. B **63**, 174501.

Bokil, H. S., and A. P. Young, 1995, Phys. Rev. Lett. **74**, 3021.

Bouquet, F., C. Marcenat, E. Steep, R. Calemczuk, W. K. Kwok, U. Welp, G. W. Crabtree, R. A. Fisher, N. E. Phillips, and A. Schilling, 2001, Nature (London) **411**, 448.

Brandt, E. H., 1977a, J. Low Temp. Phys. **26**, 709.

Brandt, E. H., 1977b, J. Low Temp. Phys. **26**, 735.

Brandt, E. H., 1986, Phys. Rev. B **34**, 6514.

Brandt, E. H., 1995, Rep. Prog. Phys. **58**, 1465.

Brézin, E., A. Fujita, and S. Hikami, 1990, Phys. Rev. Lett. **65**, 1949.

Brézin, E., D. R. Nelson, and A. Thiaville, 1985, Phys. Rev. B **31**, 7124.

Cha, M.-C., and H. A. Fertig, 1994a, Phys. Rev. Lett. **73**, 870.

Cha, M.-C., and H. A. Fertig, 1994b, Phys. Rev. B **50**, 14368.

Chang, D., C.-Y. Mou, B. Rosenstein, and C. L. Wu, 1998a, Phys. Rev. Lett. **80**, 145.

Chang, D., C.-Y. Mou, B. Rosenstein, and C. L. Wu, 1998b, Phys. Rev. B **57**, 7955.

Chauve, P., T. Giamarchi, and P. Le Doussal, 2000, Phys. Rev. B **62**, 6241.

Chen, Q. H., 2008, Phys. Rev. B **78**, 104501.

Chen, Q. H., and X. Hu, 2003, Phys. Rev. Lett. **90**, 117005.

Compagner, A., 1974, Physica (Amsterdam) **72**, 115.

Cooper, N. R., N. K. Wilkin, and J. M. F. Gunn, 2001, Phys. Rev. Lett. **87**, 120405.

Cornwall, J. M., R. Jackiw, and E. Tomboulis, 1974, Phys. Rev.

D **10**, 2428.
Dasgupta, C., and B. I. Halperin, 1981, Phys. Rev. Lett. **47**, 1556.
David, F., 1981, Commun. Math. Phys. **81**, 149.
de Alameida, J. R. L., and D. J. Thouless, 1978, J. Phys. A **11**, 983.
Deligiannis, K., M. Charalambous, J. Chaussy, R. Liang, D. Bonn, and W. N. Hardy, 2000, Physica C **341**, 1329.
Dietel, J., and H. Kleinert, 2006, Phys. Rev. B **74**, 024515.
Dietel, J., and H. Kleinert, 2007, Phys. Rev. B **75**, 144513.
Dietel, J., and H. Kleinert, 2009, Phys. Rev. B **79**, 014512.
Divakar, U., A. J. Drew, S. L. Lee, R. Gilardi, J. Mesot, F. Y. Ogrin, D. Charalambous, E. M. Forgan, G. I. Menon, N. Momono, M. Oda, C. D. Dewhurst, and C. Baines, 2004, Phys. Rev. Lett. **92**, 237004.
Dodgson, M. J. W., A. E. Koshelev, V. B. Geshkenbein, and G. Blatter, 2000, Phys. Rev. Lett. **84**, 2698.
Dorsey, A. T., M. Huang, and M. P. A. Fisher, 1992, Phys. Rev. B **45**, 523.
Dotsenko, V., 2001, *An Introduction to the Theory of Spin Glasses and Neural Networks* (Cambridge University Press, New York).
Duncan, A., and H. F. Jones, 1993, Phys. Rev. D **47**, 2560.
Eilenberger, G., 1967, Phys. Rev. **164**, 628.
Engels, P., I. Coddington, P. C. Haljian, and E. A. Cornell, 2002, Phys. Rev. Lett. **89**, 100403.
Ertas, D., and D. R. Nelson, 1996, Physica C **272**, 79.
Eskildsen, M. R., A. B. Abrahamsen, V. G. Kogan, P. L. Gammel, K. Mortensen, N. H. Andersen, and P. C. Canfield, 2001, Phys. Rev. Lett. **86**, 5148.
Faleski, M. C., M. C. Marchetti, and A. A. Middleton, 1996, Phys. Rev. B **54**, 12427.
Fangohr, H., and S. J. Cox, 2001, Phys. Rev. B **64**, 064505.
Fangohr, H., A. E. Koshelev, and M. J. W. Dodgson, 2003, Phys. Rev. B **67**, 174508.
Feng, B., Z. Wu, and D. Li, 2009, Int. J. Mod. Phys. B **23**, 661.
Fischer, K. H., and J. A. Hertz, 1991, *Spin Glasses* (Cambridge University Press, New York).
Fisher, D. S., M. P. A. Fisher, and D. A. Huse, 1991, Phys. Rev. B **43**, 130.
Fisher, M. P. A., 1989, Phys. Rev. Lett. **62**, 1415.
Fuchs, D. T., E. Zeldov, T. Tamegai, S. Ooi, M. Rappaport, and H. Shtrikman, 1998, Phys. Rev. Lett. **80**, 4971.
Fruchter, L., A. Aburto, and C. Pham-Phu, 1997, Phys. Rev. B **56**, R2936.
Giamarchi, T., and S. Bhattacharya, 2002, in *High Magnetic Fields: Applications in Condensed Matter Physics and Spectroscopy*, edited by C. Berthier *et al.* (Springer-Verlag, Berlin), p. 314.
Giamarchi, T., and P. Le Doussal, 1994, Phys. Rev. Lett. **72**, 1530.
Giamarchi, T., and P. Le Doussal, 1995a, Phys. Rev. Lett. **75**, 3372.
Giamarchi, T., and P. Le Doussal, 1995b, Phys. Rev. B **52**, 1242.
Giamarchi, T., and P. Le Doussal, 1996, Phys. Rev. Lett. **76**, 3408.
Giamarchi, T., and P. Le Doussal, 1997, Phys. Rev. B **55**, 6577.
Giamarchi, T., and P. Le Doussal, 1998, Phys. Rev. B **57**, 11356.
Gilardi, R., J. Mesot, A. Drew, U. Divakar, S. L. Lee, E. M. Forgan, O. Zaharko, K. Conder, V. K. Aswal, C. D. Dewhurst, R. Cubitt, N. Momono, and M. Oda, 2002, Phys. Rev. Lett. **88**, 217003.
Ginzburg, V. L., 1960, Fiz. Tverd. Tela (Leningrad) **2**, 203 [Sov. Phys. Solid State **2**, 1824 (1961)].
Ginzburg, V. L., and L. D. Landau, 1950, Zh. Eksp. Teor. Fiz. **20**, 1064.
Guida, R., K. Konishi, and H. Suzuki, 1995, Ann. Phys. (N.Y.) **241**, 152.
Guida, R., K. Konishi, and H. Suzuki, 1996, Ann. Phys. (N.Y.) **249**, 109.
Halperin, B. I., T. C. Lubensky, and S.-K. Ma, 1974, Phys. Rev. Lett. **32**, 292.
Herbut, I. F., 2007, *A Modern Approach to Critical Phenomena* (Cambridge University Press, Cambridge).
Herbut, I. F., and Z. Tešanović, 1994, Phys. Rev. Lett. **73**, 484.
Herbut, I. F., and Z. Tešanović, 1996, Phys. Rev. Lett. **76**, 4588.
Hikami, S., A. Fujita, and A. I. Larkin, 1991, Phys. Rev. B **44**, 10400.
Houghton, A., R. A. Pelcovits, and A. Sudbø, 1989, Phys. Rev. B **40**, 6763.
Hu, J., and A. H. MacDonald, 1993, Phys. Rev. Lett. **71**, 432.
Hu, J., and A. H. MacDonald, 1997, Phys. Rev. B **56**, 2788.
Hu, J., A. H. MacDonald, and B. D. Mckay, 1994, Phys. Rev. B **49**, 15263.
Hu, X., M. B. Luo, and Y. Q. Ma, 2005, Phys. Rev. B **72**, 174503.
Hu, X., S. Miyashita, and M. Tachiki, 1997, Phys. Rev. Lett. **79**, 3498.
Huh, Y. M., and D. K. Finnemore, 2002, Phys. Rev. B **65**, 092506.
Ikeda, R., 1995, J. Phys. Soc. Jpn. **64**, 1683.
Ikeda, R., T. Ohmi, and T. Tsuneto, 1990, J. Phys. Soc. Jpn. **59**, 1740.
Itzykson, C., and J. Drouffe, 1991, *Statistical Field Theory* (Cambridge University Press, Cambridge).
Jaiswal-Nagar, D., A. D. Thakur, S. Ramakrishnan, A. K. Grover, D. Pal, and H. Takeya, 2006, Phys. Rev. B **74**, 184514.
Jevicki, A., 1977, Phys. Lett. **71**, 327.
Johnson, S. T., E. M. Forgan, S. H. Lloyd, C. M. Aegerter, S. L. Lee, R. Cubitt, P. G. Kealey, C. Ager, S. Tajima, A. Rykov, and D. McK. Paul, 1999, Phys. Rev. Lett. **82**, 2792.
Junod, A., J. Y. Genuod, G. Triscone, and T. Schneider, 1998, Physica C **294**, 115.
Kato, Y., and N. Nagaosa, 1993, Phys. Rev. B **48**, 7383.
Kawamura, H., 2003, Phys. Rev. B **68**, 220502.
Keimer, B., W. Y. Shih, R. W. Erwin, J.-W. Lynn, F. Dogan, and I. A. Aksay, 1994, Phys. Rev. Lett. **73**, 3459.
Ketterson, J. B., and S. N. Song, 1999, *Superconductivity* (Cambridge University Press, New York).
Kienappel, A. K., and M. A. Moore, 1997, Phys. Rev. B **56**, 8313.
Kierfeld, J., and V. Vinokur, 2000, Phys. Rev. B **61**, R14928.
Kim, P., Z. Yao, C. A. Bolle, and C. M. Lieber, 1999, Phys. Rev. B **60**, R12589.
Kleinert, H., 1990, *Path Integrals in Quantum Mechanics, Statistics, and Polymer Physics* (World Scientific, Singapore).
Klironomos, A. D., and A. T. Dorsey, 2003, Phys. Rev. Lett. **91**, 097002.
Kokkaliaris, S., A. A. Zhukov, P. A. J. de Groot, R. Gagnon, L. Taillefer, and T. Wolf, 2000, Phys. Rev. B **61**, 3655.
Kokubo, N., T. Asada, K. Kadowaki, K. Takita, T. G. Sorop, and P. H. Kes, 2007, Phys. Rev. B **75**, 184512.
Kokubo, N., R. Besseling, and P. H. Kes, 2004, Phys. Rev. B **69**, 064504.
Kokubo, N., K. Kadowaki, and K. Takita, 2005, Phys. Rev. Lett. **95**, 177005.

Kopnin, N. B., 2001, *Theory of Nonequilibrium Superconductivity* (Oxford University Press, New York).
Korshunov, S. E., 1990, Europhys. Lett. **11**, 757.
Korshunov, S. E., 1993, Phys. Rev. B **48**, 3969.
Koshelev, A. E., 1994, Phys. Rev. B **50**, 506.
Kovner, A., P. Kurzepa, and B. Rosenstein, 1993, Mod. Phys. Lett. **8**, 1343.
Kovner, A., and B. Rosenstein, 1992, J. Phys.: Condens. Matter **4**, 2903.
Larkin, A. I., 1970, Zh. Eksp. Teor. Fiz. **58**, 1466.
Larkin, A., and A. Varlamov, 2005, *Theory of Fluctuations in Superconductors* (Oxford University Press, New York).
Lasher, G., 1965, Phys. Rev. **140**, A523.
Lawrence, W. E., and S. Doniach, 1971, in *Proceedings of the 12th International Conference on Low Temperature Physics*, Kyoto, 1970, edited by E. Kanda (Academic, Kyoto), p. 361.
Lawrie, I. D., 1994, Phys. Rev. B **50**, 9456.
Lee, P. A., and S. R. Shenoy, 1972, Phys. Rev. Lett. **28**, 1025.
Leote de Carvalho, R. J. F., R. Evans, and Y. Rosenfeld, 1999, Phys. Rev. E **59**, 1435.
Levanyuk, A. P., 1959, Zh. Eksp. Teor. Fiz. **36**, 810.
Li, D., P.-J. Lin, B. Rosenstein, B. Ya. Shapiro, and I. Shapiro, 2006, Phys. Rev. B **74**, 174518.
Li, D., A. M. Malkin, and B. Rosenstein, 2004, Phys. Rev. B **70**, 214529.
Li, D., and B. Rosenstein, 1999a, Phys. Rev. B **60**, 9704.
Li, D., and B. Rosenstein, 1999b, Phys. Rev. B **60**, 10460.
Li, D., and B. Rosenstein, 2001, Phys. Rev. Lett. **86**, 3618.
Li, D., and B. Rosenstein, 2002a, Phys. Rev. B **65**, 220504.
Li, D., and B. Rosenstein, 2002b, Phys. Rev. B **65**, 024513.
Li, D., and B. Rosenstein, 2002c, Phys. Rev. B **65**, 024514.
Li, D., and B. Rosenstein, 2003, Phys. Rev. Lett. **90**, 167004.
Li, D., and B. Rosenstein, 2004, Phys. Rev. B **70**, 144521.
Li, D., B. Rosenstein, and V. Vinokur, 2006, J. Supercond. Novel Magn. **19**, 369.
Li, M. S., and T. Nattermann, 2003, Phys. Rev. B **67**, 184520.
Liang, R., D. A. Bonn, and W. N. Hardy, 1996, Phys. Rev. Lett. **76**, 835.
Lin, P.-J., and B. Rosenstein, 2005, Phys. Rev. B **71**, 172504.
Lobb, C. J., 1987, Phys. Rev. B **36**, 3930.
Lopatin, A. V., 2000, Europhys. Lett. **51**, 635.
Lopatin, A. V., and G. Kotliar, 1999, Phys. Rev. B **59**, 3879.
Lortz, R., F. Lin, N. Musolino, Y. Wang, A. Junod, B. Rosenstein, and N. Toyota, 2006, Phys. Rev. B **74**, 104502.
Lortz, R., N. Musolino, Y. Wang, A. Junod, and N. Toyota, 2007, Phys. Rev. B **75**, 094503.
Lovett, R., 1977, J. Chem. Phys. **66**, 1225.
Madison, K. W., F. Chevy, W. Wohlleben, and J. Dalibard, 2000, Phys. Rev. Lett. **84**, 806.
Maki, K., and H. Takayama, 1971, Prog. Theor. Phys. **46**, 1651.
Matl, P., N. P. Ong, R. Gagnon, and L. Taillefer, 2002, Phys. Rev. B **65**, 214514.
Mazenko, G. F., 2006, *Nonequillibrium Statistical Mechanics* (Wiley-VCH, Weinheim).
McK. Paul, D., C. V. Tomy, C. M. Aegerter, R. Cubitt, S. H. Lloyd, E. M. Forgan, S. L. Lee, and M. Yethiraj, 1998, Phys. Rev. Lett. **80**, 1517.
Menon, G. I., 2002, Phys. Rev. B **65**, 104527.
Menon, G. I., and C. Dasgupta, 1994, Phys. Rev. Lett. **73**, 1023.
Menon, G. I., C. Dasgupta, and T. V. Ramakrishnan, 1999, Phys. Rev. B **60**, 7607.
Mermin, N. D., and H. Wagner, 1966, Phys. Rev. Lett. **17**, 1133.
Mezard, M., and G. Parisi, 1991, J. Phys. I **1**, 809.
Mezard, M., G. Parisi, and M. A. Virasoro, 1987, *Spin Glass Theory and Beyond* (World Scientific, Singapore).
Mikitik, G. P., and E. H. Brandt, 2001, Phys. Rev. B **64**, 184514.
Mikitik, G. P., and E. H. Brandt, 2003, Phys. Rev. B **68**, 054509.
Monarkha, Y., and K. Kono, 2004, *Two-Dimensional Coulomb Liquids and Solids* (Springer, New York).
Moore, M. A., 1989, Phys. Rev. B **39**, 136.
Moore, M. A., 1992, Phys. Rev. B **45**, 7336.
Moore, M. A., 1997, Phys. Rev. B **55**, 14136.
Moore, M. A., T. J. Newman, A. J. Bray, and S.-K. Chin, 1998, Phys. Rev. B **58**, 936.
Mukerjee, S., and D. A. Huse, 2004, Phys. Rev. B **70**, 014506.
Nattermann, T., 1990, Phys. Rev. Lett. **64**, 2454.
Nattermann, T., and S. Scheidl, 2000, Adv. Phys. **49**, 607.
Newman, T. J., and M. A. Moore, 1996, Phys. Rev. B **54**, 6661.
Nguyen, A. K., and A. Sudbø, 1998, Phys. Rev. B **60**, 15307.
Nikulov, A. V., 1995, Phys. Rev. B **52**, 10429.
Nikulov, A. V., D. Yu. Remisov, and V. A. Oboznov, 1995, Phys. Rev. Lett. **75**, 2586.
Nishizaki, T., K. Shibata, T. Sasaki, and N. Kobayashi, 2000, Physica C **341-348**, 957.
Nonomura, Y., and X. Hu, 2001, Phys. Rev. Lett. **86**, 5140.
Oganesyan, V., D. A. Huse, and S. L. Sondhi, 2006, Phys. Rev. B **73**, 094503.
Okazaki, R., Y. Kasahara, H. Shishido, M. Konczykowski, K. Behnia, Y. Haga, T. D. Matsuda, Y. Onuki, T. Shibauchi, and Y. Matsuda, 2008, Phys. Rev. Lett. **100**, 037004.
Okopinska, A., 1987, Phys. Rev. D **35**, 1835.
Olson, C. J., C. Reichhardt, and S. Bhattacharya, 2001, Phys. Rev. B **64**, 024518.
Olsson, P., 2007, Phys. Rev. Lett. **98**, 097001.
Olsson, P., and S. Teitel, 2001, Phys. Rev. Lett. **87**, 137001.
Olsson, P., and S. Teitel, 2003, Phys. Rev. B **67**, 144514.
O'Neill, J. A., and M. A. Moore, 1993, Phys. Rev. B **48**, 374.
Pal, D., S. Ramakrishnan, and A. K. Grover, 2002, Phys. Rev. B **65**, 096502.
Pal, D., S. Ramakrishnan, A. K. Grover, D. Dasgupta, and B. K. Sarma, 2001, Phys. Rev. B **63**, 132505.
Paltiel, Y., E. Zeldov, Y. Myasoedov, M. L. Rappaport, G. Jung, S. Bhattacharya, M. J. Higgins, Z. L. Xiao, E. Y. Andrei, P. L. Gammel, and D. J. Bishop, 2000, Phys. Rev. Lett. **85**, 3712.
Paltiel, Y., E. Zeldov, Y. Myasoedov, H. Shtrikman, S. Bhattacharya, M. J. Higgins, Z. L. Xiao, E. Y. Andrei, P. L. Gammel, and D. J. Bishop, 2000, Nature (London) **403**, 398.
Parisi, G., 1980, J. Phys. A **13**, 1101.
Park, H., and J. Yeo, 2008, J. Korean Phys. Soc. **52**, 1093.
Park, K., and D. A. Huse, 1998, Phys. Rev. B **58**, 9427.
Pastoriza, H., M. F. Goffman, A. Arribêre, and F. de la Cruz, 1994, Phys. Rev. Lett. **72**, 2951.
Pethick, C. J., and H. Smith, 2008, *Bose-Einstein Condensation in Dilute Gases* (Cambridge University Press, Cambridge).
Pierson, S. W., J. Buan, B. Zhou, C. C. Huang, and O. T. Valls, 1995, Phys. Rev. Lett. **74**, 1887.
Pierson, S. W., T. M. Katona, Z. Tešanović, and O. T. Valls, 1996, Phys. Rev. B **53**, 8638.
Pierson, S. W., O. T. Valls, Z. Tešanović, and M. A. Lindemann, 1998, Phys. Rev. B **57**, 8622.
Pierson, S. W., and O. T. Walls, 1998, Phys. Rev. B **57**, R8143.
Pourret, A., H. Aubin, J. Lesueur, C. A. Marrache-Kikuchi, L. Berge, L. Dumoulin, and K. Behnia, 2006, Nat. Phys. **2**, 683.
Prange, R. E., 1969, Phys. Rev. B **1**, 2349.
Radzyner, Y., A. Shaulov, and Y. Yeshurun, 2002, Phys. Rev. B

65, 100513.
Rajaraman, R., 1982, *Solitons and Instantons* (North-Holland, Amsterdam).
Reichhardt, C., C. J. Olson, J. Groth, S. Field, and F. Nori, 1996, Phys. Rev. B **53**, R8898.
Reichhardt, C., A. van Otterlo, and G. T. Zimanyi, 2000, Phys. Rev. Lett. **84**, 1994.
Revaz, B., A. Junod, and A. Erb, 1998, Phys. Rev. B **58**, 11153.
Rosenstein, B., 1999, Phys. Rev. B **60**, 4268.
Rosenstein, B., and A. Knigavko, 1999, Phys. Rev. Lett. **83**, 844.
Rosenstein, B., B. Ya. Shapiro, R. Prozorov, A. Shaulov, and Y. Yeshurun, 2001, Phys. Rev. B **63**, 134501.
Rosenstein, B., Ya. Shapiro, I. Shapiro, Y. Bruckental, A. Shaulov, and Y. Yeshurun, 2008, Phys. Rev. B **72**, 144512.
Rosenstein, B., and V. Zhuravlev, 2007, Phys. Rev. B **76**, 014507.
Roulin, M., A. Junod, A. Erb, and E. Walker, 1996, J. Low Temp. Phys. **105**, 1099.
Roulin, M., A. Junod, and E. Walker, 1996, Science **273**, 1210.
Ruggeri, G. J., 1978, Phys. Rev. B **20**, 3626.
Ruggeri, G. J., and D. J. Thouless, 1976, J. Phys. F: Met. Phys. **6**, 2063.
Ryu, S., A. Kapitulnik, and S. Doniach, 1996, Phys. Rev. Lett. **77**, 2300.
Saint-James, D., G. Sarma, and E. Thomas, 1969, *Type II Superconductivity* (Pergamon, Oxford).
Salem-Sugui, S., and E. Z. Dasilva, 1994, Physica C **235**, 1919.
Salem-Sugui, S., M. Friesen, A. D. Alvarenga, F. G. Gandra, M. M. Doria, and O. F. Schilling, 2002, Phys. Rev. B **66**, 134521.
Sasagawa, T., Y. Togawa, J. Shimoyama, A. Kapitulnik, K. Kitazawa, and K. Kishio, 2000, Phys. Rev. B **61**, 1610.
Sasik, R., and D. Stroud, 1995, Phys. Rev. Lett. **75**, 2582.
Schilling, A., R. A. Fisher, N. E. Phillips, U. Welp, D. Dasgupta, W. K. Kwok, and G. W. Crabtree, 1996, Nature (London) **382**, 791.
Schilling, A., R. A. Fisher, N. E. Phillips, U. Welp, W. K. Kwok, and G. W. Crabtree, 1997, Phys. Rev. Lett. **78**, 4833.
Schilling, A., U. Welp, W. K. Kwok, and G. W. Crabtree, 2002, Phys. Rev. B **65**, 054505.
Senatore, C., R. Flkiger, M. Cantoni, G. Wu, R. H. Liu, and X. H. Chen, 2008, Phys. Rev. B **78**, 054514.
Shibata, K., T. Nishizaki, T. Sasaki, and N. Kobayashi, 2002, Phys. Rev. B **66**, 214518.
Shibauchi, T., M. Sato, S. Ooi, and T. Tamegai, 1998, Phys. Rev. B **57**, R5622.
Sinova, J., C. B. Hanna, and A. H. MacDonald, 2002, Phys. Rev. Lett. **89**, 030403.
Sok, J., M. Xu, W. Chen, B. J. Suh, J. Gohng, D. K. Finnemore, M. J. Kramer, L. A. Schwartzkopf, and B. Dabrowski, 1995, Phys. Rev. B **51**, 6035.
Sonin, E. B., 2005, Phys. Rev. A **72**, 021606.
Stevens, M., and M. Robbins, 1993, J. Chem. Phys. **98**, 2319.
Stevenson, P. W., 1981, Phys. Rev. D **23**, 2916.
Taylor, B. J., S. Li, M. B. Maple, and M. P. Maley, 2003, Phys. Rev. B **68**, 054523.
Taylor, B. J., and M. B. Maple, 2007, Phys. Rev. B **76**, 014517.
Tešanović, Z., 1999, Phys. Rev. B **59**, 6449.
Tešanović, Z., and A. V., Andreev, 1994, Phys. Rev. B **49**, 4064.
Tešanović, Z., L. Xing, L. Bulaevskii, Q. Li, and M. Suenaga, 1992, Phys. Rev. Lett. **69**, 3563.
Tešanović, Z., and I. F. Herbut, 1994, Phys. Rev. B **50**, 10389.
Tešanović, Z., and L. Xing, 1991, Phys. Rev. Lett. **67**, 2729.
Thakur, A. D., S. S. Banerjee, M. J. Higgins, S. Ramakrishnan, and A. K. Grover, 2005, Phys. Rev. B **72**, 134524.
Thompson, R. S., and C. R. Hu, 1971, Phys. Rev. Lett. **27**, 1352.
Thouless, D. J., 1975, Phys. Rev. Lett. **34**, 946.
Tinh, B.-D., and B. Rosenstein, 2009, Phys. Rev. B **79**, 024518.
Tinkham, M., 1996, *Introduction to Superconductivity* (McGraw-Hill, New York).
Troy, R. J., and A. T. Dorsey, 1993, Phys. Rev. B **47**, 2715.
Ullah, S., and A. T. Dorsey, 1990, Phys. Rev. Lett. **65**, 2066.
Ullah, S., and A. T. Dorsey, 1991, Phys. Rev. B **44**, 262.
Ussishkin, I., 2003, Phys. Rev. B **68**, 024517.
Ussishkin, I., S. L. Sondhi, and D. A. Huse, 2002, Phys. Rev. Lett. **89**, 287001.
van Otterlo, A., R. T. Scalettar, and G. T. Zimanyi, 1998, Phys. Rev. Lett. **81**, 1497.
Wang, Y., L. Li, and N. P. Ong, 2006, Phys. Rev. B **73**, 024510.
Wang, Y., N. P. Ong, Z. A. Xu, T. Kakeshita, S. Uchida, D. A. Bonn, R. Liang, and W. N. Hardy, 2002, Phys. Rev. Lett. **88**, 257003.
Welp, U., J. A. Fendrich, W. K. Kwok, G. W. Crabtree, and B. W. Veal, 1996, Phys. Rev. Lett. **76**, 4809.
Welp, U., S. Fleshler, W. K. Kwok, R. A. Klemm, V. M. Vinokur, J. Downey, B. Veal, and G. W. Crabtree, 1991, Phys. Rev. Lett. **67**, 3180.
Wilkin, N. K., and H. J. Jensen, 1997, Phys. Rev. Lett. **79**, 4254.
Wilkin, N. K., and M. A. Moore, 1993, Phys. Rev. B **47**, 957.
Willemin, M., A. Schilling, H. Keller, C. Rossel, J. Hofer, U. Welp, W. K. Kwok, R. J. Olsson, and G. W. Crabtree, 1998, Phys. Rev. Lett. **81**, 4236.
Wu, Z., B. Feng, and D. Li, 2007, Phys. Rev. A **75**, 033620.
Xiao, Z. L., E. Y., Andrei, Y. Paltiel, E. Zeldov, P. Shuk, and M. Greenblatt, 2002, Phys. Rev. B **65**, 094511.
Xiao, Z. L., O. Dogru, E. Y. Andrei, P. Shuk, and M. Greenblatt, 2004, Phys. Rev. Lett. **92**, 227004.
Yeo, J., and M. A. Moore, 1996a, Phys. Rev. Lett. **76**, 1142.
Yeo, J., and M. A. Moore, 1996b, Phys. Rev. B **54**, 4218.
Yeo, J., and M. A. Moore, 2001, Phys. Rev. B **64**, 024514.
Yeo, J., H. Park, and S. Yi, 2006, J. Phys.: Condens. Matter **18**, 3607.
Zeldov, E., D. Majer, M. Konczykowski, V. B. Geshkenbein, V. M. Vinokur, and H. Shtrikman, 1995, Nature (London) **375**, 373.
Zhou, B., J. Buan, S. W. Pierson, C. C. Huang, O. T. Valls, J. Z. Liu, and R.-N. Shelton, 1993, Phys. Rev. B **47**, 11631.
Zhuravlev, V., and T. Maniv, 1999, Phys. Rev. B **60**, 4277.
Zhuravlev, V., and T Maniv, 2002, Phys. Rev. B **66**, 014529.